T-3631

A NEW FILTERING TECHNIQUE FOR CORRECTING TIME VARIATIONS IN MAGNETIC DATA

by

Mohammad Nurul Hasan

T-3631

A thesis submitted to the Faculty and the Board of Trustees of the Colorado School of Mines in partial fulfillment of the requirements for the degree of Master of Science (Geophysics).

Golden, Colorado

Date Nov. 7, '88

Signed: M. Nurul Hasan
Mohammad Nurul Hasan

Approved: R. O. Hansen
Dr. Richard O. Hansen
Thesis Advisor

Golden, Colorado

Date 9 Nov 88

P R Romig
Dr. Phillip R. Romig
Head
Geophysics Department

ABSTRACT

Time variations in magnetic data distort the anomalies due to the geology. The standard method for removing time variations from magnetic data is based on the assumption that the time variations measured at the base station and those encountered at the field stations are exactly the same, and accordingly the time variations are removed from the field data simply by subtracting the base station reading from the corresponding field station reading. This assumption is practically true for very local land-based surveys, in which the base and field stations are close to one another. For large-scale surveys, when the base and field stations are at a considerable distance apart, the standard method introduces errors because, although the time variations measured at two different places are practically identical in shape, they differ in amplitude and phase depending on the separation between the base station and survey location.

Dr. R. O. Hansen at the Colorado School of Mines has formulated a new filtering technique for correcting time variations in magnetic data. The technique is based on the base and field data only and is capable of taking care of the differences in amplitude and phase between the time

variations in the base and field data. Results obtained by applying the filter to model and real data demonstrate that the new filtering technique successfully removes the time variations from the field data by compensating for the differences in amplitude and phase between the time variations in the base and field data.

TABLE OF CONTENTS

LIST OF FIGURES

ACKNOWLEDGEMENTS

I would like to express my gratitude to my advisor, Dr. Richard O. Hansen, for allowing me to take his proposed new filtering technique for correcting time variations in magnetic data as my Master's thesis topic. I am grateful to him for guiding my research and helping me throughout my studies. I would also like to express my gratefulness to my graduate committee members Dr. Norman Harthill, Dr. Abdelwahid A. Ibrahim and Dr. M. Dean Kleinkopf for their help and encouragement in my studies.

I appreciate very much the permission of the TerraSense, Inc. to use some of their data for my research.

I gratefully acknowledge the use of software and computer facilities at the Center for Potential Fields Studies (CPFS) for my research. The intimate academic atmosphere at the CPFS has greatly helped me in my studies. The graduate students at the Center were all very nice and cooperative, and I enjoyed being one of them. Particularly, I would like to thank Wendy Weiland and Steve Tsai for their help. I also appreciate the help received from Helen Leek at the Center.

Finally, I would like to express my thankfulness to the Government of Bangladesh, through the Geological Survey

of Bangladesh (GSB), for giving me this opportunity for higher studies and providing me with necessary financial support.

Chapter 1

INTRODUCTION

The geomagnetic field, measured at or near the earth's surface during a magnetic survey, can be considered to be composed of three components:

a) the internal field,

b) the anomalous field, and

c) the time-varying field.

The internal field, according to present theories, is caused by electric currents circulating in the outer core region of the earth. Although the internal field varies both in magnitude and direction over geologically long times, it is practically a steady-state field for the duration of a mgnetic survey. The internal field has a magnitude of the order of tens of thousands of nT.

The anomalous field is caused by materials and structures having magnetic susceptibilities in the outer tens of kilometer of the earth; this field is also called the field due to the geology. The magnitude of the anomalous field reaches up to thousands of nT.

The time-varying field is the short-duration and small-amplitude fluctuations of the geomagnetic field. These fluctuations, about which we are concerned during

magnetic surveys, usually have periods less than a few days. The origin of this field lies primarily in the complex interactions between solar and terrestrial electromagnetic phenomena. The time-varying field that we encounter during magnetic surveys is also known as the time variations. The time variations observed at or near the earth's surface vary from tens of nT to hundreds of nT.

The objective of a magnetic survey is to map the anomalous field for locating magnetic minerals and other natural resources occuring in association with magnetic bodies. So, after the completion of a magnetic survey, the next step is to remove the internal field and the time variations from the geomagnetic field measurements, called the field data. Usually, the internal field, which is practically a steady-state field for the duration of a magnetic survey, is routinely and accurately removed from the field data through the subtraction of a geomagnetic reference field. In practice, however, because of the limited geographic coverage of most surveys (the internal field being practically a constant value over such an area) , the removal of this field is not always carried out. To remove the time variations from the field data, the standard method generally adopted is the following: In or near the survey area, at a fixed station (called the base

station) a magnetometer is read at the beginning and end of a survey and periodically (at short intervals) throughout the survey. The base station readings are called the base data. A plot of these readings against time is termed the drift curve. The drift curve is used to correct the measurements made at the field stations for time variations by noting the difference between the base station reading and a reasonably chosen baseline at the time a particular field station was occupied and then algebraically subtracting this difference from the field station reading.

This simple method works well in very local land-based surveys. However, this method also assumes that the time variations measured at the base station are exactly the same as the time variations measured at the field stations. In reality, this assumption is not true when the survey area is large and the base and field stations are a considerable distance apart. Further, if there is a phase shift between the time variations in the base and field data, this method fails to remove the time variations from the field data correctly. So, such a method is not valid for large scale surveys and impractical in oceanic and airborne operations, because in these surveys large amounts of data are collected and the base and field stations may be widely separated from one another.

Studies of the time variations (as we have done in the next chapter, Time Variations) show that the time variations measured at two different places separated by a distance of hundreds of kilometers, over wide areas of the earth in the mid-latitude zones, especially during solar quiet days when magnetic surveys are normally carried out, are practically identical to one another in shape except for differences in amplitude and phase depending on the differences in latitude and local solar time at the two places. In these areas, the storm variations observed at two different places are also identical in shape, differing only in amplitude and phase. In the equatorial, auroral and polar cap zones the same properties of the time variations are also observed between two places at a much smaller distance apart, but the time variations differ greatly both in amplitude and phase. Considering these characteristic properties of time variations, it seems hopeful that a linear filtering technique based on the base and field data only (the base and field data contain all the necessary information about the time variations measured at the base and field stations), which is also capable of taking into account the differences in amplitude and phase (if any) between the time variations in the base and field data, could be used to remove the time variations from the field

data. Such a technique, if proved successful, is expected to have wide application in magnetic survey data reduction.

With these ideas in mind, Dr. Richard O. Hansen at the Colorado School of Mines (CSM) has formulated a new filtering technique for correcting time variations in magnetic data. The new filtering technique is based on the base and field data only and is capable of taking into account the differences in amplitude and phase between the time variations in the base and field data.

In this thesis, studies on the proposed new filtering technique are reported. The sources and properties of the time variations are first discussed in an attempt to understand how these variations affect magnetic measurements and what characteristic properties need to be considered in removing their effects from the field data. Next, the mathematical formulation and implementation, along with the expected applications, of the technique are explained. Results obtained by applying the filtering technique to both model and real data are then analysed. Finally, on the basis of the results obtained here, statements about the merits and usefulness of the new filtering technique are made.

Chapter 2

TIME VARIATIONS

The earth's magnetic field fluctuates with time. The short duration and small amplitude fluctuations, about which we are mainly concerned during a magnetic survey, are here considered as the time variations. The time variations are primarily due to the complex interactions between solar and terrestrial electromagnetic phenomena.

The earth is constantly exposed to the flow of various energies from space, such as electromagnetic radiation, cosmic rays, charged particles, and neutrinos; and this flow of energies affects terrestrial phenomena in different ways (Abell, 1975). The sun is also a source of these energies and, being nearest to the earth, has the greatest effect on it. Particularly, the interactions of the electromagnetic radiation, charged particles and magnetic fields emitted from the sun with the magnetic fields of the earth and its atmosphere are the main sources of the time variations (Regan and Rodriguez, 1981). The emission of charged particles and magnetic fields from the sun gives rise to the classic shape of the earth's magnetic field, called the magnetosphere, shown in Figure 1. In the magnetosphere, due to the distortion of the nearly dipole

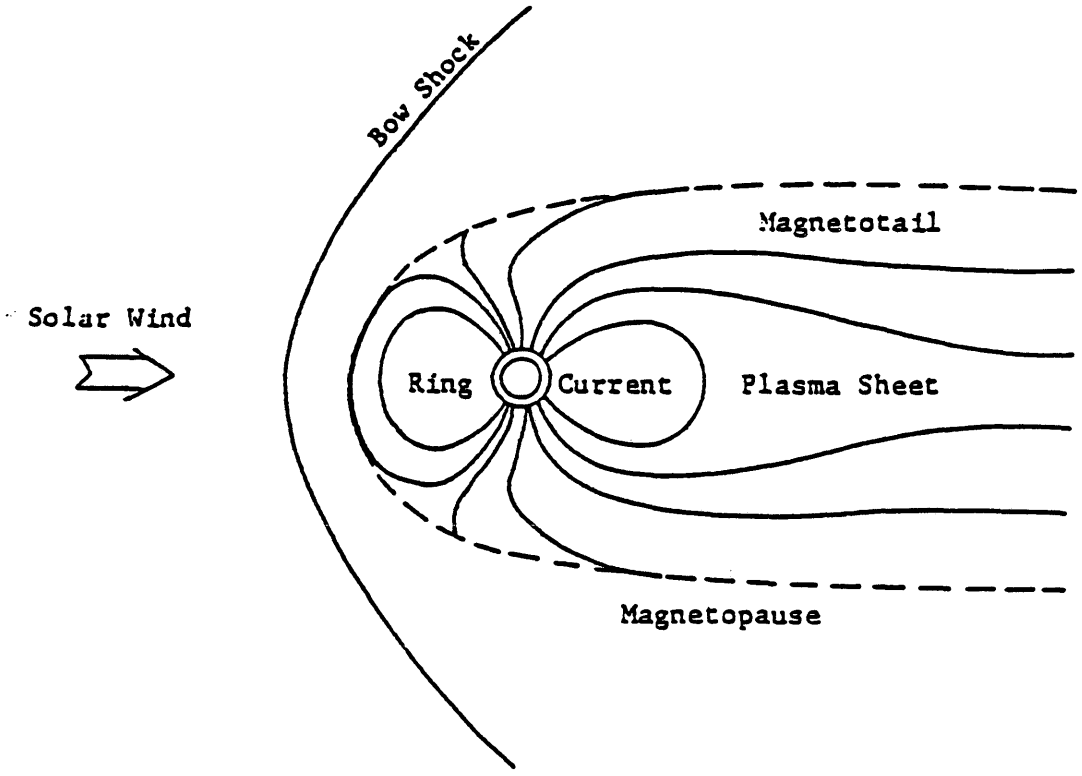

Figure 1. The magnetosphere of the earth, viewed from the plane of the ecliptic.
(Regan and Rodriguez, 1981)

geometry of the earth's magnetic field by the interaction between the solar wind (a hot, completely ionized gas or plasma, composed of mainly electrons and protons) and the geomagnetic field, three major current systems, namely the magnetopause current system, the plasma sheet current system and the ring current system, develop. These are non-steady current systems because the clouds of the ionized particles from the sun meet the outer magnetic field of the earth with a variable velocity ranging from 300 to 800 km/s (Porstendorfer, 1975). The density of these ionized particles is also highly variable, varying from 0.4 to 80 ions/cm^3 (Abell, 1975). Due to their movements in the geomagnetic field, the current systems generate time-varying magnetic fields. The variations of the fields depend on the fluctuations of velocity and density of the ionized particles on the geomagnetic field.

The magnetopause current system causes oscillations of the geomagnetic field with periods of seconds to minutes or impulsive varitions with no distinct periodicity. The amplitudes of these oscillations, known as micropulsations, are on the order of several nT. The plasma sheet current system generally finds its way into the polar regions of the earth's magnetic field and produces the well-known signature of magnetic substorms: magnetic bays (decreases

in the horizontal magnetic component) with magnitudes on the order of a hundred nT. The ring current system is a more steady-state current system other than either the magnetopause or the plasma sheet current system but, during magnetic storms, particles from the plasma sheet are injected into the ring current to produce additional magnetic field fluctuations which are detected at low latitudes on the earth's surface. On such occasions, the ring current generates a perturbation field opposite to the main geomagnetic field and thus causes depression of the field observed on the surface. The perturbation is on the order of hundreds of nT. Except during magnetic storms and substorms, periods of intense and moderate activities in the sun, the time-vaying magnetic fields generated by these current systems, which are separated from the earth's surface by a distance equal to several times the radius of the earth, have practically no effect on ground and airborne magnetic survey measurements.

The solar electromagnetic radiation gives rise to a current system, known as the ionospheric current system, in the 90 to 130 km altitude range. In this region, x-rays ionize the atmosphere, creating an ionosphere, while the ultraviolet rays provide differential heating over this density stratified medium, resulting in atmospheric

turbulence. The resulting motion of the charged particles in the presence of the earth's magnetic field generates the ionospheric current system which produces the most important time-varying magnetic field. In comparison to other current systems, the ionospheric current system is very close to the earth and, for this reason, the time-varying magnetic field produced by this current system has a profound effect on ground and airborne magnetic survey measurements. Even during solar quiet days, when there is practically no activity in the sun, this time-varying magnetic field has a magnitude on the order of tens of nT.

The external time-varying magnetic field is the combined effect of the time-varying magnetic fields generated by the various current systems discussed above (including other minor current systems, such as field-aligned current system, sporadic current system, etc.), which are external to the earth, at any single time. The external time-varying magnetic fields also induce currents in the earth, called telluric currents, whose configuration and intensity vary depending upon the conductivities of the earth's crust and its internal structure. These induced currents, in the presence of the earth's magnetic field, in turn generate a time-varying

magnetic field known as the internal (or induced) time-varying magnetic field. Thus the time variations are the resultant of the external and internal time-varying magnetic fields generated by the external and induced current systems respectively.

The above brief discussion about the sources of the time variations clearly demonstrates that, due to the constant interaction between the solar and the terrestrial electromagnetic phenomena, time variations are always present. As a result, whenever we measure the geomagnetic field at or near the earth's surface, we also measure the time variations together with the internal and anomalous field components of the geomagnetic field. During magnetic storms and substorms, the amplitudes of the time-varying magnetic fields can be on the order of hundreds of nT. Even during solar quiet days, when magnetic surveys are normally carried out, time variations of tens of nT are observed. The internal field, being practically a steady-state field for the duration of a magnetic survey, is effectively removed by subtracting a geomagnetic reference field from the survey measurements. The presence of time variations in the magnetic survey measurements distorts and obscures the anomalies due to the anomalous field caused by materials and structures having magnetic

susceptibilities in the outer tens of kilometer of the earth. To extract the true anomalies due to the anomalous field of our interest, we are therefore also required to remove the time variation effects from the geomagnetic field measurements.

To construct an effective procedure for removing the time variations from survey measurements, the next step is to investigate the properties of the time variations, particularly the spatial variation of the time variations . Are they same all over the earth or do they vary from place to place, or even from time to time? If they vary, are there any characteristic trends in the way they vary so that knowing the time variations measured at one place, the time variations observed at a second place could be predicted?

The time variations are caused by the interaction of the solar wind with the earth's magnetic field. The solar wind and its properties are the result of activities in the sun. So, according to the level of activity in the sun, the time variations are divided into three main groups: a) storm-time variations, when there are intense activities in the sun, b) substorm-time variations, when there are moderate activities in the sun, and c) solar quiet daily variations, when there are practically no activities in the

sun - the sun is quiet. Although time variations are a worldwide phenomenon, they are not same all over the world. There are very definite regions of the earth over which the time variations effects are quite different. These regions schematically shown in Figure 2 are the equatorial, mid-latitude, auroral and polar cap zones. The time variations also vary in frequency. Micropulsations occur throughtout a range of freqencies from 0.001 to 1 Hz and mostly take place, with maximum probability and amplitude, in the auroral zones during times when there are severe magnetic and auroral disturbances (McPherron, 1968). Smooth and low-frequency time variations having periods from tens of minute to hours long are predominant in the mid-latitude zones.

Intense magnetic storms usually start suddenly at almost the same instant, within half a minute, all over the earth (Jacobs, 1968). The intensity of magnetic disturbances increases from low to high latitudes up to about magnetic latitude 65°, the latitude of the auroral zones. Within these zones the intensity, although considerable, decreases slightly towards the magnetic poles. The records of individual storm differ greatly among themselves. The time variations due to magnetic storms are generally analysed into three main parts, namely a) a part

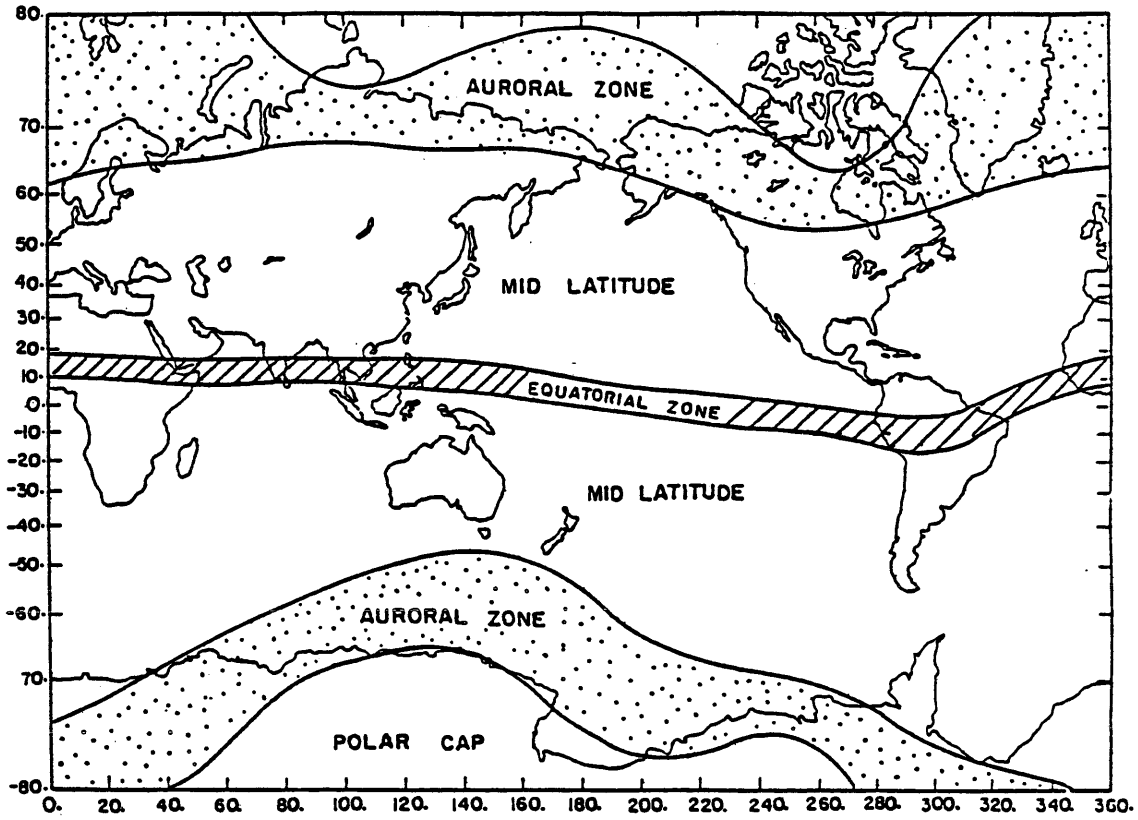

Figure 2. Regions of various observed time variations effects.
(Regan and Rodriguez, 1981)

depending on time measured from the commencement of the storm, which is known as storm-time variations, b) a daily variation in addition to that present on quiet days and much greater in intensity and markedly different in character, known as disturbance daily variations, and c) an irregular part most marked at high latitudes.

At middle and lower latitudes, the storm-time part of the horizontal intensity H of the time variations rises to a maximum within an hour or two of the commencement of the storm and remains above its initial value for a period of 2 to 6 hours. This is called the initial phase. H then decreases, attaining after several hours a minimum which is much more below the initial undisturbed value. This is called the main phase, and is followed by a gradual recovery, called the recovery phase, which may last for several days. The main phase generally lasts from 12 to 14 hours and tends to be noisy. Execpt at high latitudes, the declination D shows little or no storm-time change, while Z, the vertical component of the storm-time variations, shows changes much smaller than those in H. H has the same direction in both northern and southern hemisphere, whereas Z has opposite direction north and south of the magnetic equator. The storm-time variations in H decrease with increasing latitude, being greatest at the equator. In the

auroral zones the storm variations are markedly different form those in lower latitudes and are characterized by extremely large and often rapid changes. Figure 3 shows the striking difference in the storm-time variations at low latitudes (Honolulu) and those in the auroral Zone (College, Alaska). Crossing the auroral zone towards the magnetic pole, the characteristics of storm-time variations undergo a further transition to yet another type peculiar to the polar cap as at Godhaven in Figure 3.

The disturbance daily variations depend on local time but are not constant in intensity; the intensity decreases from the first to the second day of a storm. The disturbance daily variations are very different from the solar quiet daily variations (which we will discuss next) both in times of maximum and minimum and in relation to latitude. Moreover, the disturbance daily variations show no greater change in intensity during the sunlit hours than during the hours of darkness.

In general, the time variations during magnetic storms are very irregular, aperiodic and unpredictable, but the major trends of the time variations measured, at the same time, in Peru (magnetic latitude 0.6°S) and Hawaii (magnetic latitude 21.0°N) in the mid-latitude zones, appear to be very much alike except that the variations

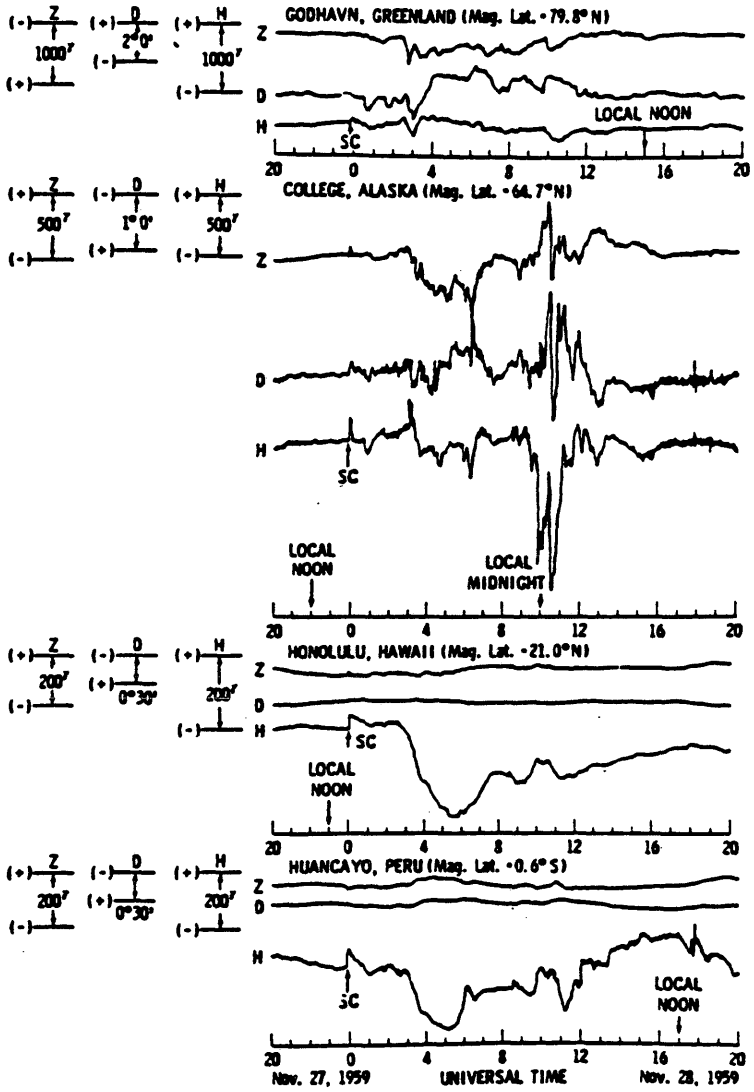

Figure 3. Storm-time variations at different geomagnetic latitudes.

(Jacobs, 1968)

measured in Peru contain more minor fluctuations than those in Hawaii. The variations observed in Peru and Hawaii also differ in amplitude and phase, but the difference in phase is very difficult to see in these plots (Figure 3).

The solar-quiet daily variations are usually known as the Sq variations (Sq stands for solar-quiet). The Sq variations are composed of the external and internal (induced) time-varying magnetic fields mainly caused by the ionospheric current system. The external and the internal time-varying fields reinforce one another so far as their horizontal components are concerned; their vertical components are opposed (Jacobs, 1968). The Sq variations also contains the lunar daily variations which, being very small, are not normally considered.

The Sq variations are functions of latitude and local solar time. The world is divided into three longitudinal zones with respect to geomagnetic (gm) longitude as shown in Figure 4: zone 1, (the Europe-Africa zone between gm 45° E and gm 165° E); zone 2, (the Asia-Australia zone between gm 165° E and gm 285° E); and zone 3, (the north-south America zone between gm 285° E and gm 45° E). Geomagnetically, the year is divided into three seasons: D months (January, February, November and December), E months (March, April, September and October), and J months (May,

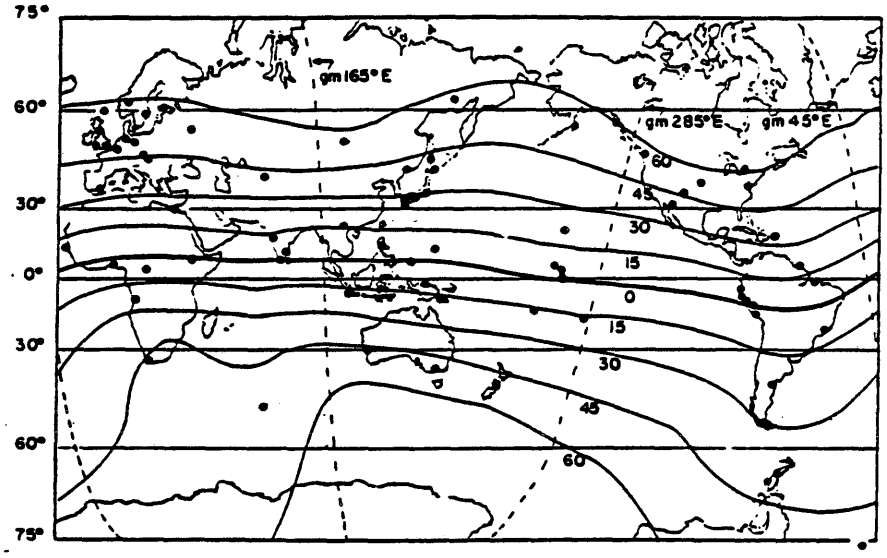

Figure 4. Distribution of 1969 IGY geomagnetic stations used in the Sq variations study, with respect to geographic latitude (ordinate) and dip latitude (solid curves). The three geomagnetic longitudes shown by the broken curves indicate the boundaries of the three longitudinal zones. (Matsushita and Campbell, 1967)

June, July and August). Using the 1969 IGY geomagnetic stations shown in Figure 4, in all the three zones during the three seasons, the Sq variations were studied by Matsushita and Campbell (1967). The worldwide average of the Sq variations for the E months are shown in Figure 5. For stations in the southern latitudes the curves for H are approximately the same as those obtained at stations in the corresponding northern latitudes. The curves for D and Z at the southern latitudes are also same as those at the corresponding northern latitudes, except that they change direction on crossing the equator. At the centre of a narrow belt no more than 2 to 3 degrees of latitude in width, approximately centred on the magnetic equator, the daily range of the horizontal intensity is nearly 3 times as large as the range at points no more than 500 km to the north or south.

From these curves it is not possible to predict a common rate of change of amplitude of the Sq variations at different latitudes; Riddihough (1971) while studying the time variations in Ireland pointed out that the amplitude and range differences of the Sq variations, though geographically distributed, are not simply related to distance - their pattern is likely to be permanent and determinable and is probably related to geology and

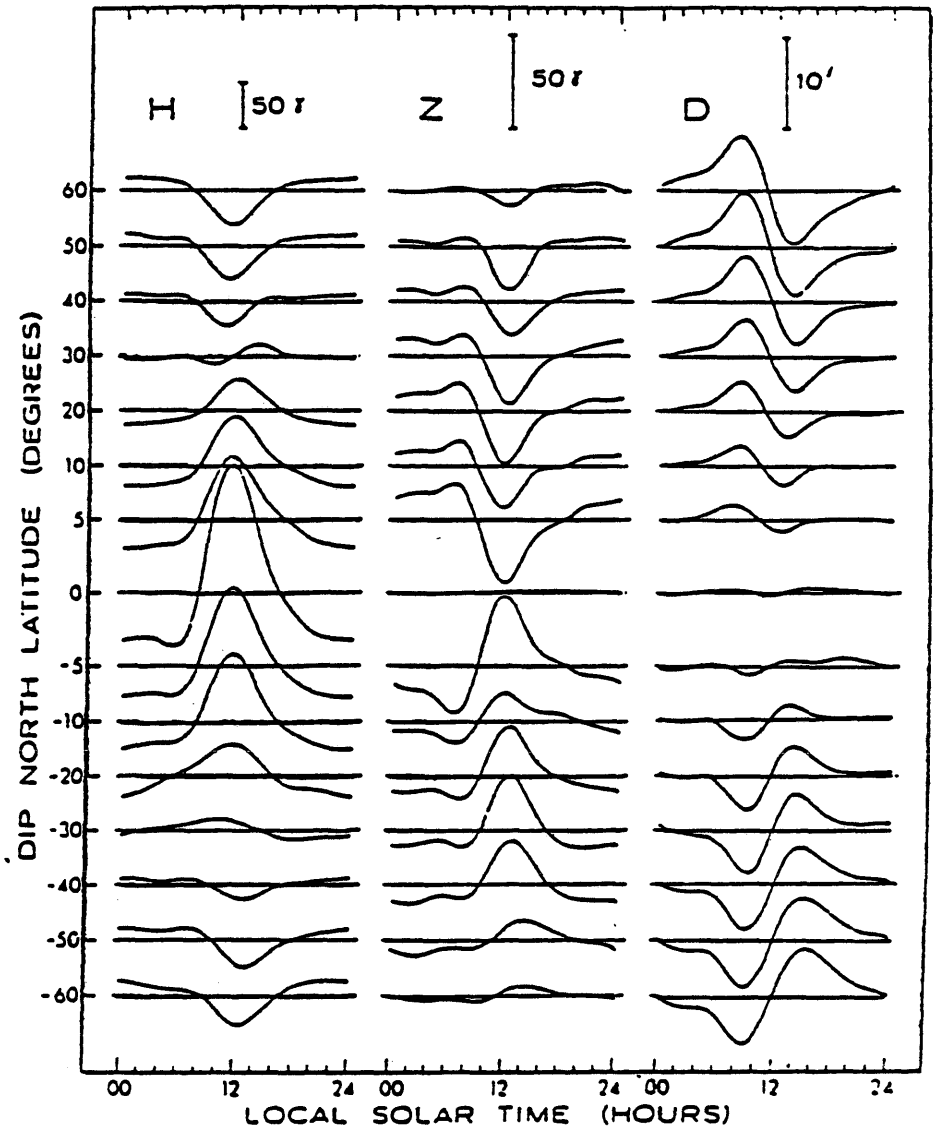

Figure 5. Worldwide average of the solar quiet daily variations for the months of March, April, September and October, 1958.
(Regan and Rodriguez, 1981)

structural features on a large scale. However, if we consider two adjacent curves, separated by 10 degrees of latitude, we can fairly accurately estimate the rate. For example, the rate of decrease in amplitude is 2 nT per degree latitude from the H-curve at 10° latitdue to the H-curve at 20° latitude. A separation of 10 degrees of latitude is approximately equal to 1150 km. Except in rare oceanic and airborne operations, the base and field stations are not set at such a huge separation from one another. So, for most surveys, knowing how far apart are the base and field stations in latitude, we can make an estimate of the difference in amplitude between the Sq variations measured at those two stations. On the other hand, if two stations lie along a common latitude, we do not expect to find any considerable change in amplitude between the Sq variations measured at these two stations. However, since the Sq variations are also functions of the solar local time, we expect to find a difference in phase between the Sq variations at two stations, if the stations are situated along a common latitude. The earth completes one revolution in 24 hours by rotating from west to east; so, the Sq variations measured at two stations separated by a distance of 1 degree of longitude will show a phase difference equivalent to 4 minutes of time difference.

Thus, knowing the difference between the local solar times at two different stations where the Sq variations are measured, we can estimate the phase shift between the two measurements. In general the Sq variations are smooth, periodic (1/24 cph = cycle per hour) and predictable. For example, the H-amplitude at 5° and 20° latitudes has the same shape, differing only in amplitude and phase (the phase difference depending on the difference of solar local times at these two stations).

The Sq variations are larger and more rapid during the hours of daylight than of darkness. There is also a seasonal effect; the amplitudes of the Sq variations are greater at stations more exposed to the sun. The amplitudes of the Sq variations are also some 50 to 100 percent greater in years of sunspot maximum than in years of sunspot minimum (Jacobs, 1968). Vestine and others (1947) also reported on the average behavior of all types of time variations at different latitudes and locations throughout the earth at differnt times of the year.

The worldwide average studies on the time variations indicate some characteristic properties of these variations. However, before making any general statements about the properties of the time variations which could be utilized in designing a technique for removing these

variations from the magnetic measurements, it is important that we also study the nature of the time variations over more localized areas comparable to areas normally covered during magnetic surveys.

Schmucker (1970) reported on studies of the time variations in the southwestern United States. Figure 6 shows the sequence of storm-time variations recorded at the IGY stations in the midwestern United states. The reduction of Z-amplitude between Burlington in the great plains and Leadville in the Rocky Mountains suggests high internal conductivities beneath the Rockies. The general increase of the H-amplitude towards north reflects the increasing closeness of the auroral zone. All the H curves are almost alike; although highly irregular and aperiodic, these curves have the same trend of variations. The H-fields measured at Espanola and Casper, separated by a distance of about 800 km, are practically identical except for having differences in amplitude and, in this case (since the stations lie approximately on the same longitude), a possible small phase shift which is very difficult to see from these curves. If we keep in mind the difference in internal conductivities at the different stations, the Z curves also appear to be alike. Figure 7 shows fast fluctuations (about 60 cph) along two profiles

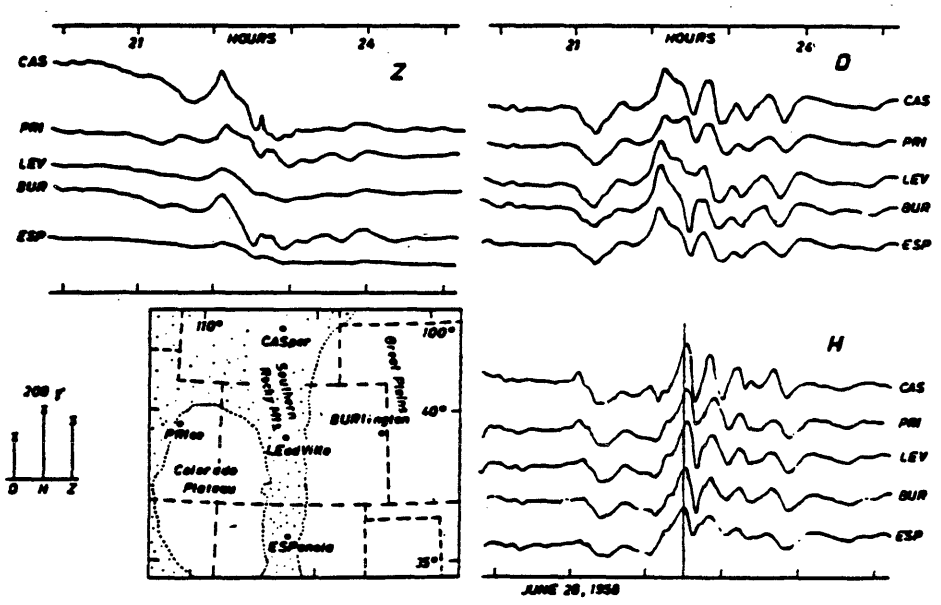

Figure 6. Sequence of storm-time variations recorded at IGY stations in the mid-western United States. (Schmucker, 1970)

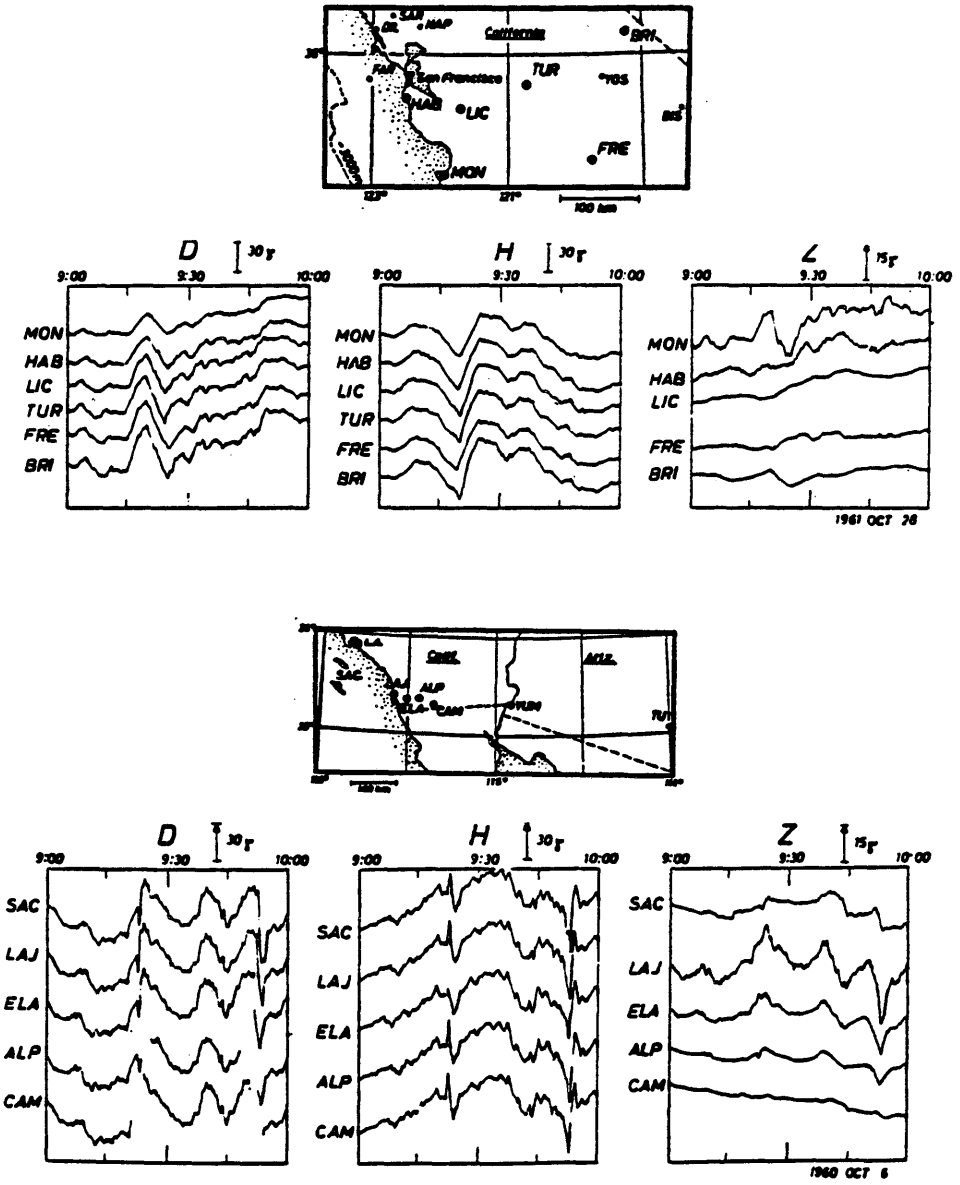

Figure 7. Flast fluctuations along two profiles (Monterey-Bridgeport and San Clemente Island - Cameron) through central and southern California. (Schmucker, 1970)

(Monterey-Bridgeport and San Clemente Island-Cameron) through central and southern California. The H curves, in either of the profiles, are similar in shape among themselves. The strong Z-fluctuation along both the profiles disappears at the coast towards inland because of the decrease of internal conductivity toward inland. Figure 8 shows two bays (magnetic substorms) as recorded on the profile Farallon Islands - Fallon, Nevada. In each bay record, the H curves have the same shape except for having, in these examples, small differences in amplitude and phase; the H curves in each bay record are almost identical. The Farallon Islands and Fallon are about 400 km apart, yet the H-amplitdue measured at these two stations have the same shape, differing only in amplitude and phase. The change in amplitude from off-shore stations to inland stations is clearly visible in the Z curves. The reversal of Z-amplitude between Carson City and Fallon is due to the change in internal conductivities between these two stations.

Figure 9 shows the Sq variations measured near the coast of California. In contrast to storm-time and substorm-time variations and fast fluctuations, the Sq variations are very smooth and periodic (1/24 cph). The Z-amplitude is nearly doubled at the California coast

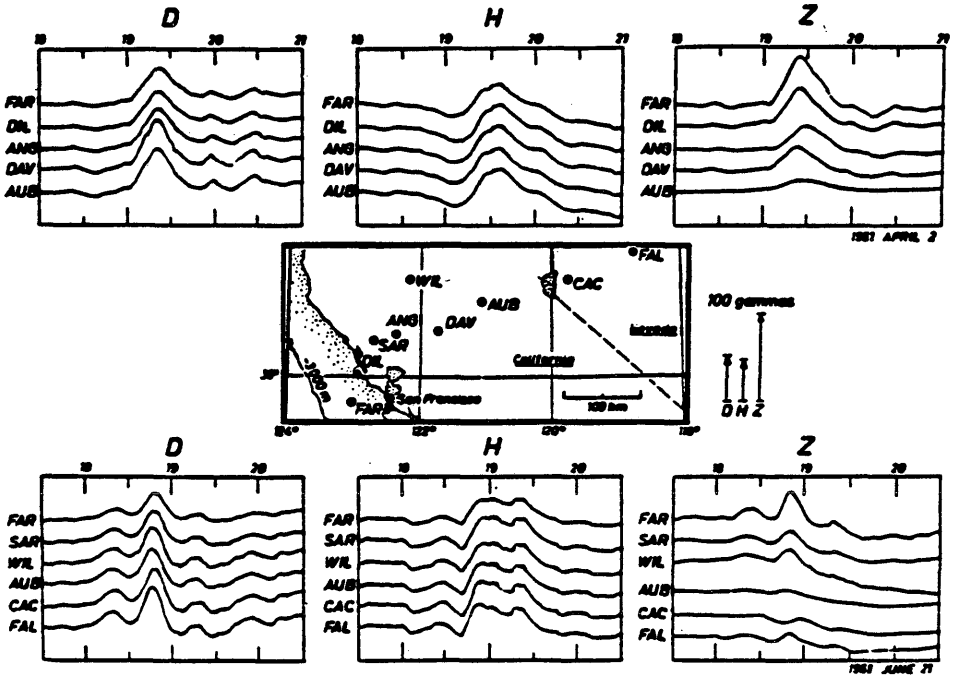

Figure 8. Two bays (sub-storm variations) as recorded on the profile Farallon Islands - Fallon, Nevada. (Schmucker, 1970)

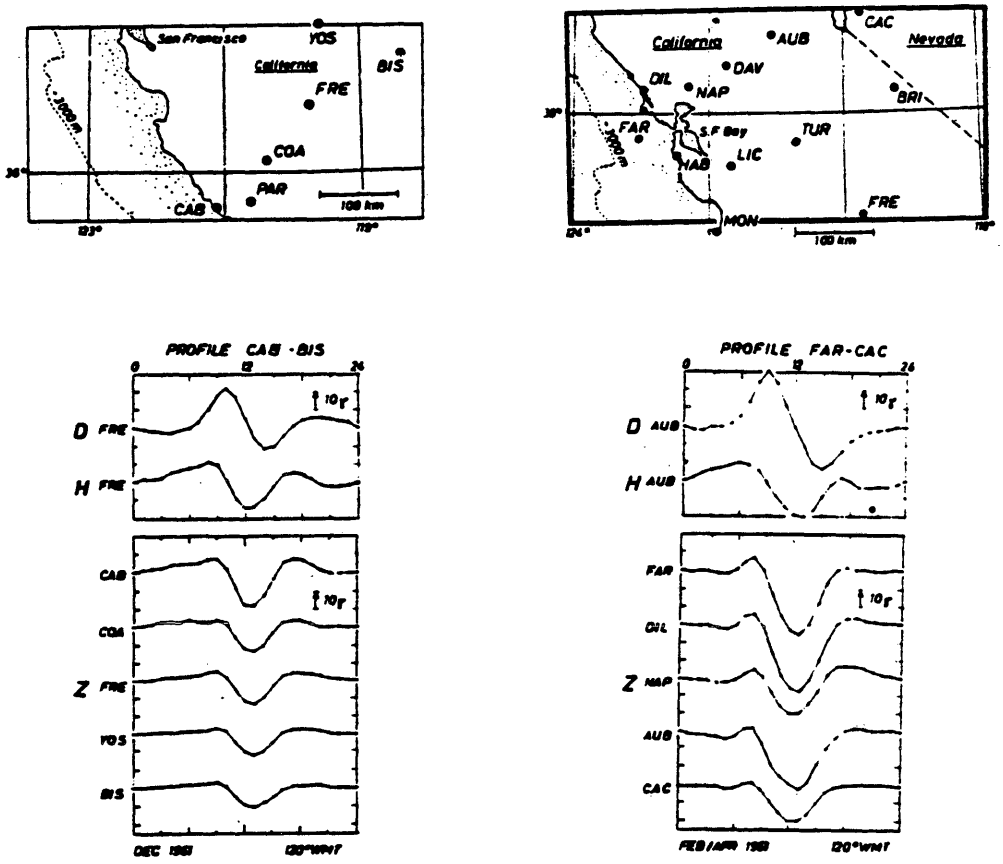

Figure 9. The Sq variations measured along two profiles (Cambria - Bishop and Farallon Islands - Carson City) near the coast of California. (Schmucker, 1970)

relative to inland, (this is known as the coastal effect), while the H-amplitudes hardly vary along the two profiles shown. The Z curves are all similar in shape, differing only in amplitude and phase.

Lilley (1982) reported on the time variations observed in western Queensland and south-east Australia. Figure 10 shows the time variations observed in western Queensland during magnetic substorms (bays). Along the profile D1-D14, a distance of about 600 km, the total field (F) variations measured at these fourteen stations are practically identical in shape except for differences in amplitude and phase. The phase shift between the two most widely separated stations, D1 and D14, is equivalent to about a time difference of 11 minutes which is, however, very difficult to see in the plots of these magnetograms. Among stations E1 to E7, we also observe the same trend of variations. Similar trends of variations are also observed in all the Z curves; the Z curves are much reduced in amplitude compared to the corresponding F curves. The reversal of anomalies in the Z curves at stations E3 and E4 is due to the difference in internal conductivities at the two stations.

Figure 11 shows the Sq variations observed in south-east Australia. The Sq variations of the total field

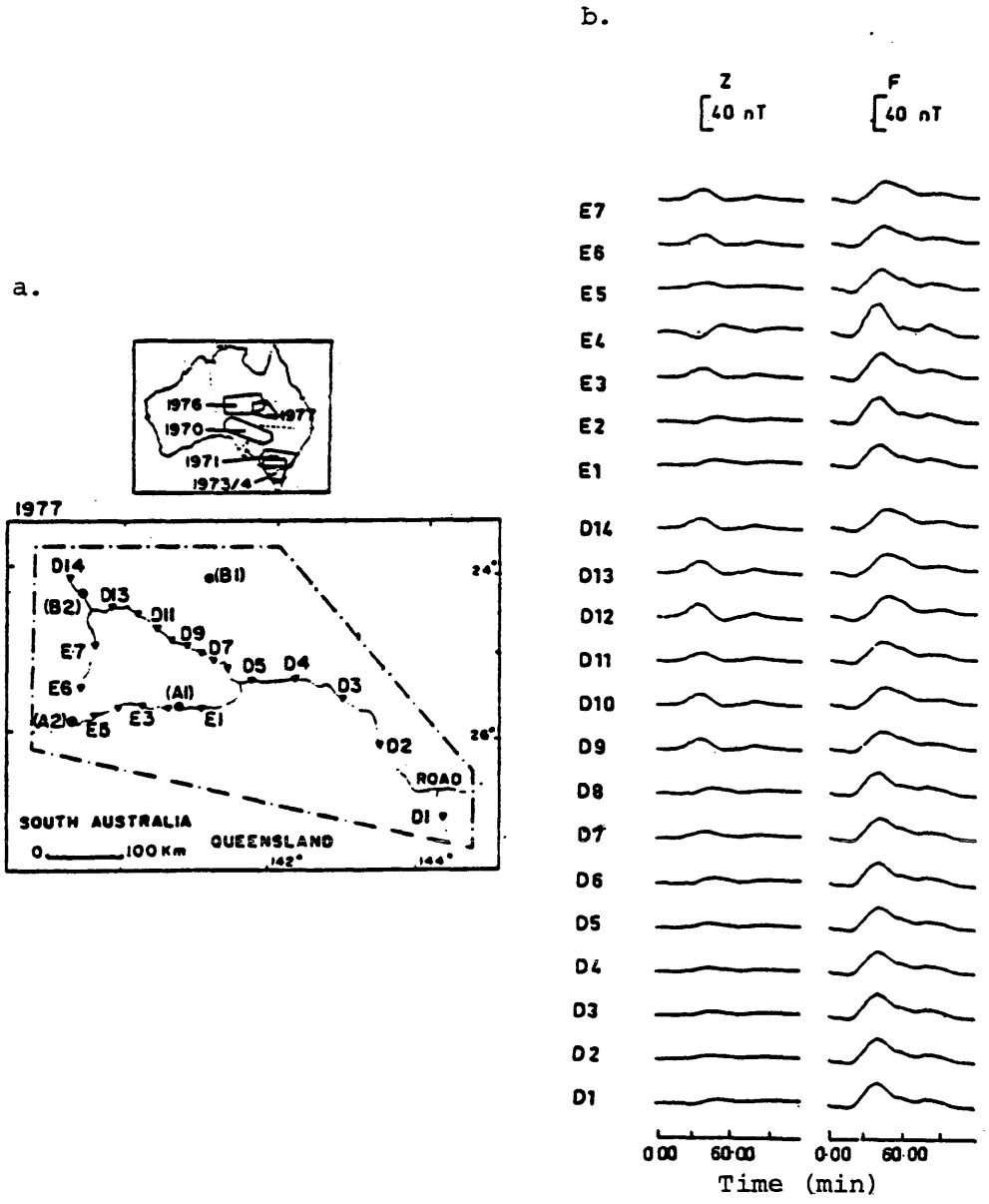

Figure 10. a. Sites of the 1977 magnetometer array study in western Queensland.
b. Records of a magnetic substorm (bay) observed at the sites of the 1977 array.
(Lilley, 1982)

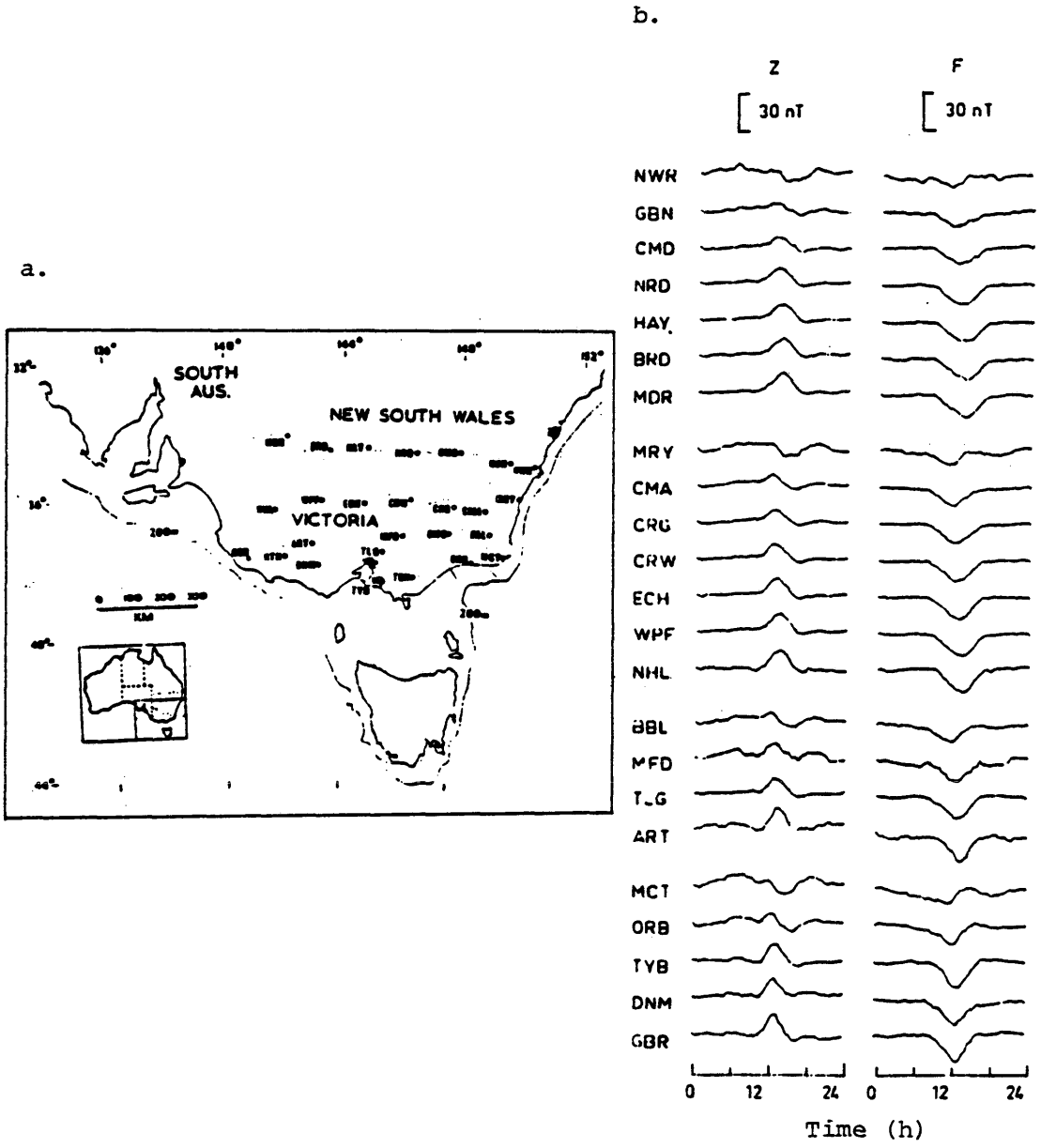

Figure 11. a. Sites of the 1971 magnetometer array study in south-east Australia.
b. The Sq variations recorded at the sites of 1971 array.
(Lilley, 1982)

F and the Z component, show similar trends of variations at all observation points, exept that the reversal of anomalies between the stations at ART and MCT is attributed to a difference in internal conductivity at these two stations. Diminution of amplitude at the coast towards inland (profile NWR-MDR) is also noticed here. Hill and Mason (1962) also reported the same effect: that the Sq variations at sea are greater in range than those on shore.

Riddihough (1971) studied the Sq variations in Ireland. The Sq variations observed at the Valentine Observatory were compared with those measured at a series of stations in Ireland. In Ireland too, it was observed that the Sq variations measured at different stations and at Valentine were identical in shape except for differences in amplitude and phase. The same coastal effect and distortion of shape of variations between two stations due to the difference in internal conductivities at the two stations were also observed in Ireland.

Morley (1953) reported on the time variations in the auroral regions. Even during magnetic quiet days, there are always some disturbances in the auroral and polar cap regions. The time variations in these regions have no characteristic shape; the trend of anomalies in the time variations varies from time to time. Figures 12 and 13 show

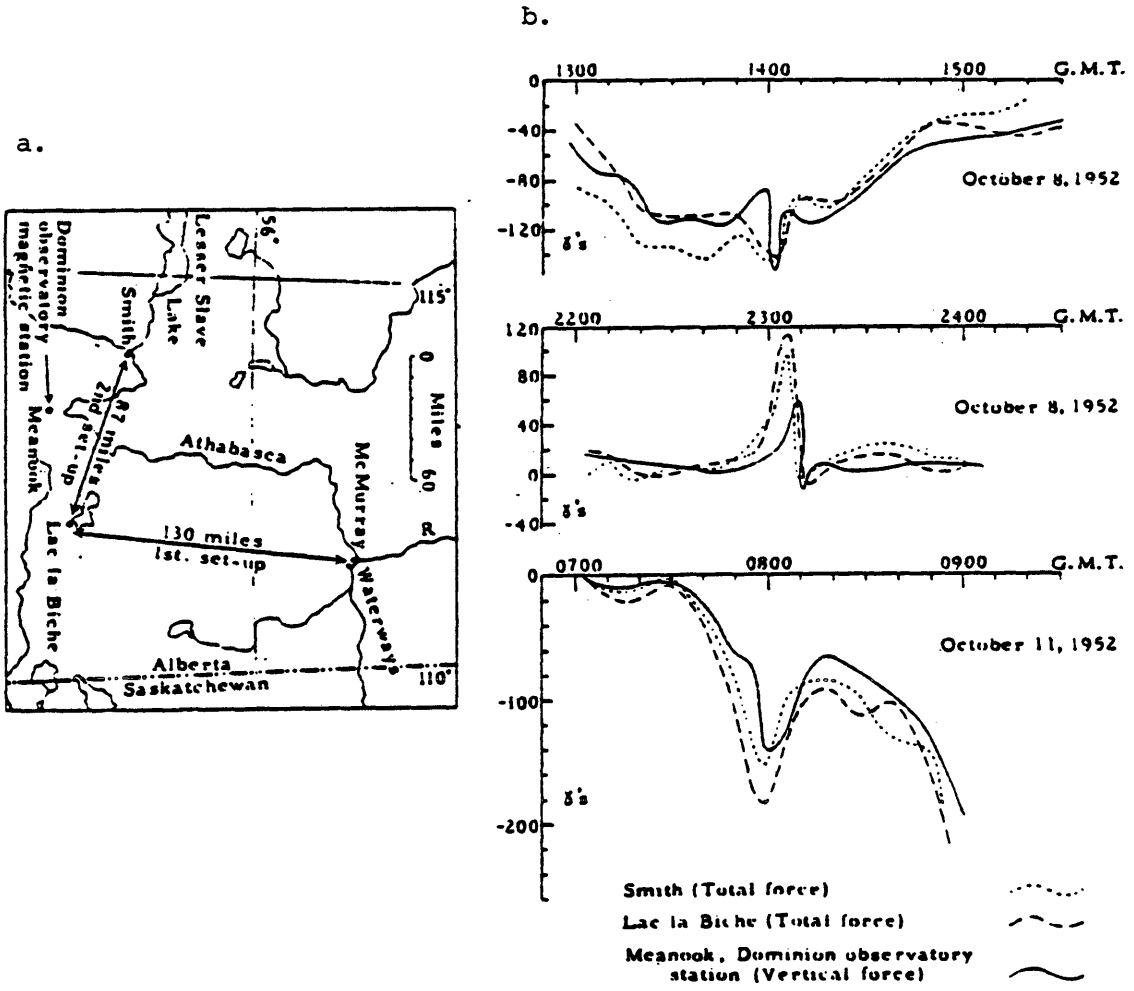

Figure 12. a. Sketch map showing locations of observation points.
b. Comparison of time variations measured at Smith, Lac la Biche and Meanook. (Morley, 1953)

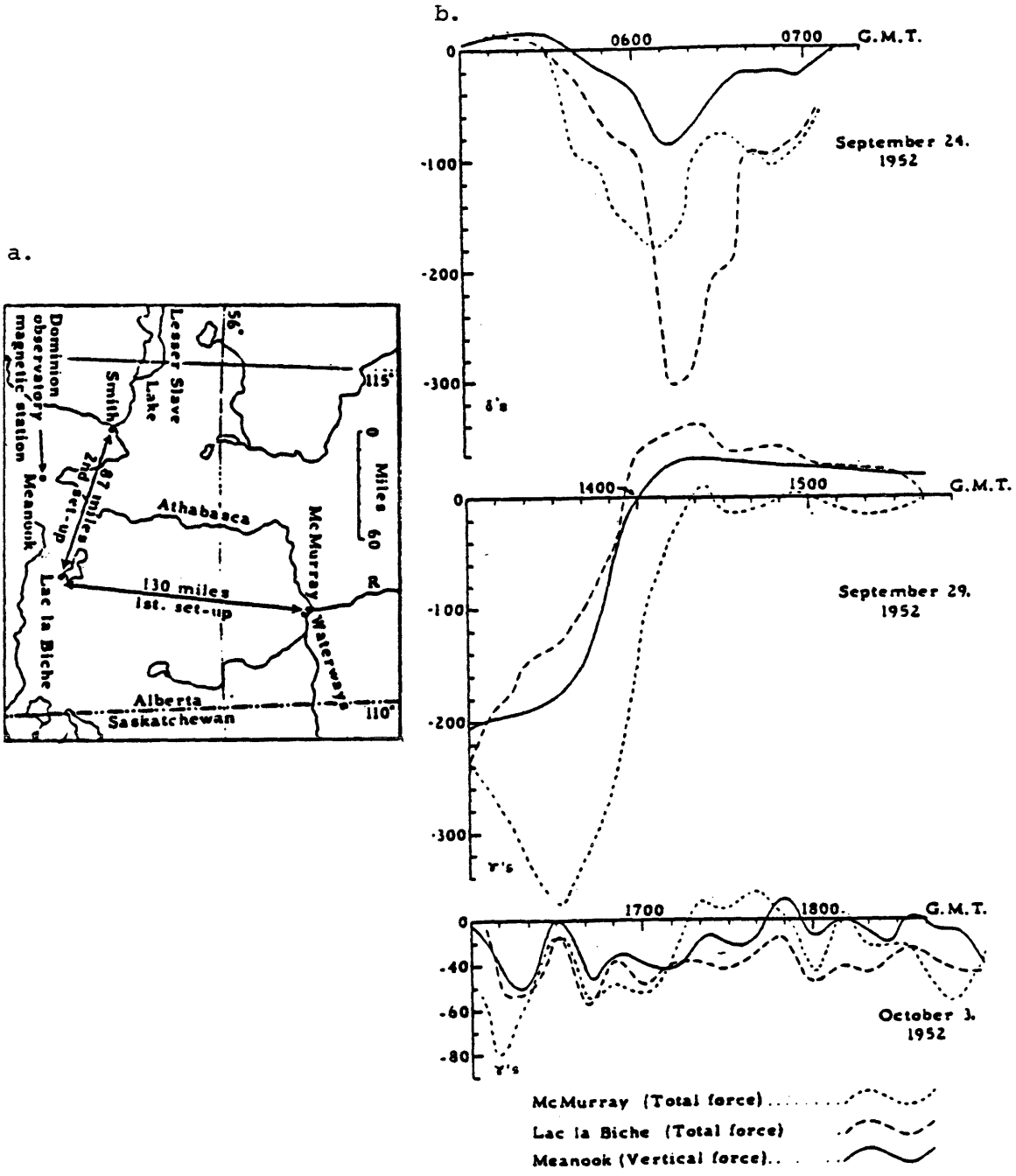

Figure 13. a. Sketch map showing locations of observation points.
b. Comparison of time variations observed at McMurray, Lac la Biche and Meanook. (Morley, 1953)

time variations in the auroral zone. Micropulsations are more frequent in these regions, and examples of micropulsations are shown in Figure 14. The time variations were measured at the stations at Smith, Lac la Biche and McMurray and then compared with the time variations observed at Dominion Observatory at Meanook (locations of these stations are shown in the sketch map in Figure 12). The distance between the Smith and Lac la Biche is 87 miles (140 km) and between Lac la Biche and McMurray 130 miles (209 km). The amplitude and phase of the time variations observed simultaneously at these stations at such separations are expected to be nearly identical, but this is not the case. However, the general shapes of the corresponding curves are similar. It is found that when conditions are disturbed at one location, they are also disturbed at other location. Similarly, quiet conditions at one station correspond to quiet conditions at other station. The agreement between the curves from Lac la Biche and Smith in the east-west direction (Figure 12) is better than those of McMurray and Lac la Biche in the north-south direction (Figure 13). It is not known whether this is due to the greater distance between the two latter stations or the fact that they are in a north-south line rather than an east-west line. A clear-cut phase reversal

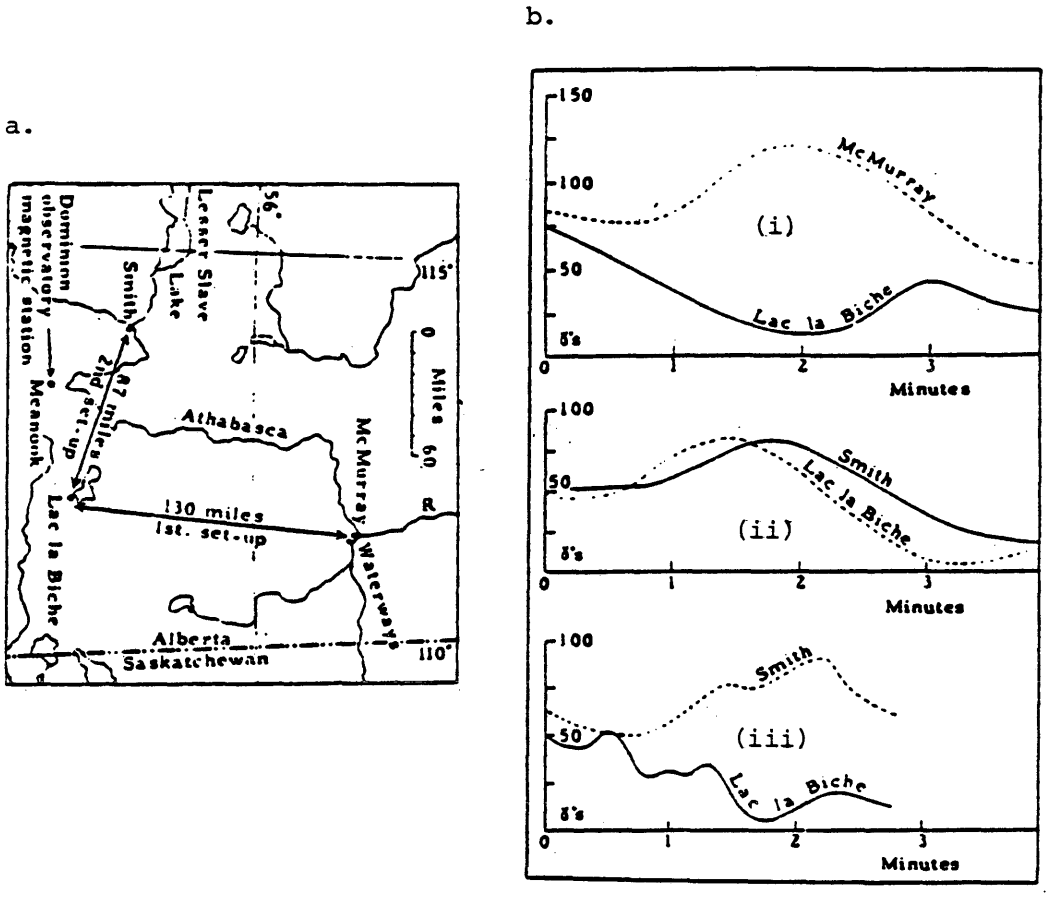

Figure 14. a. Sketch map showing locations of observation points.
b. Records of micropulsations showing
(i) Phase reversal,
(ii) Phase displacement, and
(iii) Different Character.
(Morley, 1953)

of the micropulsations exists between the McMurray and Lac la Biche stations, but no such reversal is seen in the Lac la Biche and Smith stations, as shown in Figure 14. The bottom curves in Figure 14 show that some minor pulsations appearing in one trace are absent on the other.

The different types of time variations, such as the Sq variations, storm variations, micropulsations etc. propagate with different velocities and they differ greatly in intensity and frequency content. So, in general, the time variations are frequency-dependent; and as a consequence, the differences in amplitude and phase between the time variations measured at two different places are also frequency-dependent (Lilley, 1981). However, if measurements are made during solar quiet days, the differences in amplitude and phase between the time variations at two different places may be considered to be independent of frequency, because the Sq variations are practically functions only of solar local time and latitude (difference in solar local times at two places causes the phase shift, and difference in latitudes of the two places causes the difference in amplitude).

On the basis of our above studies on time variations, we note the following characteristic properties of these variations:

1. The Sq variations observed at two different places, at a separation of hundreds of kilometers over wide areas of the earth in the mid-latitude zones, are practically similar in shape. The Sq variations depend on latitude and solar local time. Thus, the variations measured at two different places in the mid-latitude zones mainly differ in amplitude and phase depending on the locations of the places and these differences in amplitude and phase are fairly predictable. The Sq variations are smooth and periodic (1/24 cph).

2. The time variations observed, even during magnetic storms and substorms, at two different places hundreds of kilometer apart in the mid-latitude zones, are also practically similar in shape, although these storm-time and substorm-time variations are highly irregular and aperiodic. Unlike the Sq variations, these variations measured at the same place during two different storms may differ greatly. Further, the differences in amplitude and phase of these variations at two different places are not predictable.

3. In the equatorial, auroral and polar cap zones, where magnetic disturbances of some kind are always present, the observed time variations at two different places are also nearly similar in shape, but they differ

greatly in amplitude and phase even when the stations are only 100 km apart. The time variations in these regions also differ greatly at two different times. Micropulsations are most common in these regions, and the pulsations in the time variations measured at two different places may be completely out of phase and different in character.

4. The presence of materials and structures having different conductivities at two places greatly influences the shape of the time variations measured at these places; in some cases, the time variations at two such places may be completely different in shape. The enhancement of amplitude of the time variations at sea and decrease at the coast towards inland due to the differences in conductivity of the sea water and the inland geology is a common observation throughout the earth.

5. The differences in amplitude and phase between the time variations measured at two different places are in general frequency-dependent. However, during solar quiet days when magnetic surveys are normally conducted, this effect is practically insignificant.

In consideration of the above properties of the time variations, the limitations of the standard method (explained in the Introduction) for correcting time variations in magnetic data become more obvious. Further,

taking into account these properties, the development of a more effective method can be visualized. This method is discussed in the next chapter.

Chapter 3

THE NEW FILTERING TECHNIQUE

The standard method (as explained in the Introduction) for correcting time variations in magnetic data is based on the assumption that the time variations measured at the base station and those encountered at the field stations are exactly identical. For local land-based surveys, when the base and field stations are not far apart, this assumption is practically true and this method of correcting the time variations works well for such surveys. However, we have observed in Chapter 2 that, as the distance between the base and field stations increases, the time variations measured at the base and field stations also differ more and more in amplitude and phase, although the shapes of the time variations remain practically the same. So, the standard method for correcting time variations in magnetic data no longer remains valid and becomes completely impractical for oceanic and large-scale airborne operations. Therefore, for oceanic and large-scale airborne operations, we require a more general technique to remove the time variations from the field data. If this technique is to be based on the base and field data only (i.e., the base and field data are assumed to contain

all the necessary information about the time variations measured at the base and field stations), then, in consideration of the properties of the time variations, the technique is also required to be capable of taking into account the differences in amplitude and phase, if any, between the time variations measured at the base stations and those encountered at the field stations.

Dr. R. O. Hansen at the Colorado School of Mines has formulated a new filtering technique for correcting time variations in magnetic data. The new filtering technique is based on the base and field data only, and the technique is also capable of taking into account the differences in amplitude and phase between the time variations measured at the base station and those encountered at the field stations. The mathematical formulation and implementation of the proposed new filtering technique are described below.

Mathematical Formulation

During a magnetic survey, we measure the geomagnetic field at the field stations (o, field data) and the geomagnetic field at the base station (b, base data). Since the internal field component of the geomagnetic field is practically a steady-state field for the duration of a

magnetic survey, the field data are considered to be the sum of the field due to the geology (g) and the time variations (t).

Mathematically,

$$o = g + t \ . \qquad (1)$$

At the base station, the field due to the geology is also constant, and therefore the anomalies in the base data are due to the time variations only.

We measure o, but we are interested in g. We can obtain g from o by removing the time variations t from it.

Now, we assume that the base and field data are random processes. We also assume that the statistics of these processes are independent of time origin. These are fairly reasonable assumptions. On the basis of these assumptions about the base and field data (more explicitly, about the field due to the geology and the time variations), we define a filter α for the base data b such that

$$\langle |T - \alpha B|^2 \rangle = \text{minimum} \ , \qquad (2)$$

where T and B correspond to frequency-domain representations of the time variations t and the base data b. The symbol $\langle \ \rangle$ stands for ensemble expectation values.

Differentiating equation (2) with respect to α^* (complex conjugate of α), we get

$$\frac{\partial}{\partial \alpha^*} < |T - \alpha B|^2 > = 0$$

$$\frac{\partial}{\partial \alpha^*} < (T - \alpha B) (T^* - \alpha^* B^*) > = 0$$

$$< (T - \alpha B) B^* > = 0$$

$$< TB^* > - \alpha < BB^* > = 0$$

$$\alpha = \frac{< TB^* >}{< BB^* >} \cdot \qquad (3)$$

Equation (3) defines α, but we can not use this equation to calculate α because it involves T, which is unknown. To get rid off this difficulty, we write from equation (1)

$$O = G + T$$

correlate O with B^*, and get

$$< OB^* > = < GB^* > + < TB^* > \cdot$$

Now, we assume that the field due to the geology g and the base data (the time variations) b are uncorrelated (which is also a reasonable assumption), that is $<GB^*> = 0$.

So, we have

$$< TB^* > = < OB^* > \cdot \qquad (4)$$

From equations (3) and (4) we find

$$\alpha = \frac{\langle OB^* \rangle}{\langle BB^* \rangle} \cdot \qquad (5)$$

Equation (5) can now be used to solve for α , because it involves only the field and base data that we collect directly during surveying.

Calculating the filter α (which we call the Base filter) according to the equation (5) and then applying the filter to the base data b, we calculate $\hat{g}$ (an estimate of the field due to the geology g) in the following way: We have

$$\hat{G} = O - \alpha B \cdot \qquad (6)$$

Taking the inverse Fourier transform of equation (6), we get

$$\hat{g} = FT^{-1}\{ \hat{G} \}$$

$$= FT^{-1}\{ O - \alpha B \} \cdot \qquad (7)$$

In this mathematical formulation of the new filtering technique, we are mainly concerned with the equations (5) and (7): the filter α is calculated, according to the equation (5), from the estimates of the auto power spectrum $\langle B\overset{*}{B} \rangle$ of the base data and the cross power spectrum $\langle O\overset{*}{B} \rangle$ of the field and base data; then applying the filter α to

the base data, according to the equation (7), the time variations are removed from the field data.

The standard method for correcting time variations in magnetic data is based on the assumption that the time variations measured at the base station and those encountered at the field stations are exactly identical in shape, with no differences either in amplitude or in phase. Considering such exactly identical time variations in both the base and field data, it can be shown (using the identity $|F(w)| = |f(t)|$ and the assumption that the time variations and the field due to the geology are uncorrelated) that the filter α , calculated according to the equation (5), is equal to unity. Now applying this filter (whose response is unity) to the base data, according to the equation (7), we subtract the base data completely from the field data; that is, since the anomalies in the base data are due to the time variations only, we completely remove the time variations from the field data. Thus, in this case, the new filtering technique reduces to the standard method.

However, the new filtering technique can deal with much more general situations. Although identical in shape, the time variations in the base and field data may differ in amplitude and phase. In this situation, the new

filtering technique is also capable of removing the errors introduced by the differences in amplitude and phase, if any, between the time variations in the base and field data.

For example, if the amplitude of the time variations measured at the base station is twice the amplitude of the time variations encountered at the field stations, then, according to the equation (7), we need a filter α = 0.5 to correctly remove the time variations from the field data. In such a case, again starting with the identity $|F(w)| = |f(t)|$ and the assumption that the time variations and the field due to the geology are uncorrelated, it can be shown that, if we calculate $\langle OB^* \rangle$ and $\langle BB^* \rangle$ and then take their ratio to calculate the filter according to the equation (5), we in fact get the required filter α = 0.5.

To determine the filter α using equation (5) we need to calculate $\langle BB^* \rangle$ and $\langle OB^* \rangle$, where BB^* is the auto power spectrum of the base data, and OB^* is the cross power spectrum of the field and base data. We can use the cross phase spectrum of the field data o and the base data b to estimate the phase shift between the time variations measured at the base station and those encountered at the field stations. Since the anomalies in the base data are due to the time variations only, the anomalies in any

portion of the field data having the same trend of anomalies as we see in the corresponding portion of the base data are also considered to be due to the time variations only. So, in practice, from the cross phase spectrum of a portion of the field data and the corresponding portion of the base data having similar trends of anomalies we will be able to estimate the phase shift between the time variations observed at the base station and those encountered at the field stations.

The differences in amplitude and phase may also be frequency-dependent. The new filtering technique is capable of taking into account this property of the time variations. In practice, we have difficulty in estimating more than one phase shift between the time variations in the base and field data. We also have difficulty in estimating more than one common difference in amplitude. Fortunately, dependence of the differences in amplitude and phase on frequency is not a serious problem if surveys are conducted during solar quiet days because, during solar quiet days, the time variations at two places differ by practically a single phase shift depending on the difference of the solar local times at the two places, and the difference in amplitude by a common factor depending on the locations (latitudes) of the two places. However, if we

could estimate the differences in amplitude and phase at different frequencies and then incorporate these differences in the calculation of the filter α , then the new filtering technique would be more versatile and more generally applicable.

Implementation

To calculate the filter α from the equation (5), we are required to find $\langle OB^* \rangle$, the expectation value of OB^* ,and $\langle BB^* \rangle$, the expectation value of BB^*. During a magnetic survey, we collect a single set of each of the base and field data, and from these two single sets of data we cannot find the above expectation values unless we are able to make some more assumptions about the base and field data. We have already assumed that the base and field data are stationary random processes. Now, we further assume that these processes are ergodic; that is, that the statistics of these random processes are determinable from a sample function (a time series) of each of these processes. All these assumptions are fairly reasonable for both the base and field data collected during a magnetic survey. So, our calculations of OB^* and BB^* from a sample function of each of the base and field data, in practice, represent reasonable estimates of the required expectation

values of OB^* and BB^*.

The cross power spectrum OB^* and the auto power spectrum BB^* are statistical estimates. The point is that the FFT estimates are high-variance estimates, containing structure which does not reflect the ensemble average (Jenkins, 1961). So, we approximate these spectra by straight-line segments as shown in Figures 15 and 16 (spectra are calculated from a portion of the base and field data collected during magnetic gradiometer survey; Hansen and Childs, 1987), and thereby we adopt a model for the spectra based on general information about the time varaition spectra. The spectra are displayed by plotting the natural logarithm of power against frequency. Such a semi-log plot of the power spectrum is convenient because the amplitude of the spectrum at low frequencies is very large compared to its high-frequency amplitude. Further, exponential behavior of the power spectra at low frequencies is an observed fact as can be seen from the power spectrum in Figure 17, which is calculated from the portion of a typical spectrum of amplitudes of electromagnetic noise (time variations) with frequencies below 1 Hz as shown in Figure 18 (keller and Frischknect, 1966). In magnetic surveys, we are not normally concerned with the time variations having frequencies greater than 1

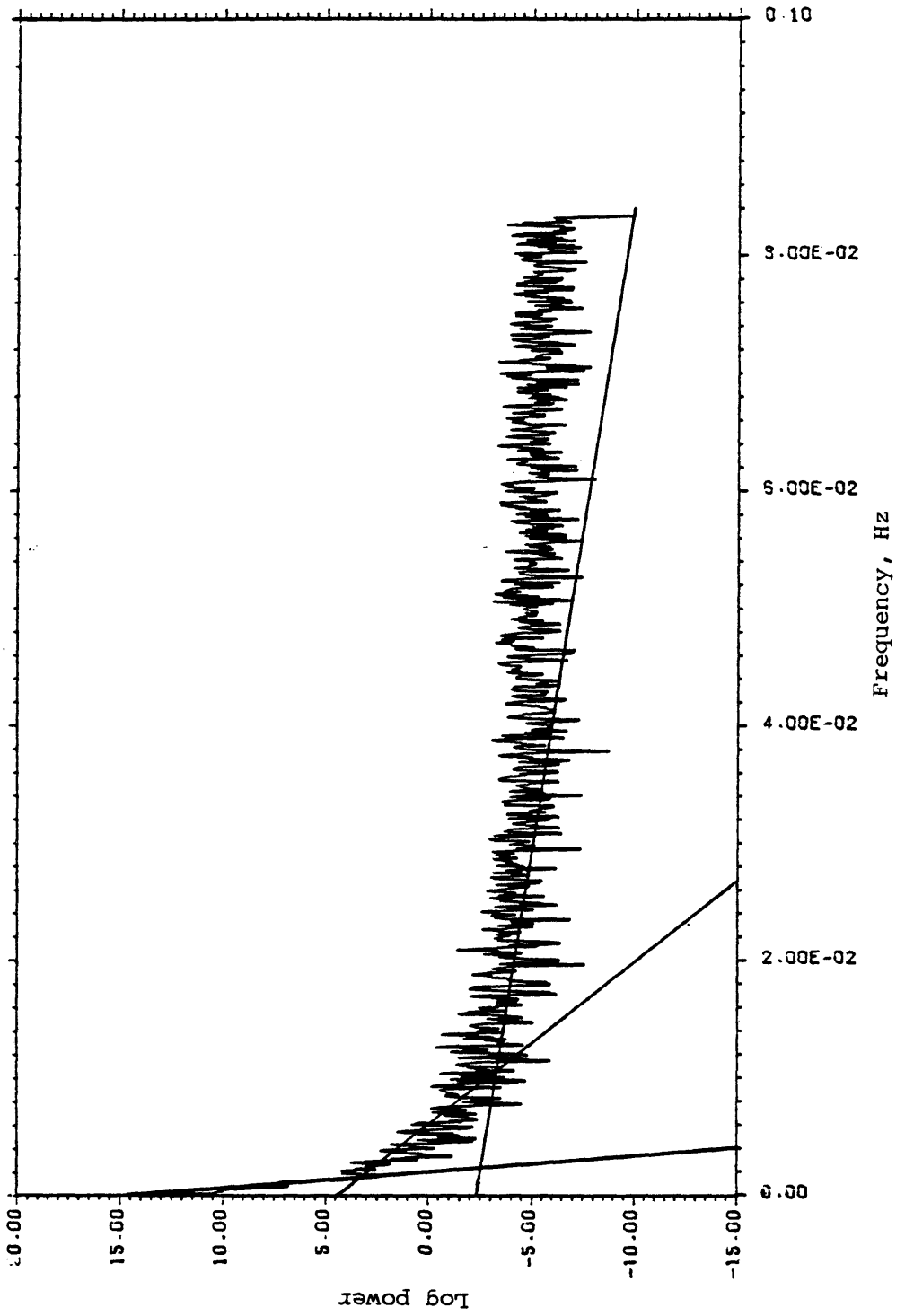

Figure 15. Cross power spectrum of the field and base data.

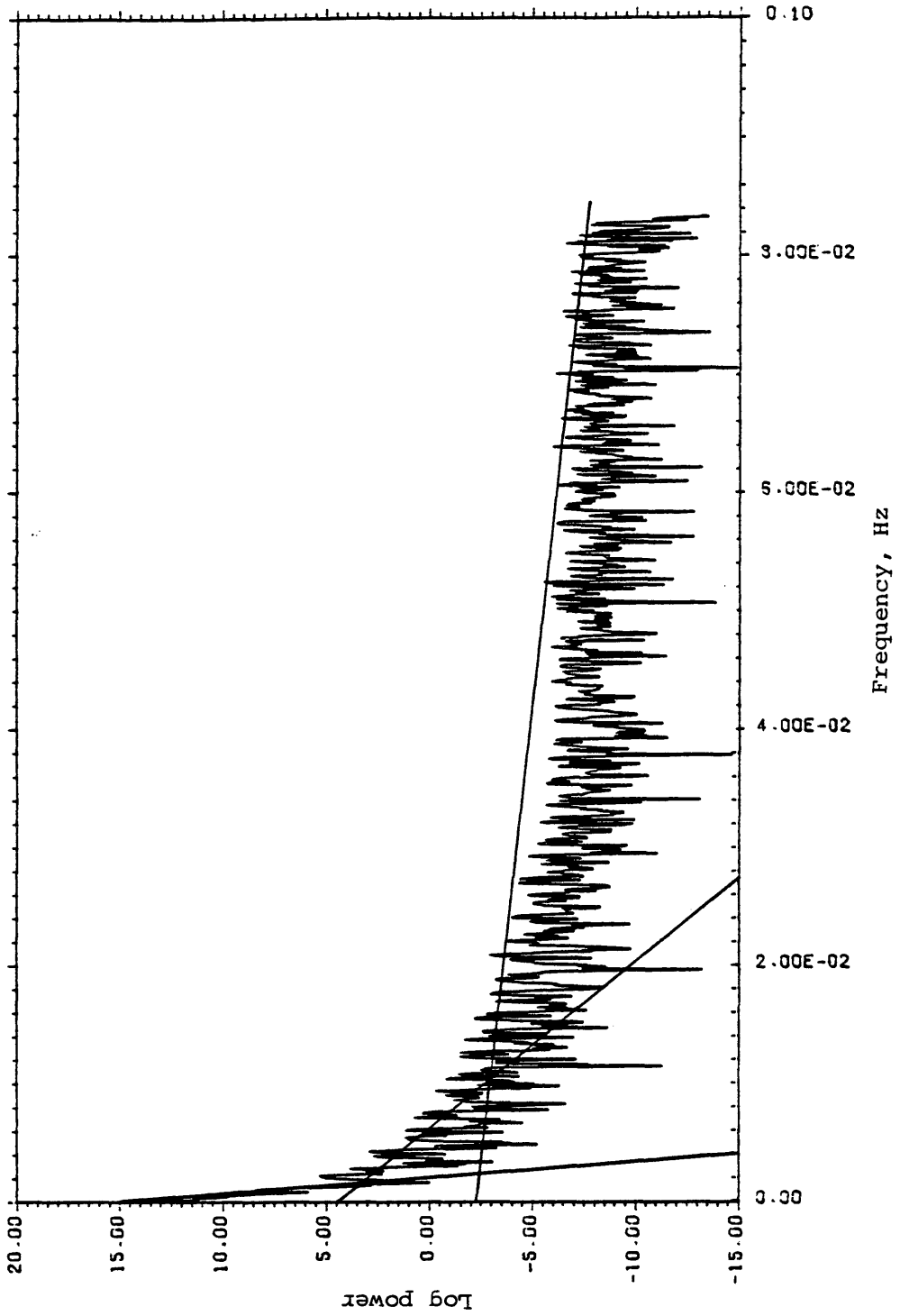

Figure 16. Auto power spectrum of the base data.

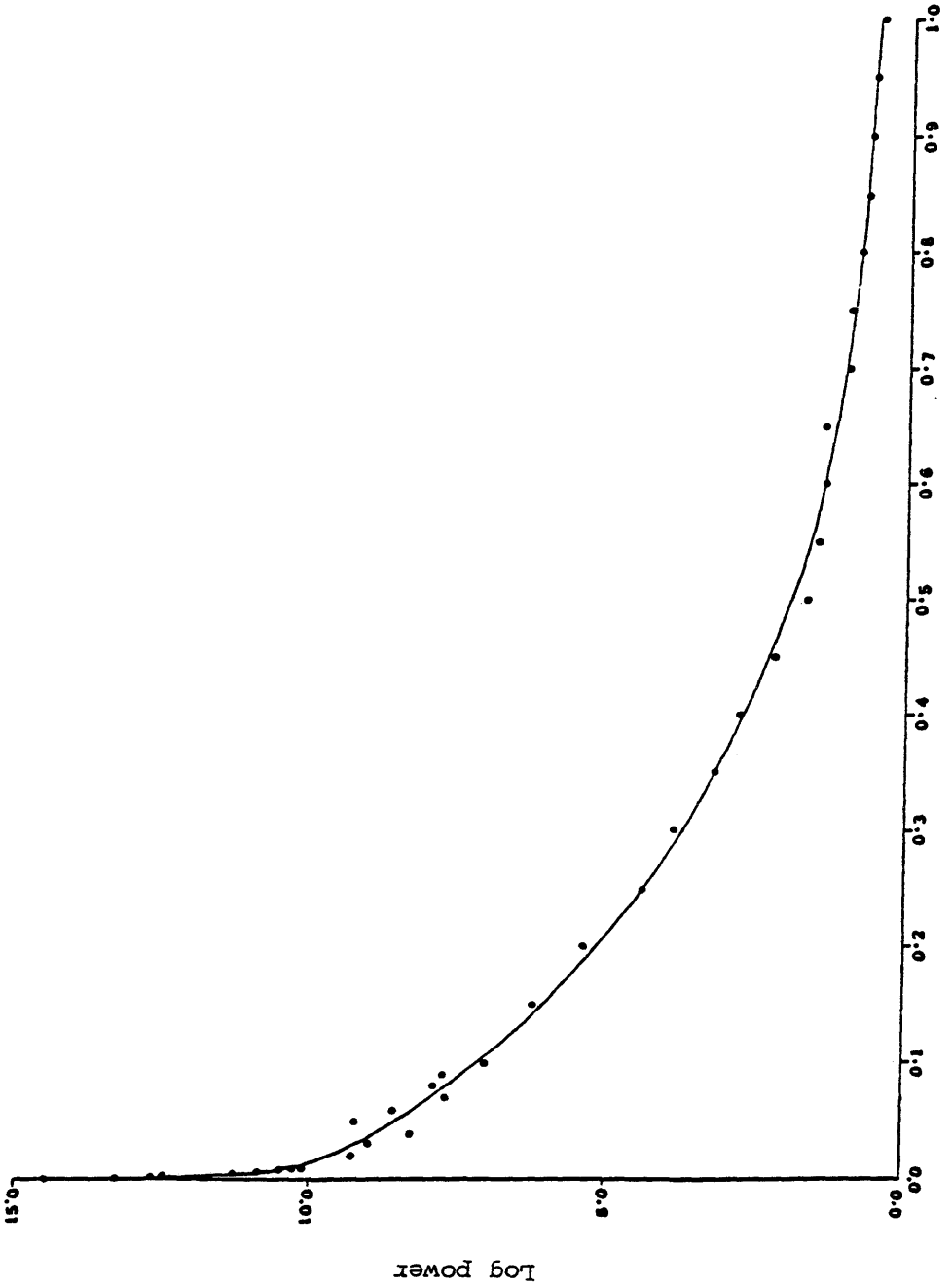

Figure 17. Power spectrum calculated from the portion of a typical spectrum of amplitudes of electromagnetic noise (time variations) with frequencies below 1 Hz as shown in Figure 18.

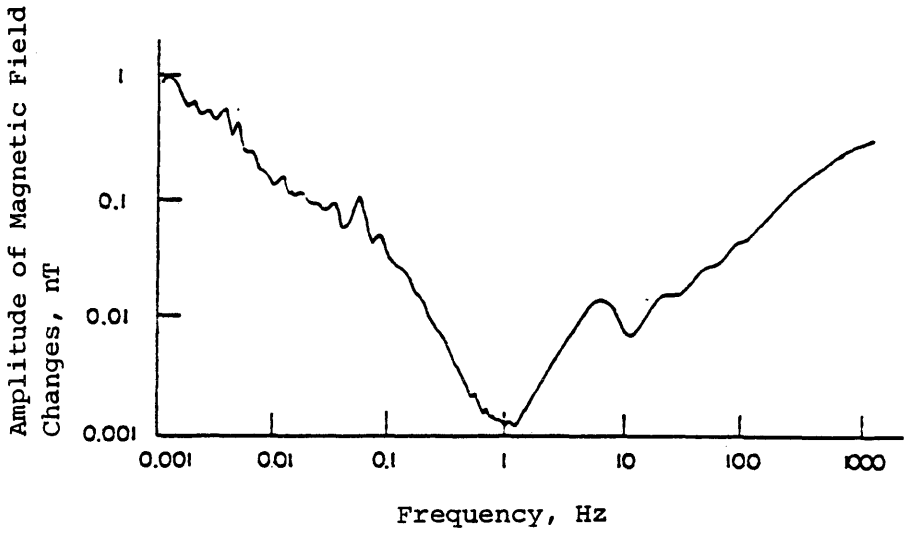

Figure 18. Typical spectrum of amplitudes of electromagnetic noise (time variations) in the extremely low frequency (ELF) range. (Keller and Frischknecht, 1966)

Hz. Such high-frequency time variations are due to the disturbances in the ionosphere caused by thunderstorms.

The flat high-frequency tails of the power spectra (Figures 15 and 16) are assumed to be white noise. Real data collected in the field are expected to contain random energies at all frequencies in equal proportion, causing the white noise tails of the power spectrum of the data. Even if there is no noise in the data, instrumental noise is also expected to generate the white noise tails. Processing finite length data and improper sampling are also possible sources of the white noise tails in the power spectra.

At this stage we would like to point out that our calculation of the cross power spectrum at the high-frequency tail is biased. The high-frequency tail of the cross power spectrum is expected to be nearly zero, much below than the corresponding high-frequency tail of the auto power spectrum. Considering the noise components, say No and Nb, of the field and base data to be completely uncorrelated, even if the expectation value of the cross power spectrum $\langle NoNb^{*} \rangle$ is equal to zero, the expectation value of the absolute value of the cross power spectrum $\langle |NoNb^{*}| \rangle$ is not equal to zero, but a positive number as can be seen from the Figure 19. In fact, we are calculating

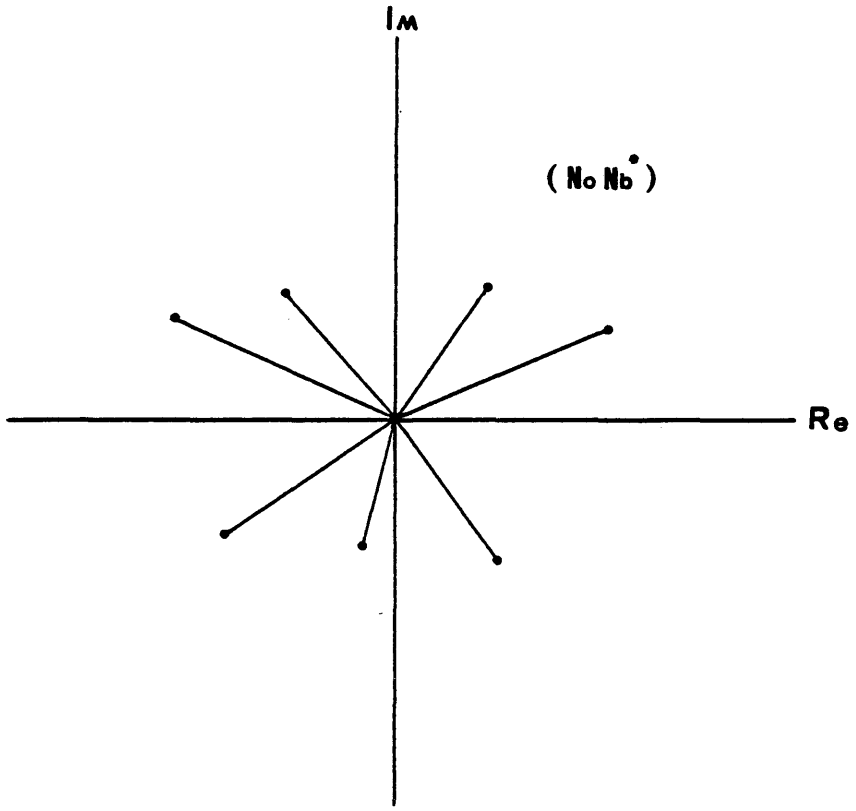

$\langle N_o N_b^* \rangle = 0$

$\langle | N_o N_b^* | \rangle =$ Positive number.

$N_o =$ Noise component of the field data.

$N_b^* =$ Noise component of the base data. (complex conjugate)

Figure 19. Random distribution of $NoNb^*$ (cross power spectrum of the noise components of the base and field data) in the complex plane.

$\langle|NoNb^{*}|\rangle$, which is greater than zero, but not the desired quantity $|\langle NoNb^{*}\rangle|$, which is equal to zero. So, the bias in the high-frequency tail of the cross power spectrum is a consequence of our computational procedure.

Therefore, as a general strategy, while taking the ratio of the power spectra to calculate the filter transfer function (also taking into consideration the phase shift, if any) care is taken to preserve the parts of the spectra due to the time variations only and to suppress the parts of the spectra due to noise. A filter transfer function, calculated in this case, is shown in Figure 20.

The anomalies in the portions of both the base and field data that we have considered here for calculating the power spectra shown in Figures 15 and 16 have the same shape, differing only by a constant phase shift as shown in Figure 21. Since the anomalies in the base and field data are similar, both the base and field data represent the time variations measured at the base and field stations respectively. So, the trend of the cross phase spectrum calculated from the base and field data is expected to represent the phase shift between the time variations in the base and field data. Figure 22 shows how the trend of the cross phase spectrum is marked by a straight line (dashed line) to represent the phase shift. In this

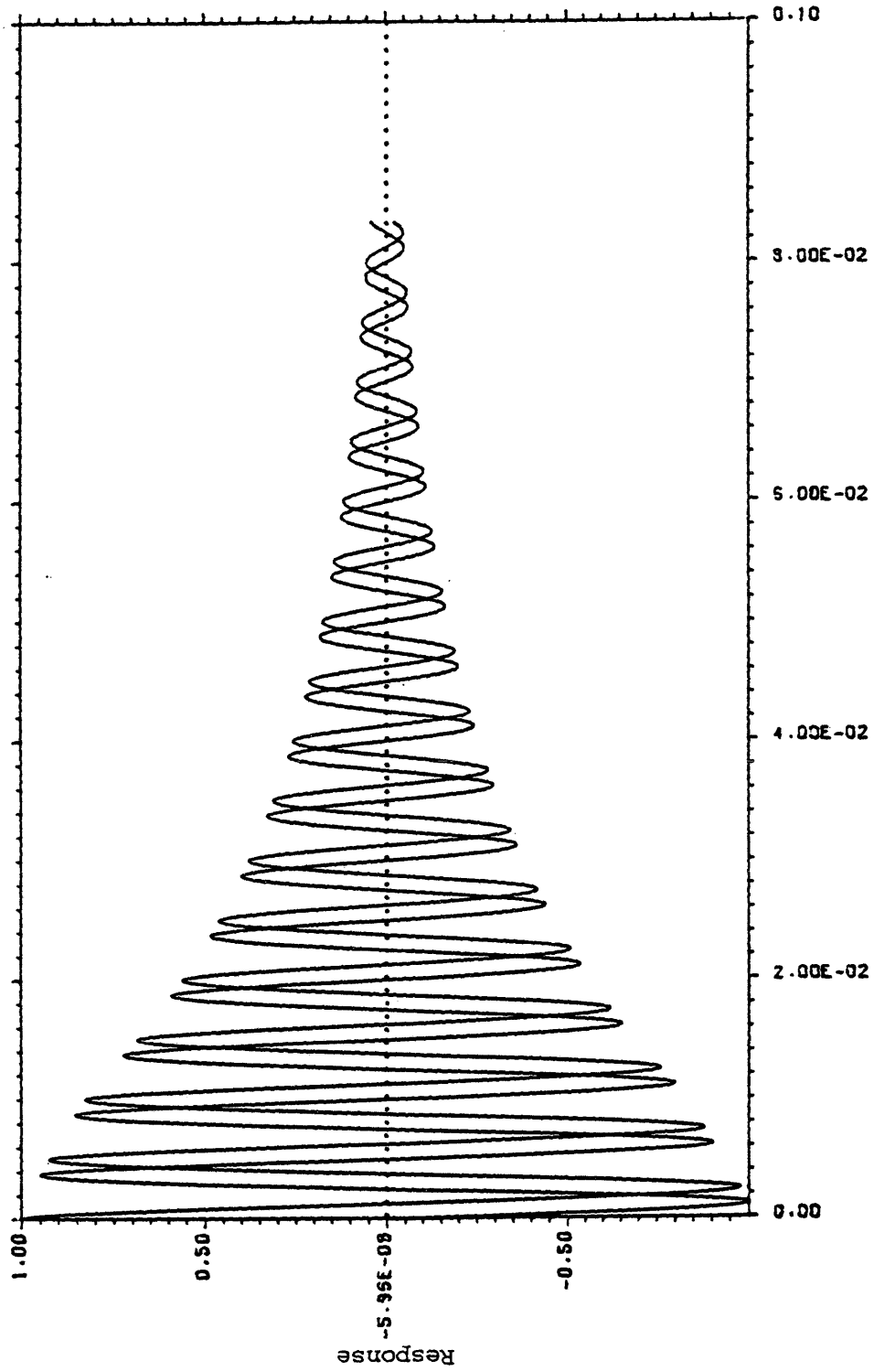

Figure 20. Filter transfer function calculated using the line segments approximation of the power spectra (Figures 15 and 16) and the straight line approximation of the phase shift (Figure 22).

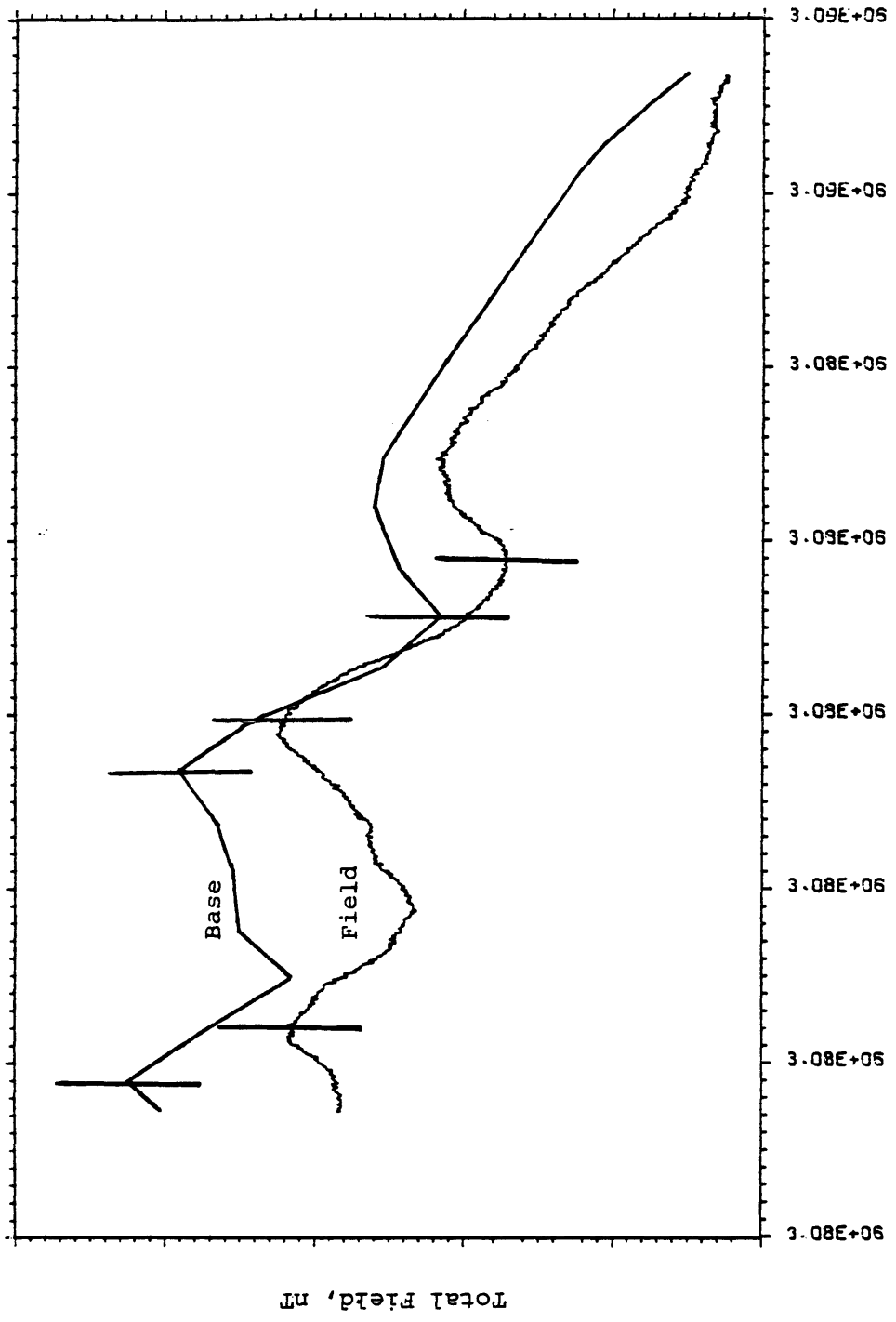

Figure 21. Field and base data plotted together to show the similar trend of anomalies and phase shift between them.

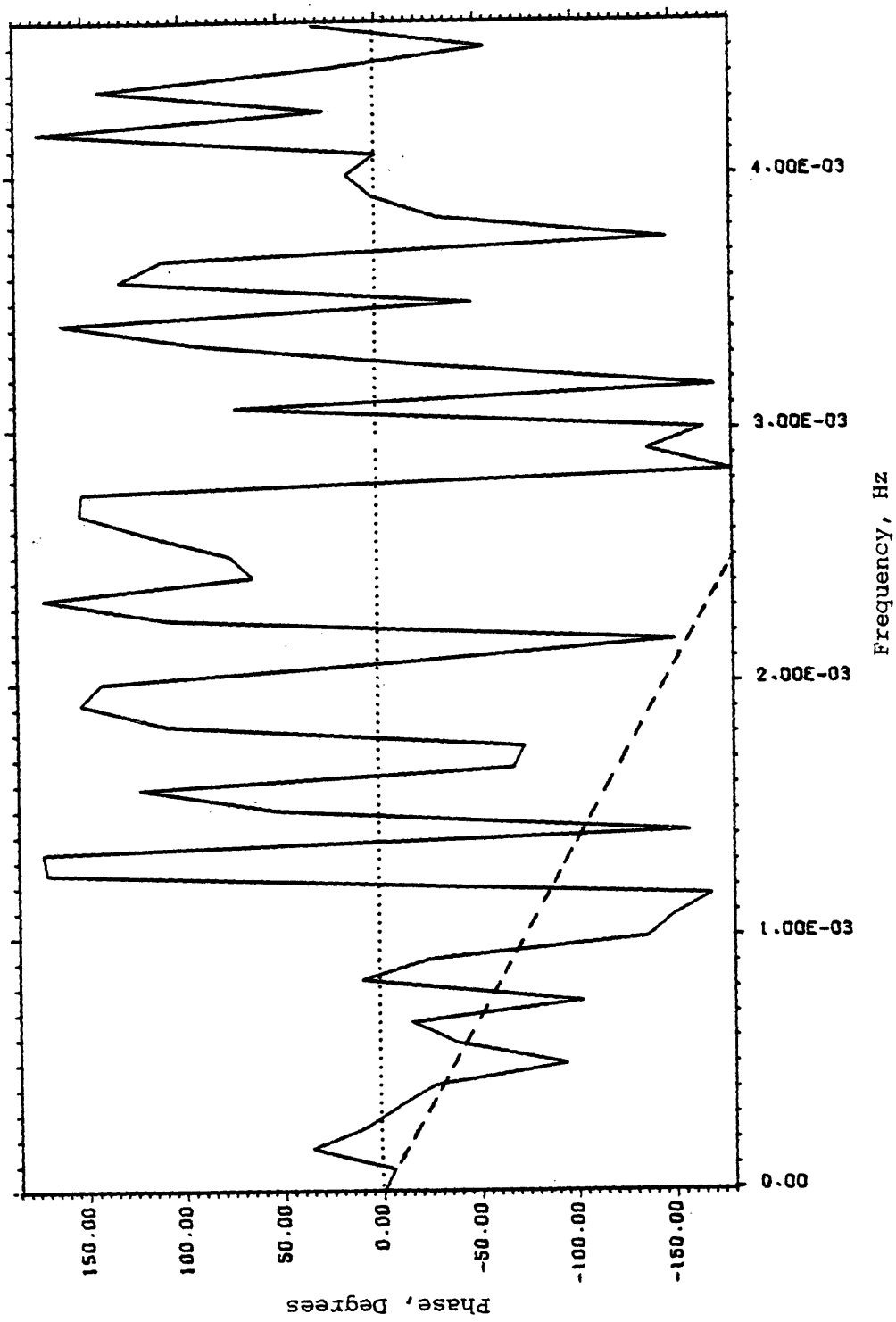

Figure 22. Cross phase spectrum of the field and base data. The trend of the cross phase spectrum marked by the dashed line represents the phase shift.

example, the dashed line passing through the points (0.0, 0.0) and (0.0025, -180.0) represents the correct phase shift. Like the power spectra, the cross phase spectrum is also a statistical estimate. So, approximating the phase shift by a straight line is also expected to be a reasonable estimate. The cross phase spectrum is plotted in degrees against frequency.

On the basis of the equations (5) and (7), and using the programs PROFFT, WDESIGN and GPROF at the Centre for the Potential Field Studies (CPFS), the new filtering technique was implemented according to the following steps:

Step1: Using the Power Spectrum option available in the PROFFT program, power spectra OB^* and BB^* and the cross phase spectrum of o and b were calculated.

Step2: Using the graphic program GPROF, power spectra were displayed by plotting natural logarithm of power against frequency, and the cross phase spectrum by plotting phase in degree against frequency.

Step3: Power spectra were approximated by straight line segments and the phase shift by a straight line, called a phase line.

Step4: Using the WDESIGN program, the filter transfer

function was calculated by representing the power spectra by the line segments and the phase shift by the phase line.

Step5: Finally, using the Base Station Filter option of the PROFFT program, and giving as inputs the field and base data and the filter transfer function to this program, the time-variation corrected field data $\hat{g}$ were calculated.

According to the mathematical formulation described above, the new filtering technique is expected to remove the time variations from the field data successfully if the time variations measured at the base station are similar in shape as the time variations encountered at the field stations, but differ only in amplitude and phase. If the time variations in the base and field data are different in shape, as may happen if the internal time-varying magnetic field at the base and field stations are quite different due to significant difference of internal conductivities at the base and field stations, then the new filtering technique will not be effective in removing the time variations from the field data correctly. For example, the time variations observed at the Smith and Lac la Biche stations as shown in the middle plots of Figure 14b (in Chapter 2) can be removed successfully by the new filtering

technique (by considering either one of the time variations as the base data and the other one as encountered in the field data) because the time variations at these two stations are practically identical in shape and also more or less in phase, but the time variations between the same two stations as shown in the bottom plots of the same figure can not be removed effectively by the same filtering technique because not only that they are completely out of phase, they also are not practically identical in shape.

Chapter 4

RESULTS

The time variations measured at the base station and those encountered at the field stations, although practically identical in shape, vary both in amplitude and phase (as explained in Chapter 2). The proposed new filtering techniquue (as explained in Chapter 3) is expected to remove the time variations from the field data by taking care of the differences in amplitude and phase, if any, between the time variations in the base and field data.

To examine the effectiveness of the new filtering technique, we are required to apply the filter to remove the time variations from the field data and then to compare the time-variation corrected field data with the corresponding time-variation free field data which we already know. Such a study is possible with model data, because during model studies we know how we have created the data and, when something is removed from them, how they should look. Such a study could also be made with real data if reliable time-variation corrected field data obtained by some other technique are also available for comparison. After model studies, we will also consider

studies with real data.

Model Data

The geomagnetic field that we measure during magnetic surveys is a superposition of the internal field, the field due to the geology and the time variations, as explained in Chapter 1. Since the internal field, which is of the order of tens of thousands of nT, is a steady-state field for the duration of a magnetic survey, the anomalies in the field data are the sum of the anomalies due to the geology and the time variations. At the base station, both the internal field and the field due to the geology are constant. So, the anomalies in the base data are due to the time variations only. In this situation, for model studies, we can therefore ignore the large, practically constant, background values in our data because by doing so we do not lose any information that we seek from the field and base data. Secondly, the programs that we used to process the data work in this sequence: first remove the mean from the data, then process and finally add back the mean to the processed data. So, even during processing, we are not losing any information from the field and base data by ignoring the large constant background values in them.

Magnetic surveys are normally carried out during solar

quiet days and during such days we observe the time variations known as the Sq variations, which are smooth and periodic (1/24 cph). Figure 23 represents a smooth and periodic model time variation, which we call the Model#1 base data (b). Figure 24 represents a model field due to the geology, which we call the Model#1 field due to the geology (g). Since the field data represent anomalies due to the geology and the time variations, we added the Model#1 base data and the Model#1 field due to the geology to create the model field data, which we call the Model#1 field data (o) as shown in Figure 25. Our Model#1 base and field data therefore contain time variations, which are exactly identical - a situation assumed in the standard method for correcting time variations in the magnetic data. Now, if we calculate the filter α from the Model#1 base and field data (according to the equation (5) in Chapter 3) and then apply the filter α to remove the time variations from the Model#1 field data (according to the equation (7) in Chapter 3) we are supposed to get back the time-variation corrected Model#1 field data, which will be exactly the same as the Model#1 field due to the geology.

The auto power spectrum of the Model#1 base data (BB^*) is shown in Figure 26, and the cross power spectrum of the Model#1 field and base data (OB^*) in Figure 27. Since the

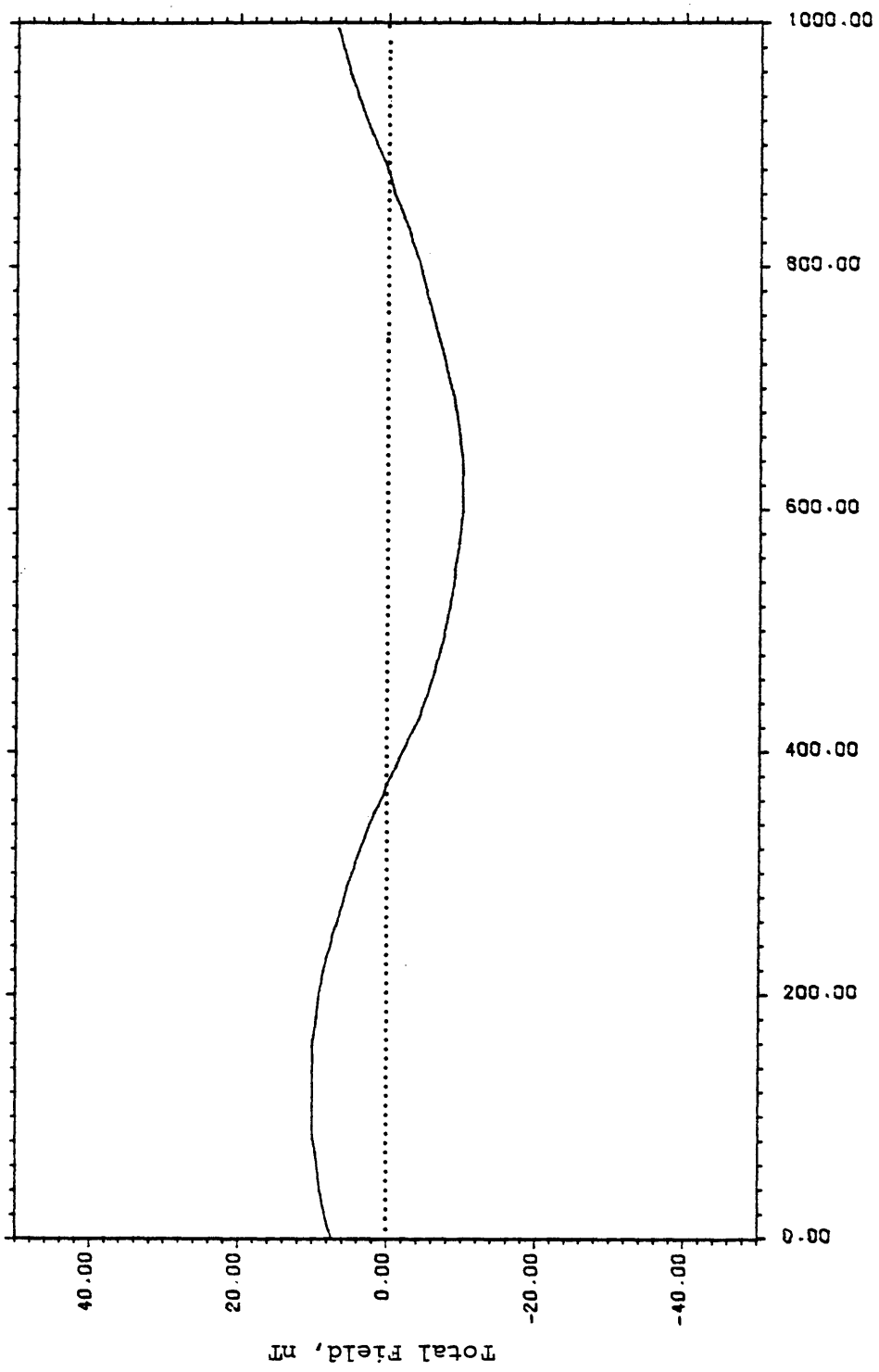

Figure 23. Model#1 base data b.

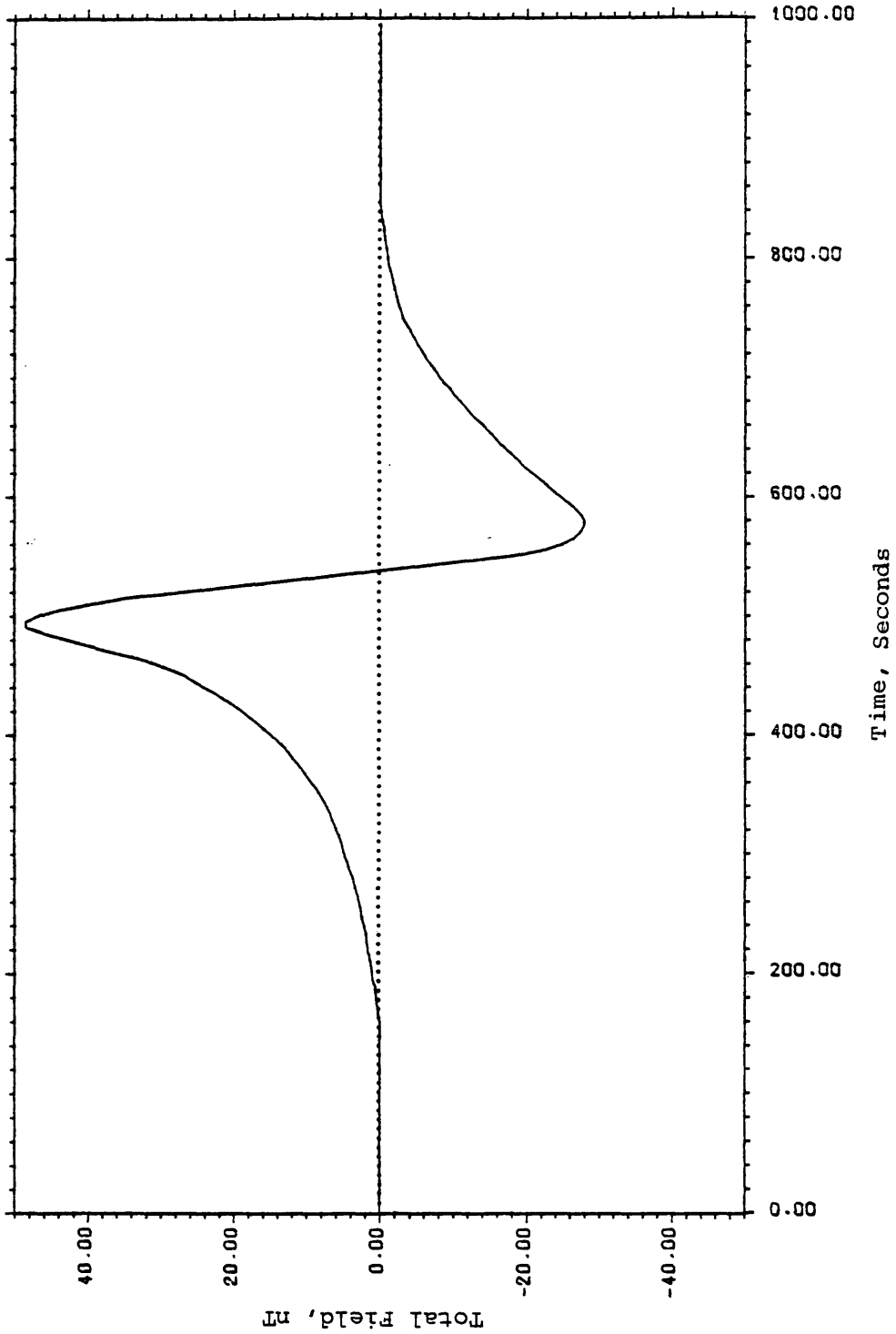

Figure 24. Model#1 field due to the geology g.

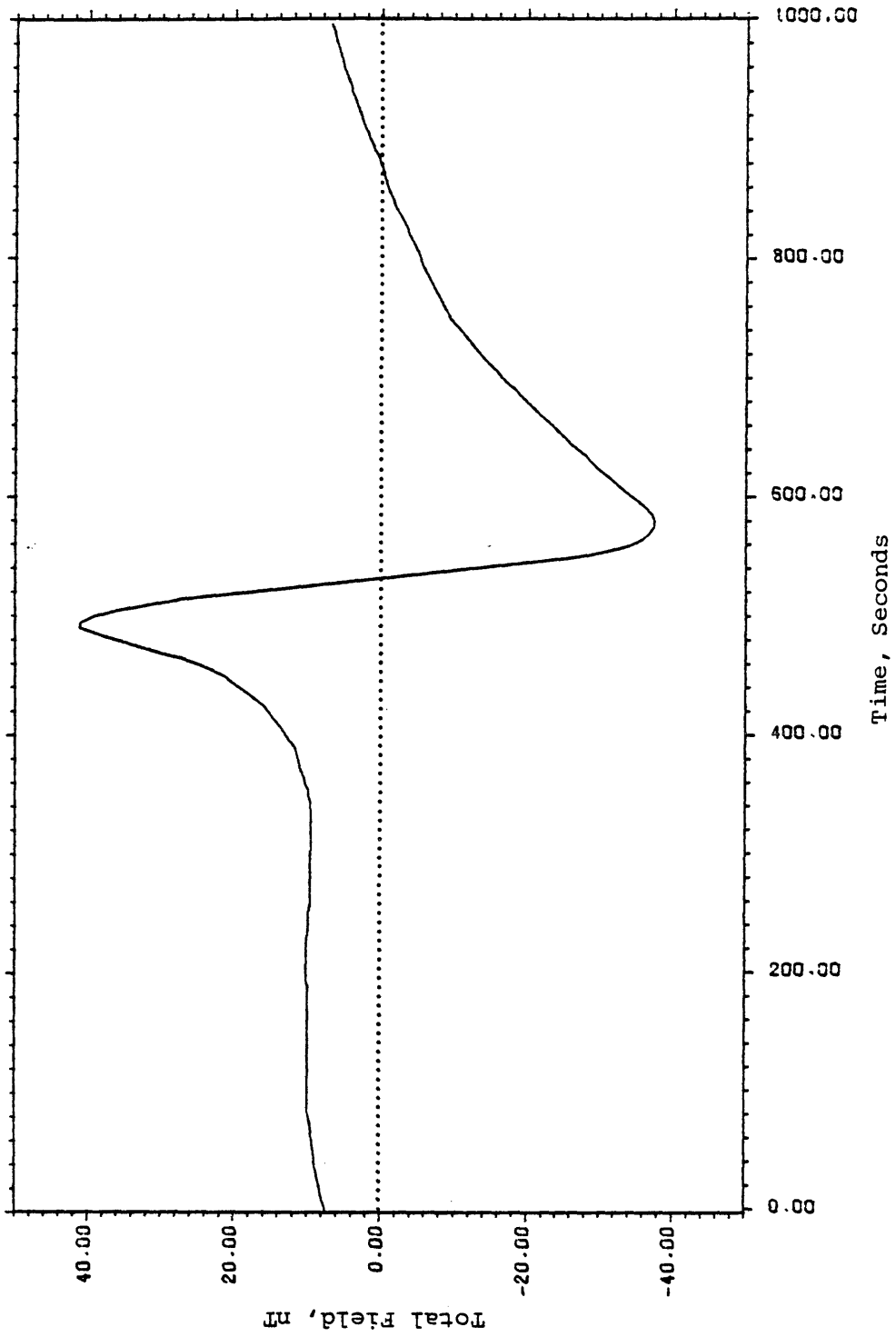

Figure 25. Model#1 field data o.

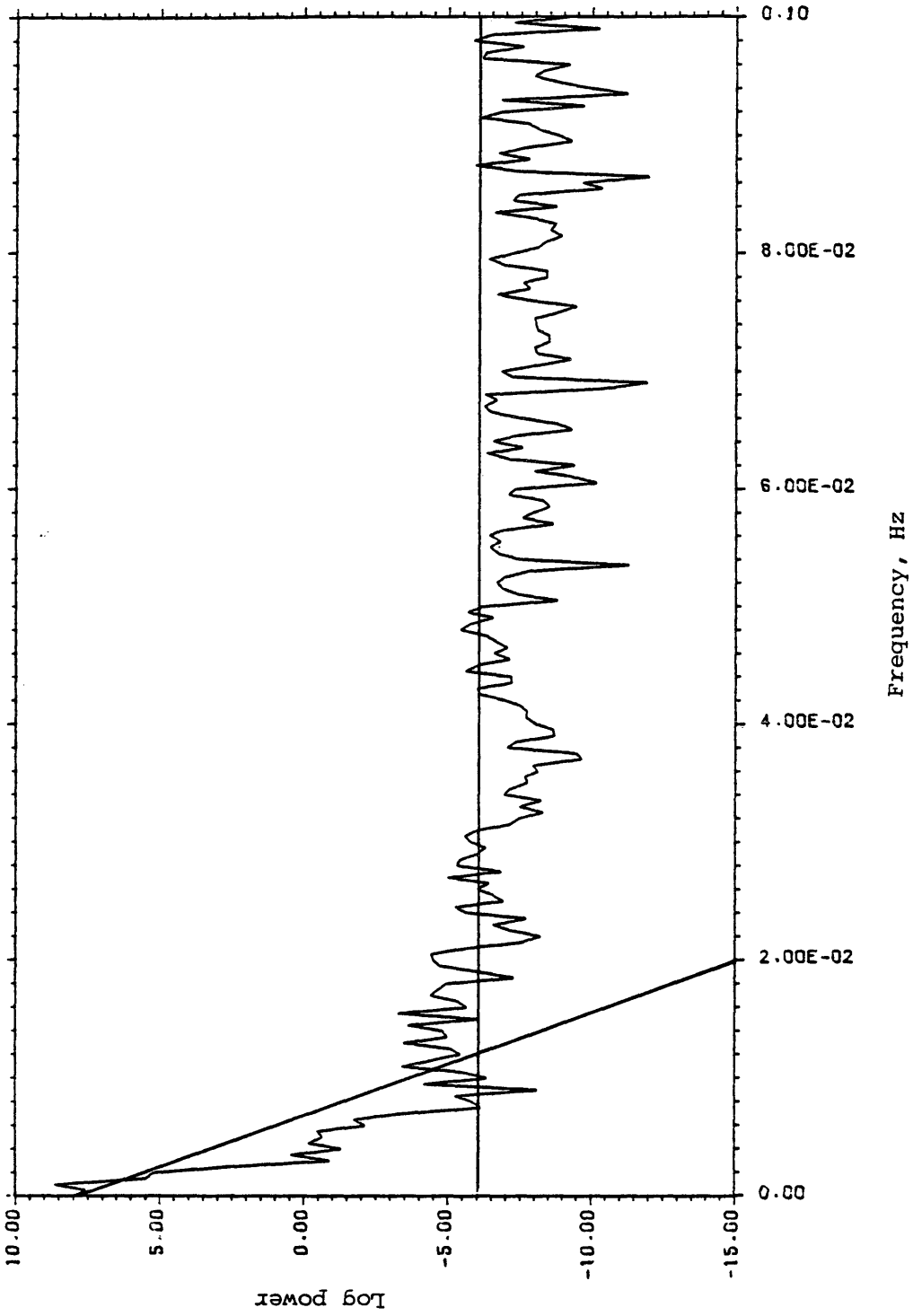

Figure 26. Auto power spectrum of the Model#1 base data 88*.

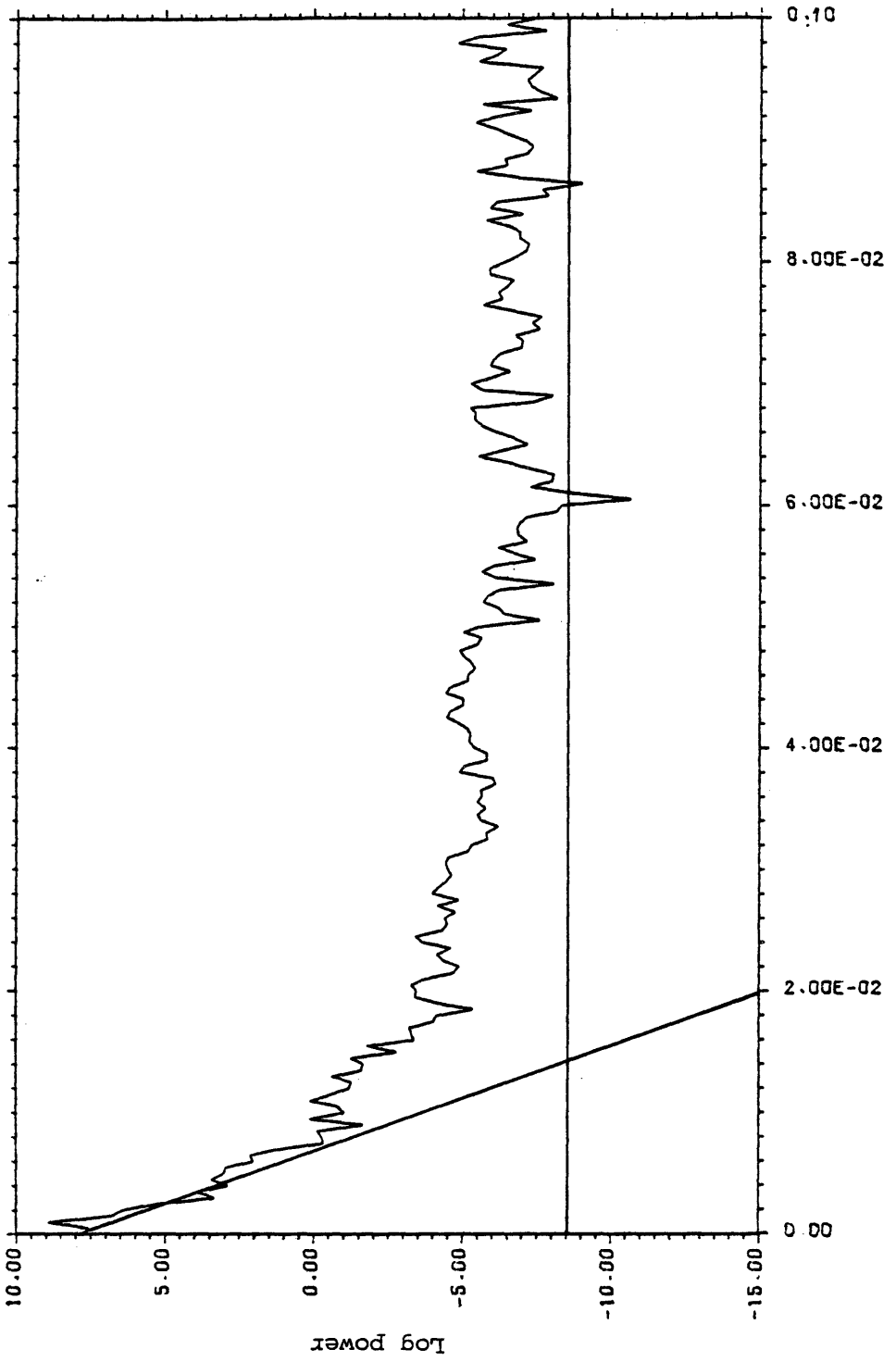

Figure 27. Cross power spectrum of the Model#1 field and base data OB.

power spectra are statistical estimates, as explained in Chapter 3, we approximated them by the line segments also shown in Figures 26 and 27. The filter α calculated, in this case, from the power spectra is shown in Figure 28. In the calculation of the filter our objective was to preserve the parts of the spectra corresponding to the signal (time variations) and to simultaneously suppress the parts of the spectra corresponding to the flat, high-frequency white noise tails. Applying the filter shown in Figure 28, we removed the time variations from the Model#1 field data. The Model#1 field due to the geology and the time-variation corrected Model#1 field data are plotted together in Figure 29. We see that the match between the two sets of data in Figure 29 is perfect; that is, the new filtering technique has completely removed the time variations from the field data.

The time variations observed in the field are not so smooth as we have considered in our Model#1 base data (Figure 23). There is always some noise in them. So, we next introduced noise to our Model#1 base data, and the Model#1 base data with noise is shown in Figure 30. We calculated the filter from the Model#1 base data with noise and the Model#1 field data, and then applied the filter to remove the time variations from the Model#1 field data. The

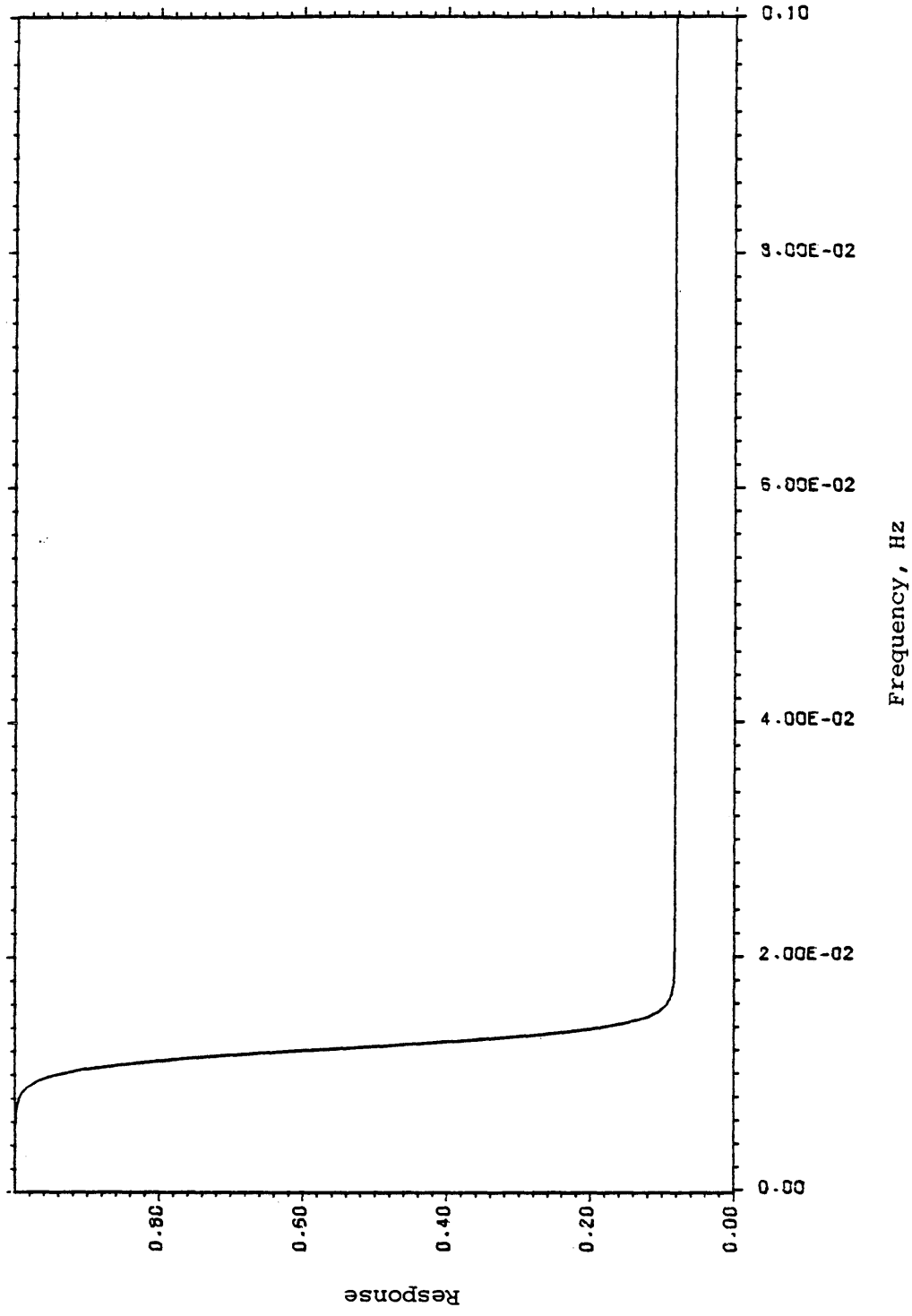

Figure 28. Filter transfer function (calculated from the power spectra in Figures 26 and 27).

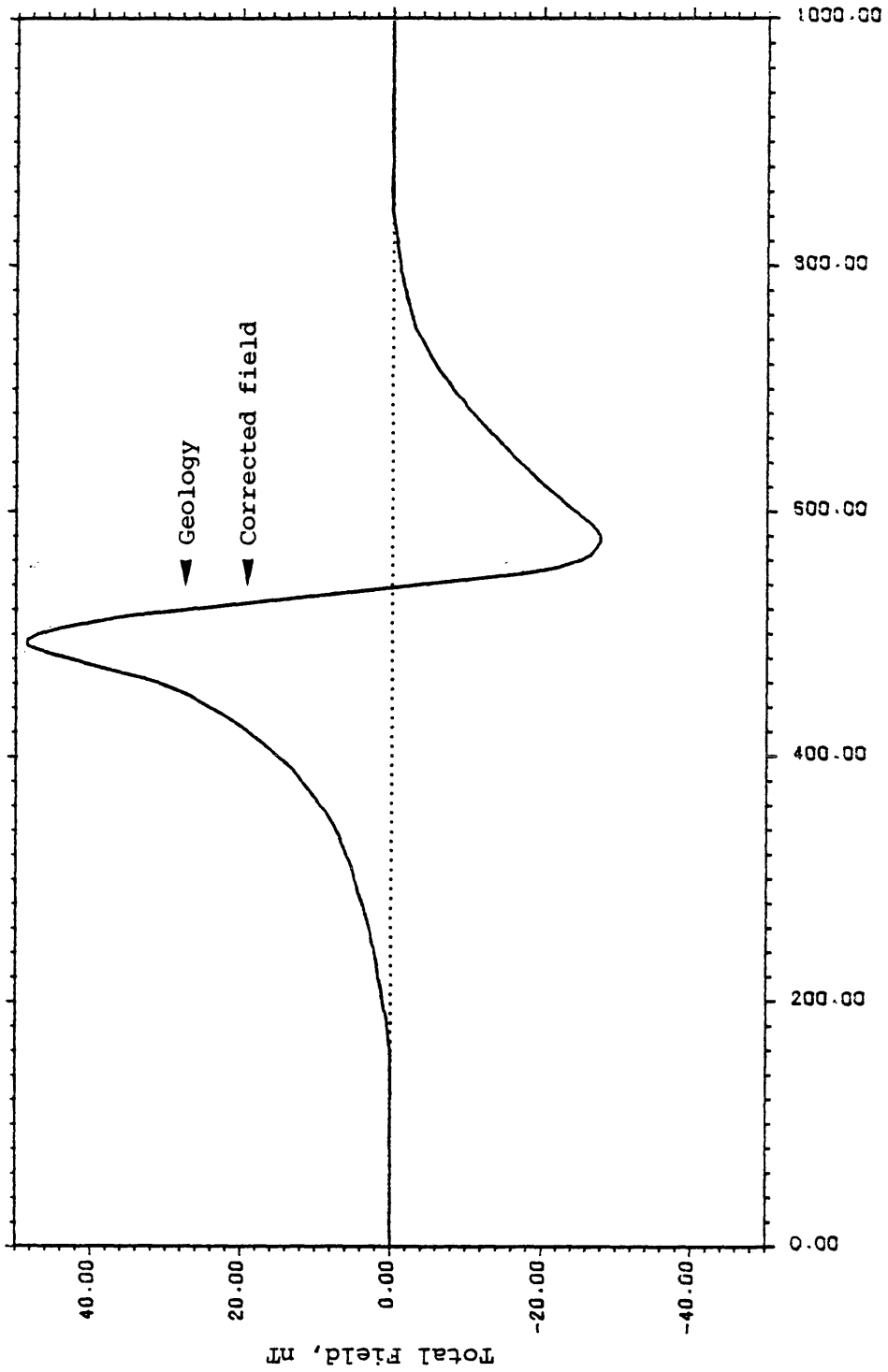

Figure 29. Model#1 field due to the geology and time-variations corrected Model#1 field data.

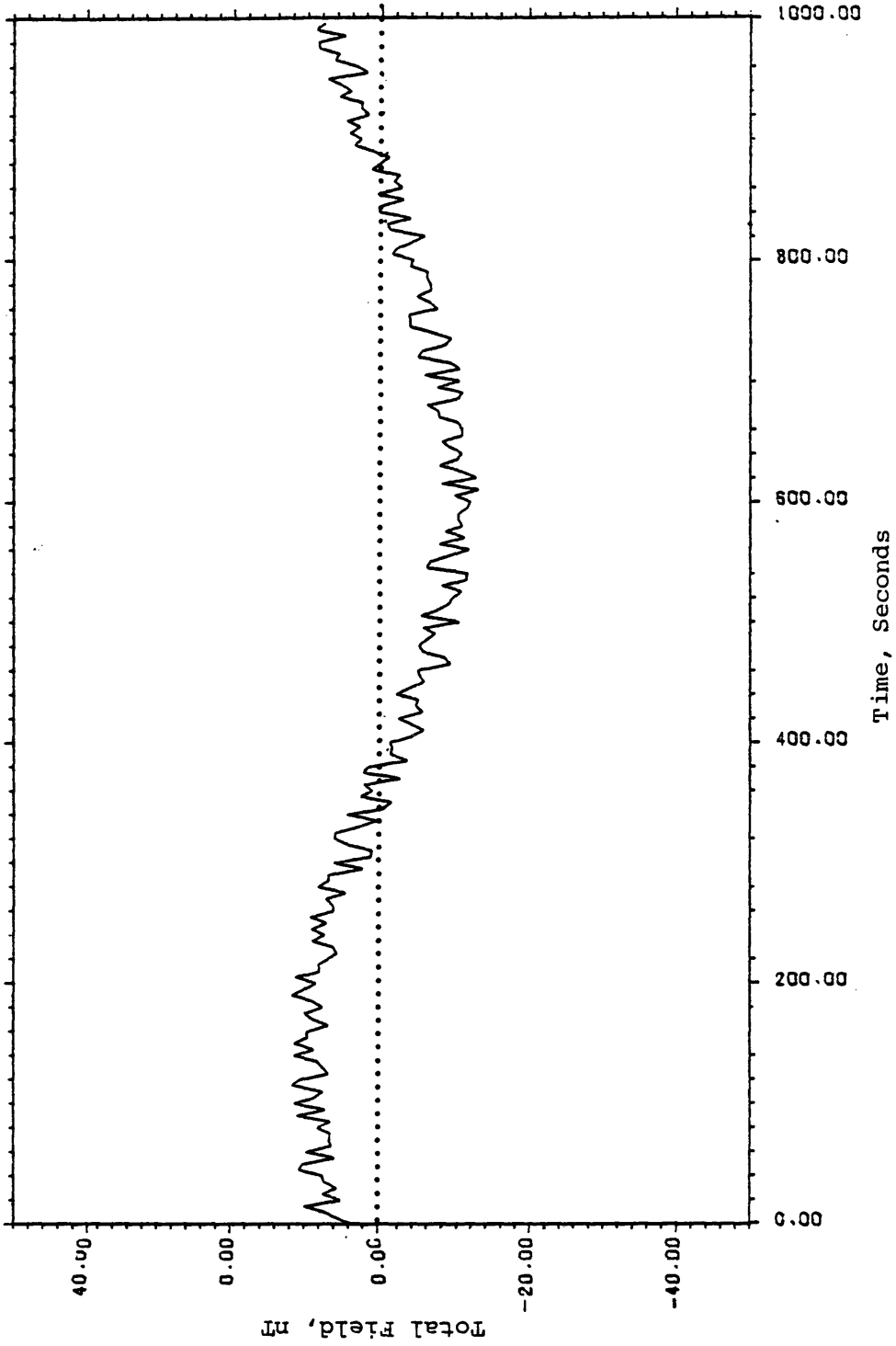

Figure 30. Model#1 base data containing noise.

time-variation corrected Model#1 field data (corrected using Model#1 base data containing noise) and the Model#1 field due to the geology are plotted together in Figure 31. The match between the two sets of data in Figure 31 demonstrates that the new filtering technique also effectively removes the noise from the base data.

The field data may also contain noise. So, we also introduced noise to our Model#1 field data, and the Model#1 field data with noise is shown in Figure 32. Calculating the filter from the Model#1 base and field data (both containing noise), we applied the filter to remove the time variations from the Model#1 field data with noise. The corrected field and the geology are plotted together in Figure 33, and these results show that the new filtering technique cannot remove the noise from the field data. This fact of the new filtering technique is also evident from equation (7) in Chapter 3.

The time variations in the base and field data may vary in phase. So, we next introduced a phase shift between the time variations in the base and field data. Figure 34 shows two Model#1 base data (two model time variations) with a phase shift equivalent to 5 sample intervals. One of these two sets of data in Figure 34 is our original Model#1 base data (Figure 23). We added the other set to the

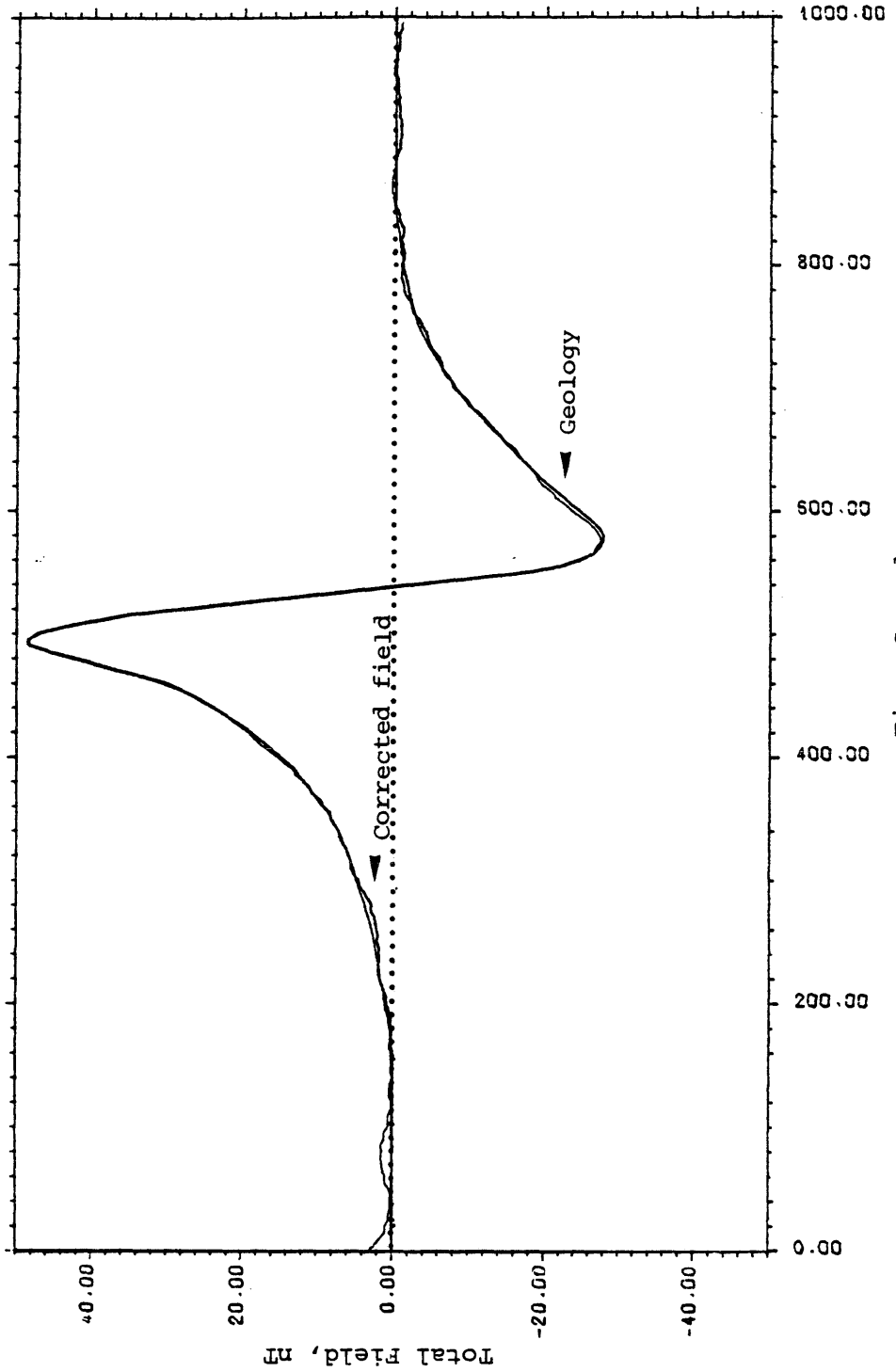

Figure 31. Model#1 field due to the geology and time-variation corrected Model#1 field data (corrected using model#1 base data containing noise.)

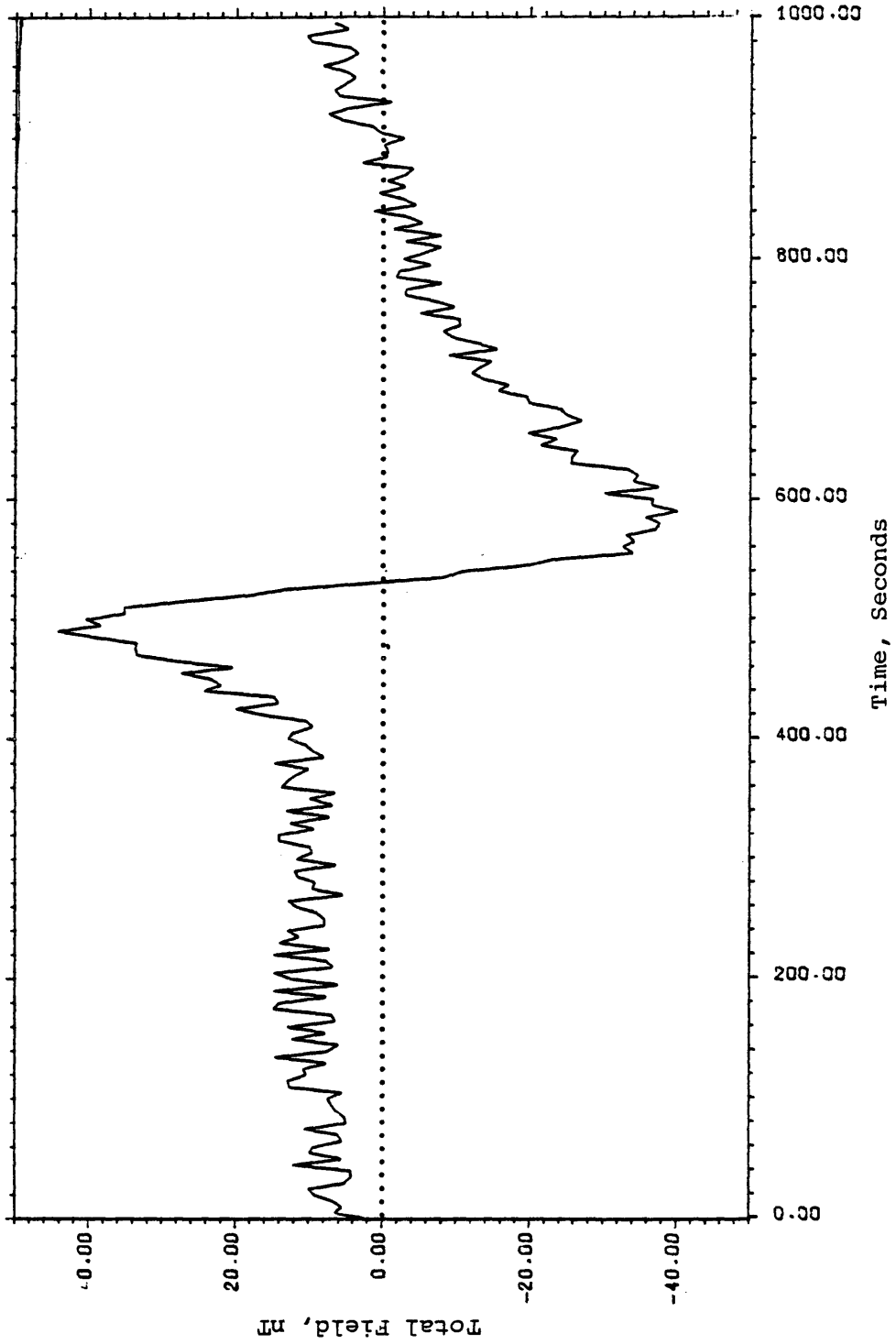

Figure 32. Model#1 field data containing noise.

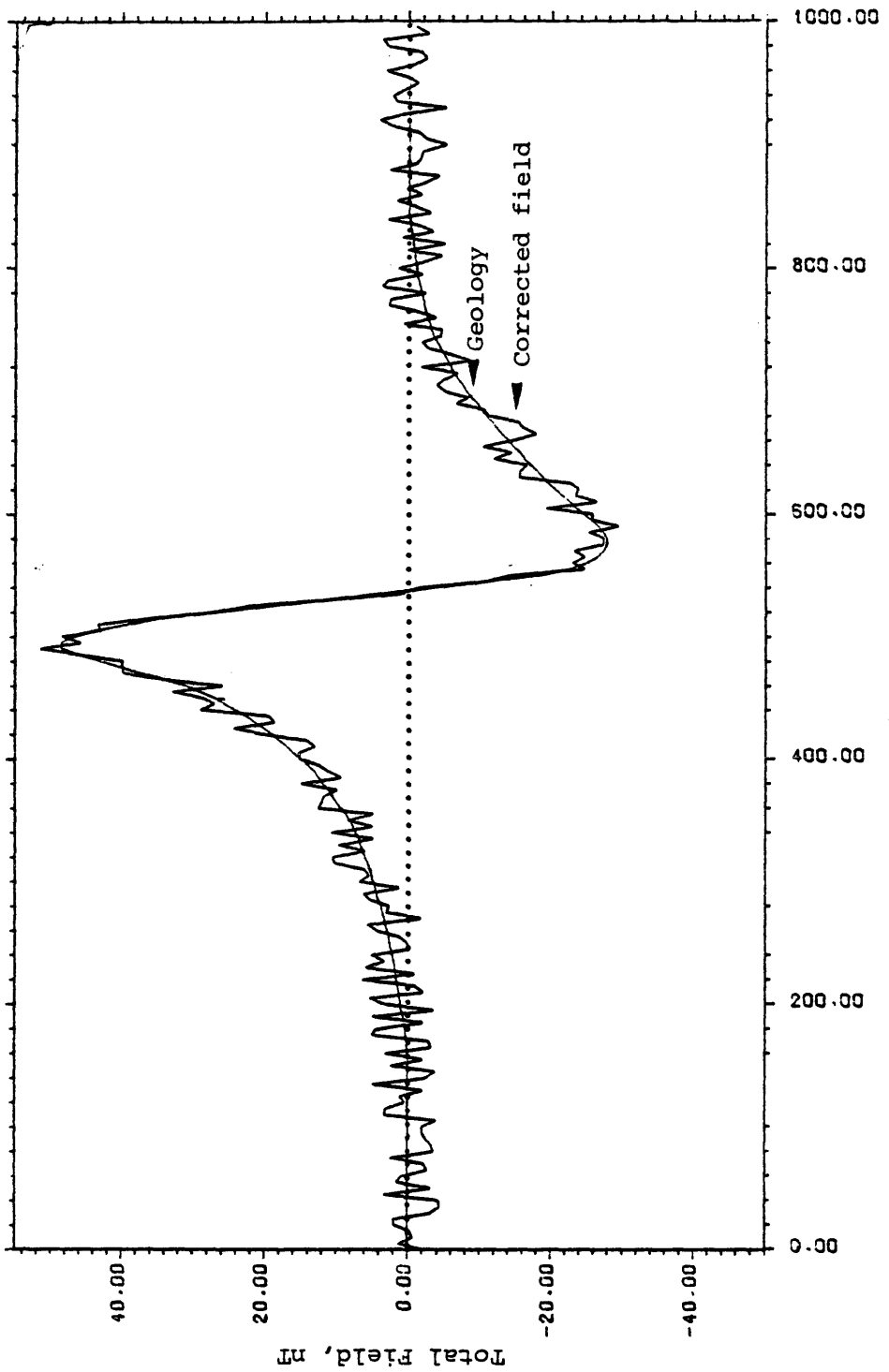

Figure 33. Model#1 field due to the geology and time-variation corrected Model#1 field data (corrected using Model#1 base and field data containg noise).

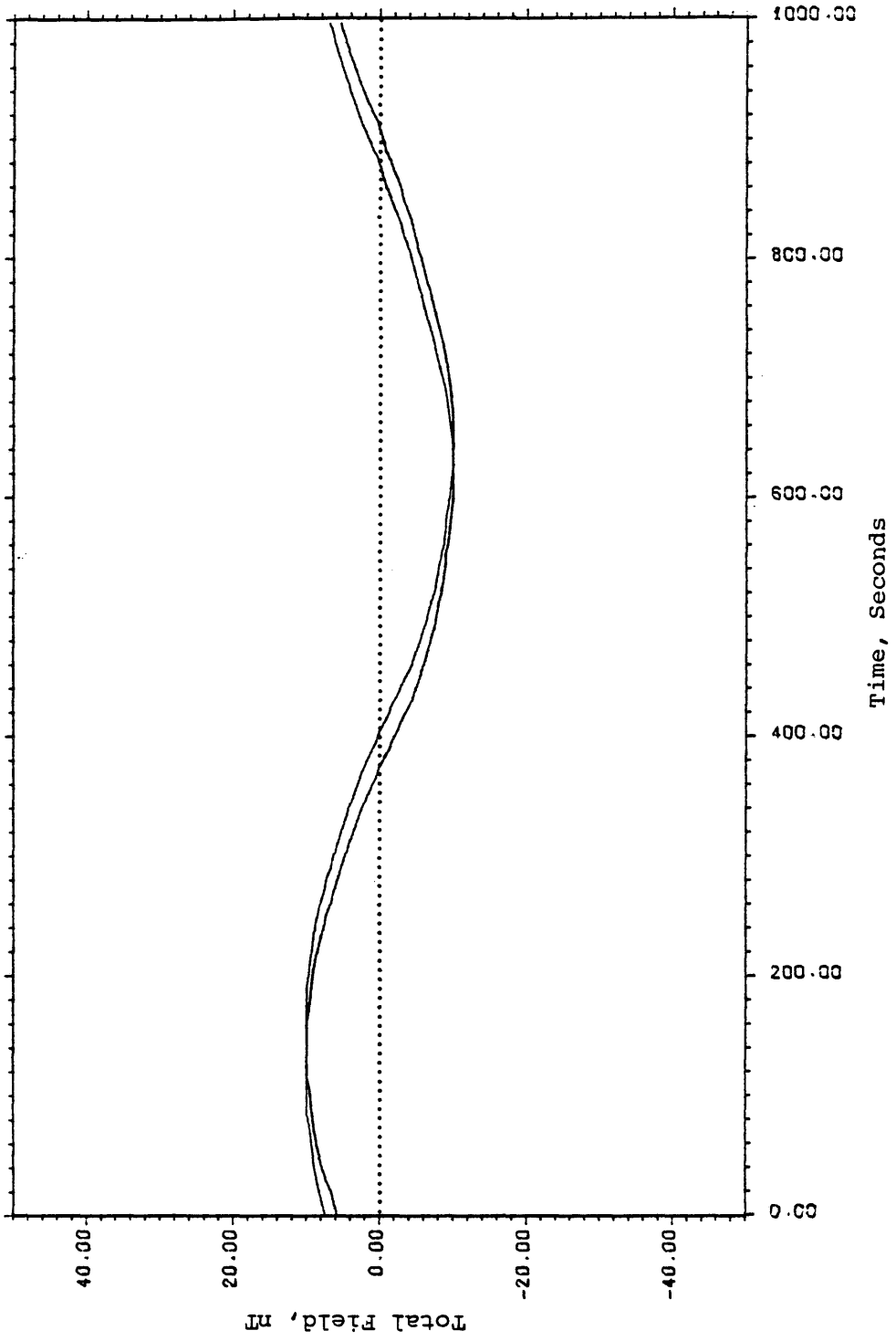

Figure 34. Two Model#1 base data differing in phase.

Model#1 field due to the geology to create new model field data, which we call the Model#2 field data as shown in Figure 35. So, our Model#1 base and Model#2 field data contain time variations differing in phase. Now, according to the theory of the new filtering technique, we expect to be able to estimate the phase shift from the cross phase spectrum of the Model#1 base and Model#2 field data, which is shown in Figure 36. The phase shift that we are considering here is equivalent to 5 sample intervals. So, the straight line represting the phase shift must pass through the point (0.01, 90.0), because the slope of the line is given by $2\pi\Delta t$ radians/frequency unit, where Δt is the total number of sample intervals equivalent to the phase shift. We see that there is no clear trend in the cross phase spectrum in Figure 36 that suggests a line passing through the point (0.01, 90.0) also shown in the same figure. This is due to the fact that the phase of the time variations in the Model#2 field data is distorted by the presence of the anomalies due to the geology in the data. This result (Figure 36) demonstrates that we cannot estimate the phase shift from the cross phase spectrum of the base and field data if the field data contain anomalies due to the geology.

However, if we take a portion of the field data having

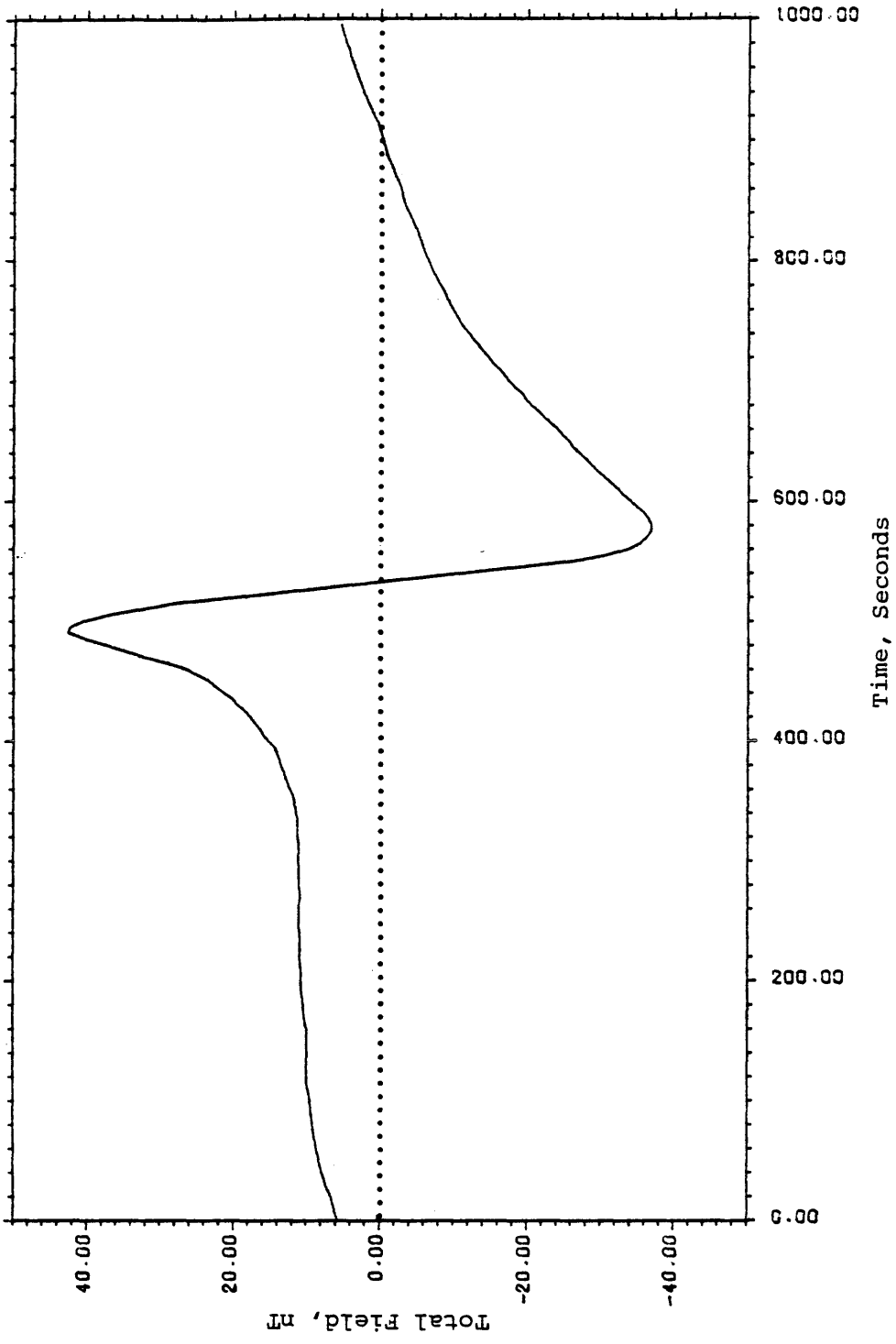

Figure 35. Model#2 field data.

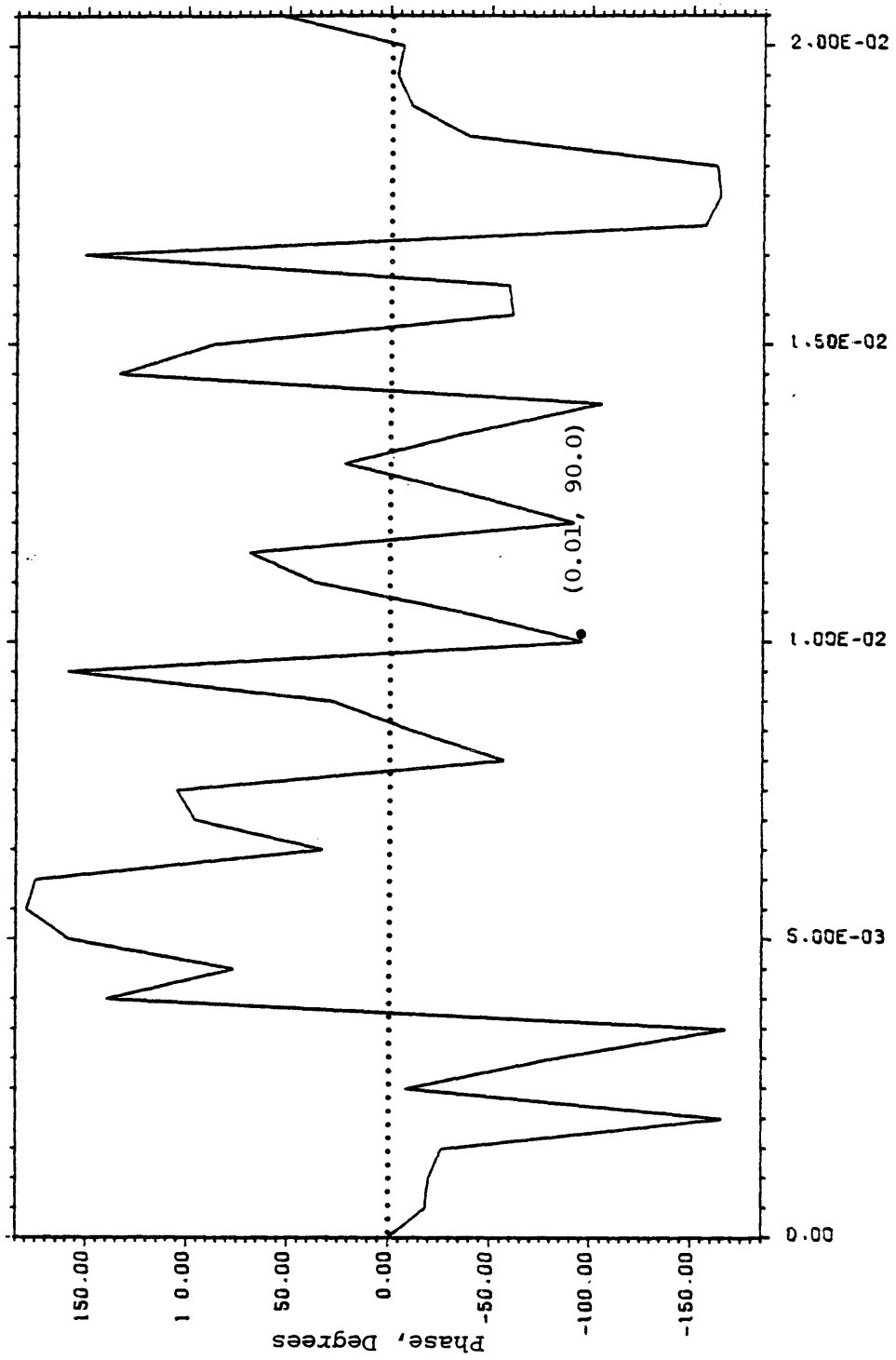

Figure 36. Cross phase spectrum of the Model#1 base and Model#2 field data.

anomalies similar to those of the corresponding portion of the base data, then the base and field data will represent the time variations measured at the base and field stations respectively. So, if we compute the cross phase spectrum of such portions of the base and field data, then we are supposed to be able to estimate the correct phase shift, if any, between the time variations in the base and field data. For our model studies, we can consider the two Model#1 base data shown in Figure 34 as the portions of the base and field data having similar trends of anomalies. During our studies with real data, we will see that to locate a portion of the field data having similar trends of anomalies as in the corresponding portion of the base data may not be very difficult. The cross phase spectrum of the two Model#1 base data (Figure 34) is shown in Figure 37. In Figure 37, the trend of the cross phase spectrum clearly suggests a straight line (dashed line) passing through the point (0.01, 90.0). We also introduced noise to the two Model#1 base data (Figure 34) and computed their cross phase spectrum as shown in Figure 38. In Figure 38 also we see that the trend of the cross phase spectrum clearly suggests a line (dashed line) passing through the point (0.01, 90.0). This result (Figure 38) further demonstrates that the presence of noise in the base and field data does

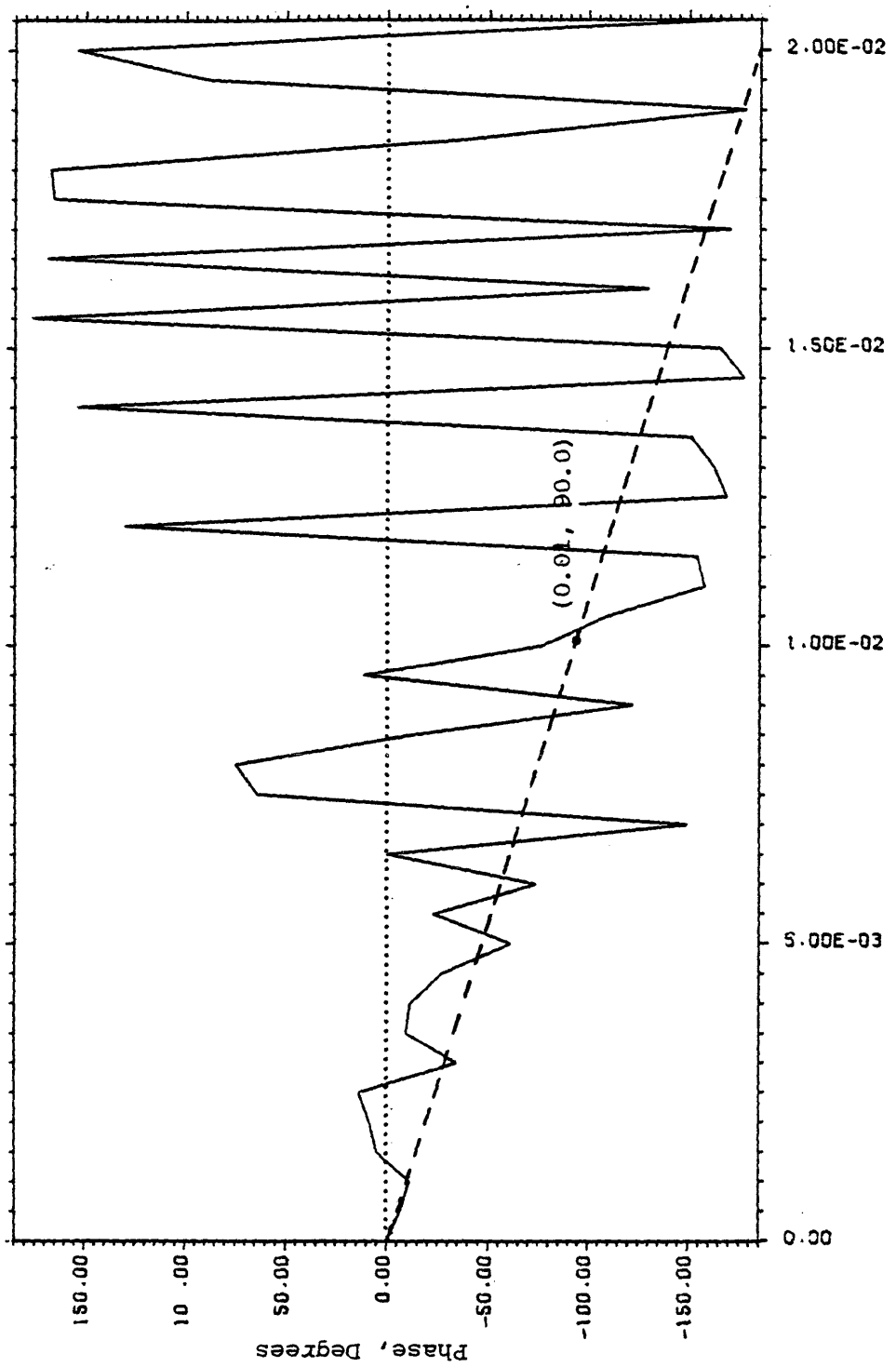

Figure 37. Cross phase spectrum of the two Model#1 base base data shown in Figure 34. The dashed line represent the phase shift.

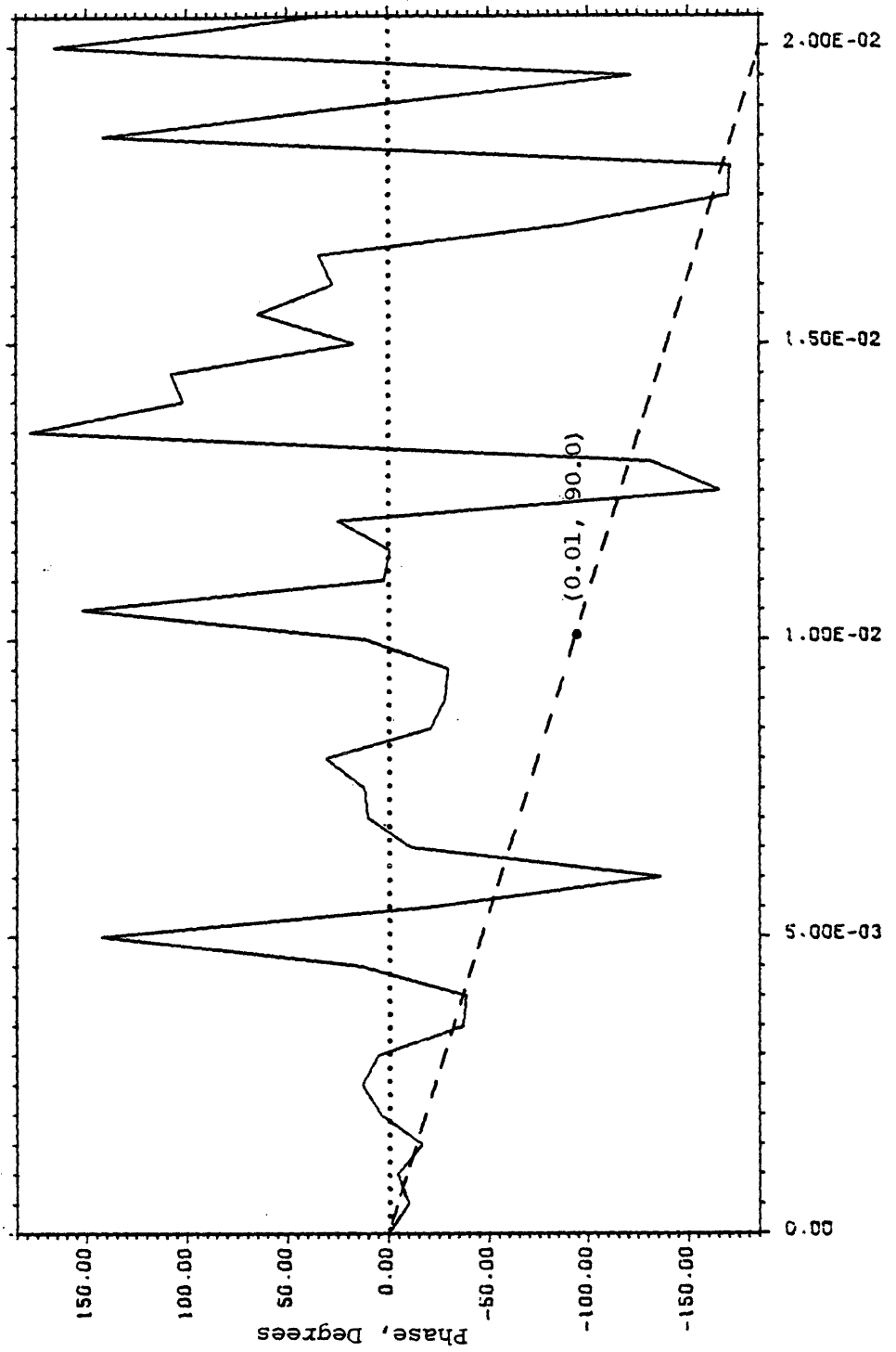

Figure 38. Cross phase spectrum of the two Model#1 base data (Figure 34) containing noise. The dashed line represents the phase shift.

not distort the trend of the cross phase spectrum between them.

The trends of the cross phase spectrum in both Figures 37 and 38 are marked by the dashed line passing through the point (0.01, 90.0) which represents the correct phase shift between the time variations in the Model#1 base and Model#2 field data. First we calculated the filter from the Model#1 base and Model#2 field data without considering the phase shift, and applied this filter to remove the time variations from the Model#2 field data. The result obtained is shown in Figure 39. In Figure 39, we see that there is a difference between the corrected field and the geology, and this difference is the error introduced in the corrected field data by the phase shift. Next, we calculated the filter by taking care of the phase shift represented by the dashed line, and then applied the filter to remove the time variations from the Model#2 field data. The result obtained this time is shown in Figure 40. In Figure 40, we see that the new filtering technique has completely removed the time variations from the field data by taking care of the difference in phase between the time variations in the base and field data.

The time variations in the base and field data may also vary in amplitude. So, we next introduced a difference

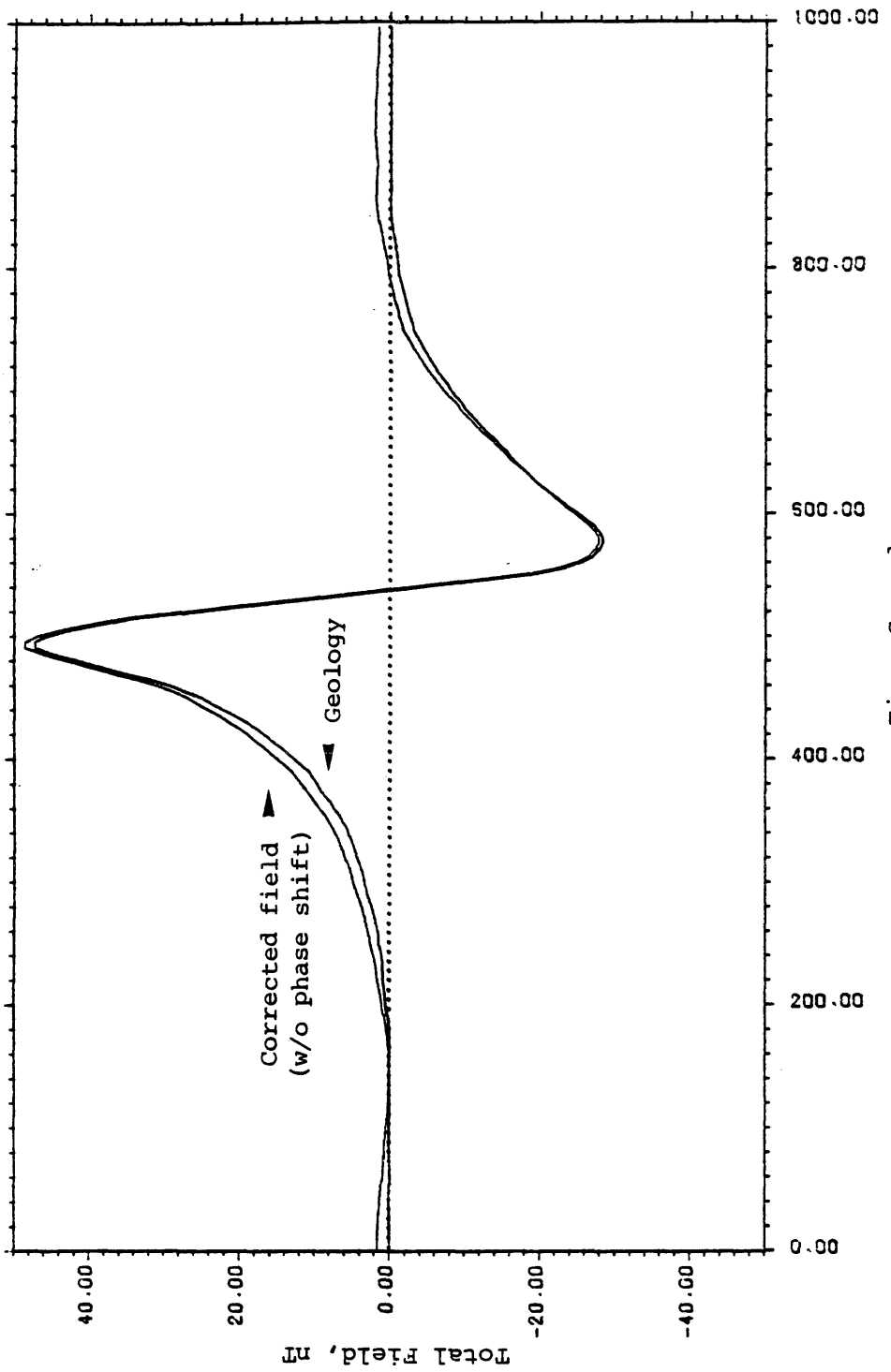

Figure 39. Model#1 field due to the geology and time-variation corrected (without phase shift) Model#2 field data.

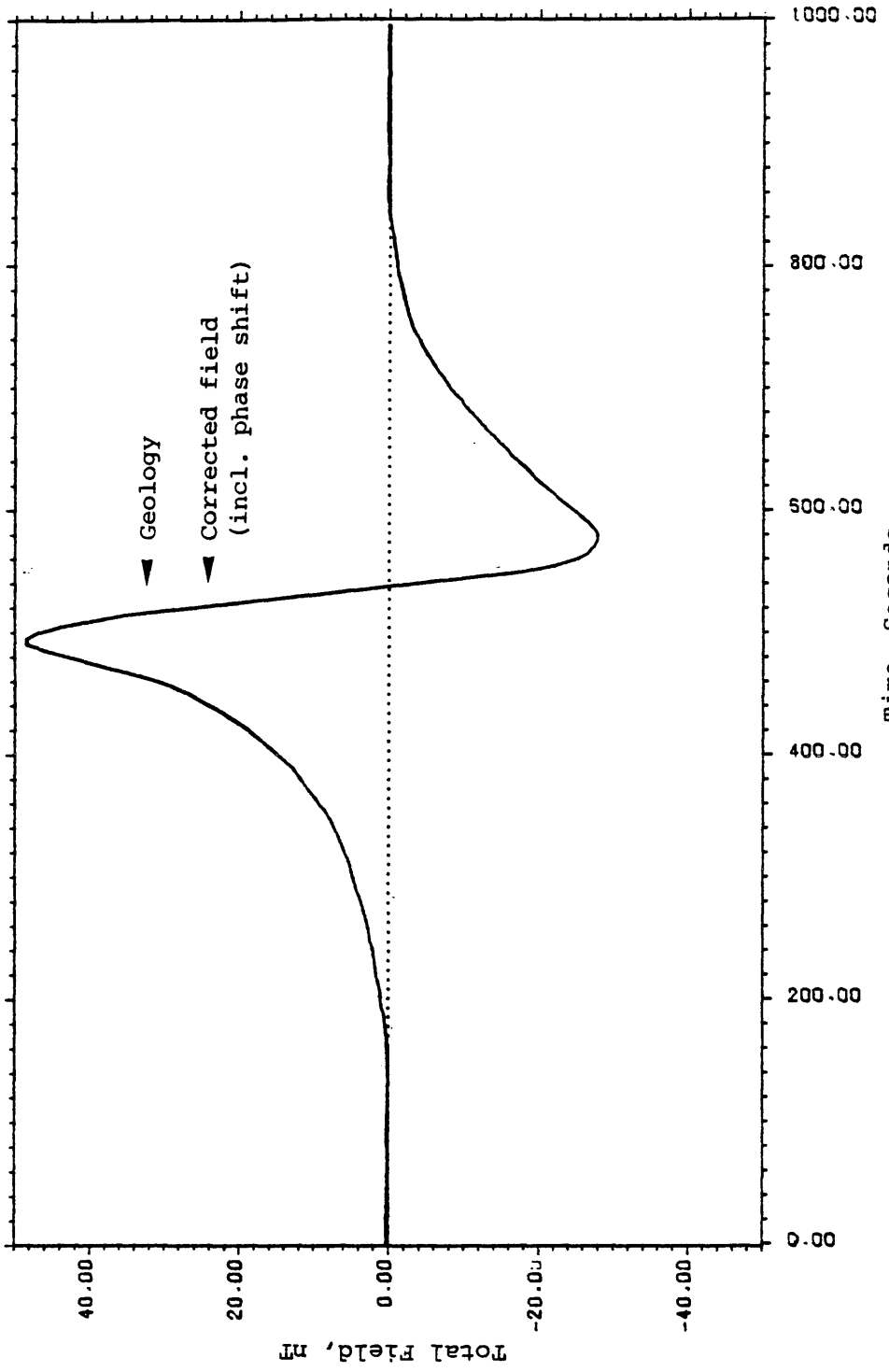

Figure 40. Model#1 field due to the geology and time-variation corrected (including phase shift) Model#2 field data.

in amplitude between the time variations in the base and field data. We constructed new model time-variation data whose amplitude is twice of the amplitude of the model time variations shown in the Model#1 base data (Figure 23). We call the new model time-variation data the Model#2 base data, as shown in Figure 41. Our Model#2 base and Model#1 field data therefore contain time variations differing in amplitude. Now considering the Model#2 base and Model#1 field data, according to the theory of the new filtering technique (equation (7) in Chapter 3), we require a filter α =0.5 to remove the time variations correctly from the Model#1 field data. We expect to be able to estimate the desired filter from the ratio of the cross power spectrum of the Model#1 field and Model#2 base data, and the auto power spectrum of the model#2 base data.

The cross power spectrum of the Model#1 field and Model#2 base data is shown in Figure 42 and the auto power spectrum of the Model#2 base data in Figure 43. Since the time variations that we are considering here are of very low frequency, all the energy is expected to be concentrated near the origin of the power spectrum. Thus, if we take the ratio of the cross and auto power spectra at the origin, we are supposed to get the desired filter response. At the origin, the ratio exp(8.5)/exp(9.20) =

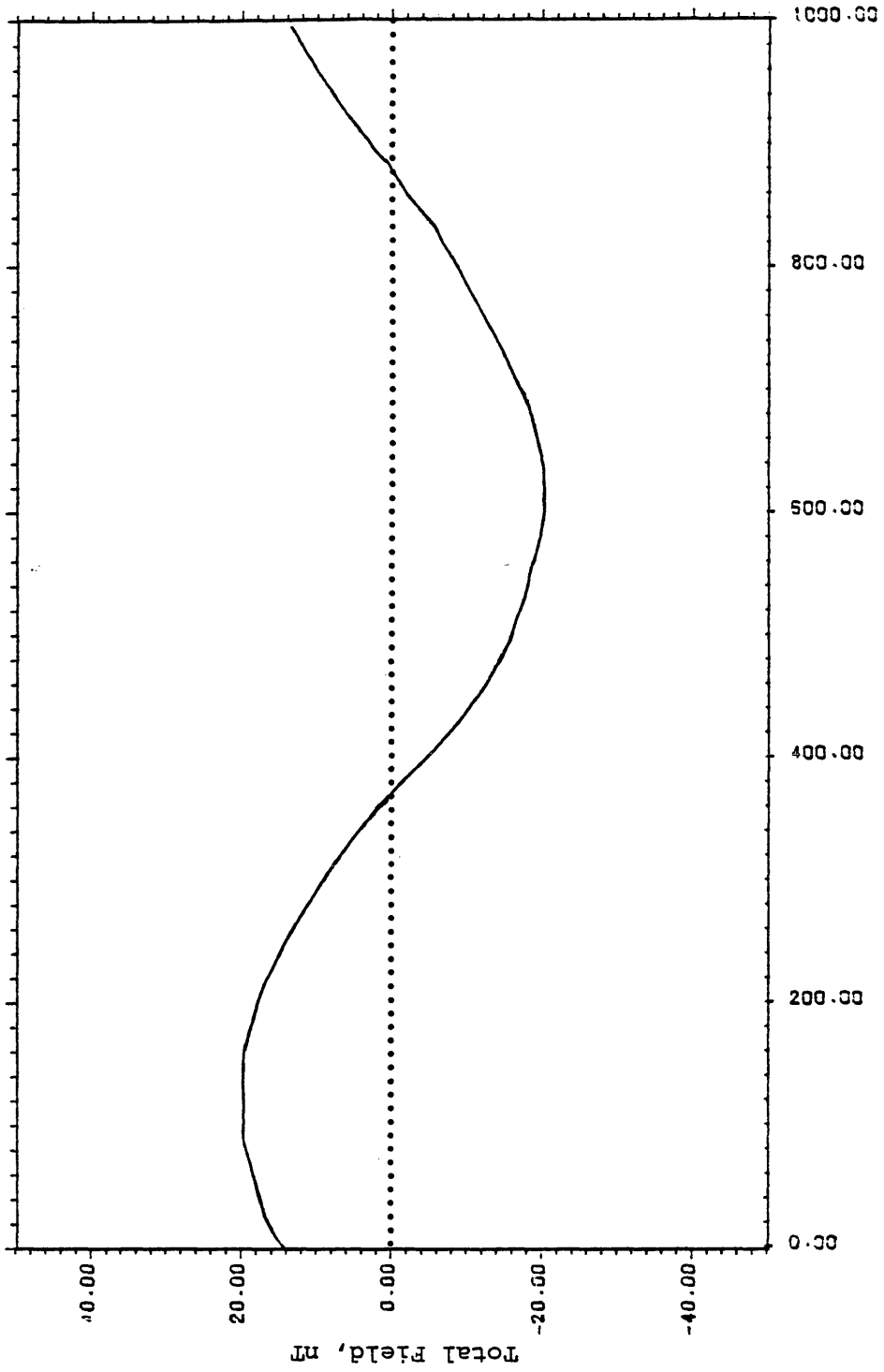

Figure 41. Model#2 base data.

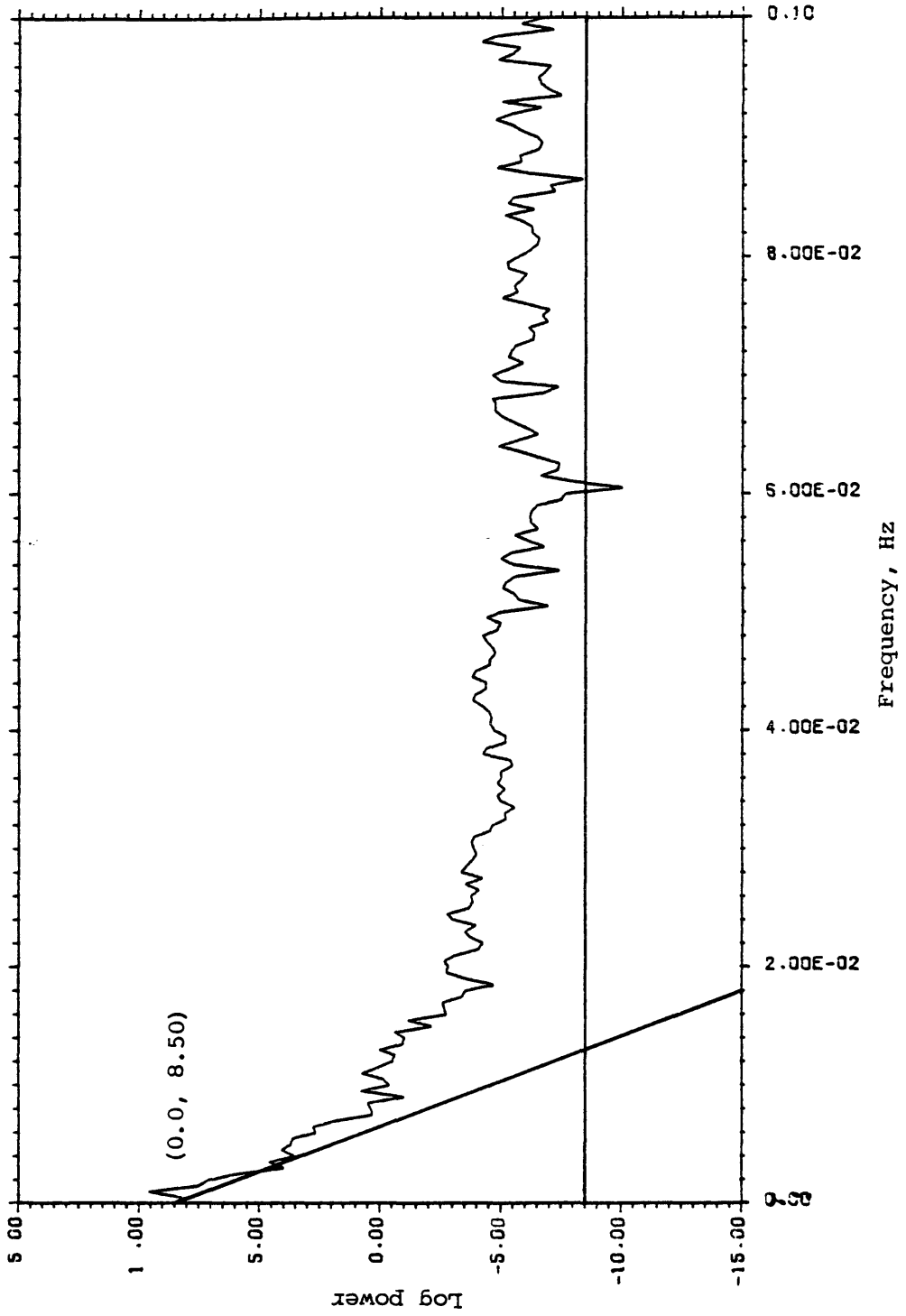

Figure 42. Cross power spectrum of the Model#1 field and Model#2 base data.

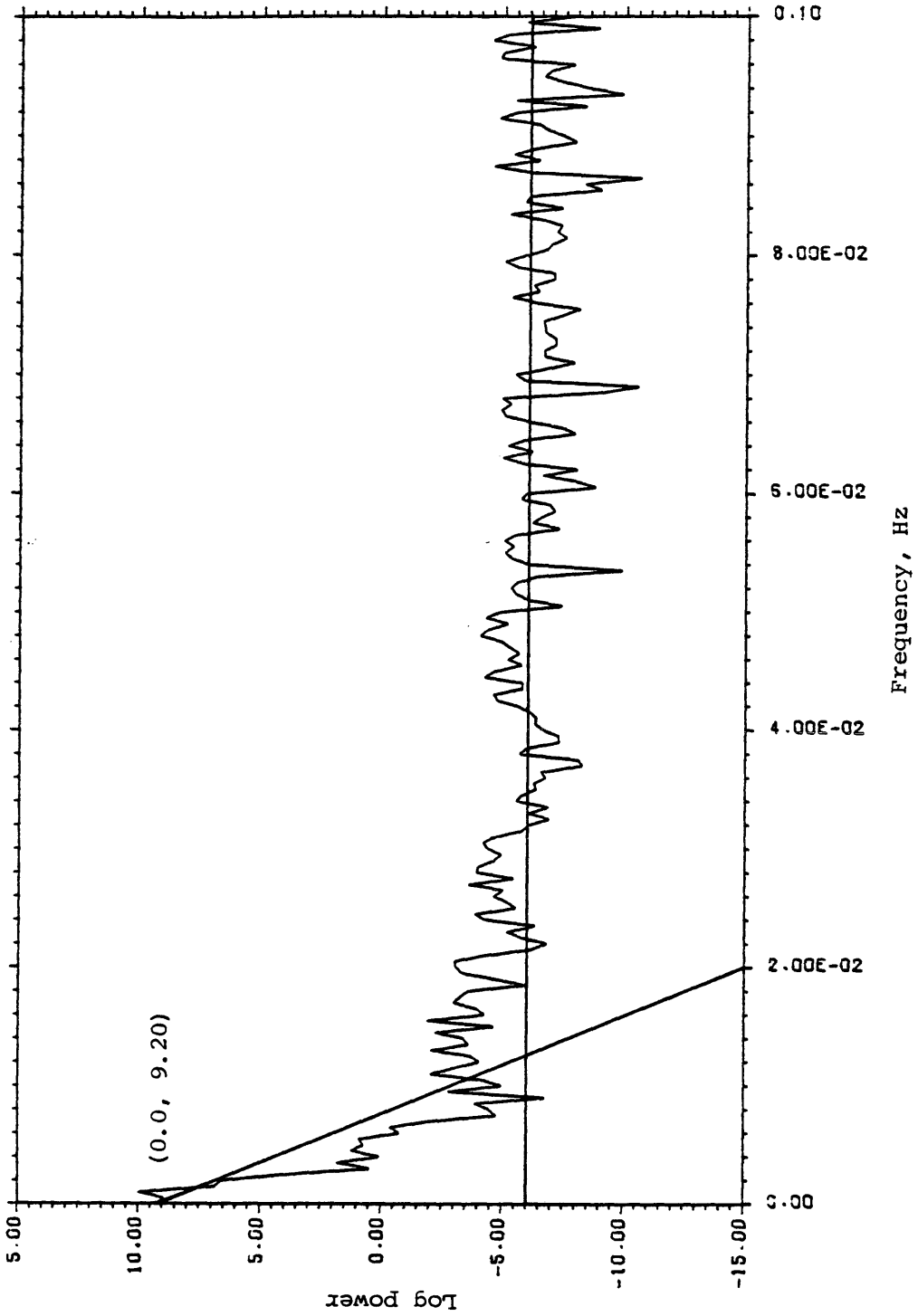

Figure 43. Auto power spectrum of the Model#2 base data.

0.496, which is practically the same as the desired value, 0.5. So, from the cross and auto power spectra, we obtained a filter whose response is equal to 0.496 near the origin, and applied this filter to remove the time variations from the Model#1 field data.

The corrected field (without considering the difference in amplitude) and the geology are plotted together in Figure 44, and these results clearly demonstrate that we introduce errors in our corrected field data if we do not take care of the difference in amplitude between the time variations in the base and field data. The corrected field, taking into account the difference in amplitude, and the geology are shown in Figure 45, and these results demonstrate that the new filtering technique also successfully removes the time variations from the field data by taking care of the difference in amplitude between the time variations in the base and field data.

So far, we have considered smooth and periodic time variations. However, in general (as seen in the examples of the observed time variations in Chapter 2), the time variations are not so smooth and periodic; they are irregular and aperiodic. So, we next considered irregular and aperiodic time variations as shown in Figure 46, which we call the Model#3 base data. We also considered a

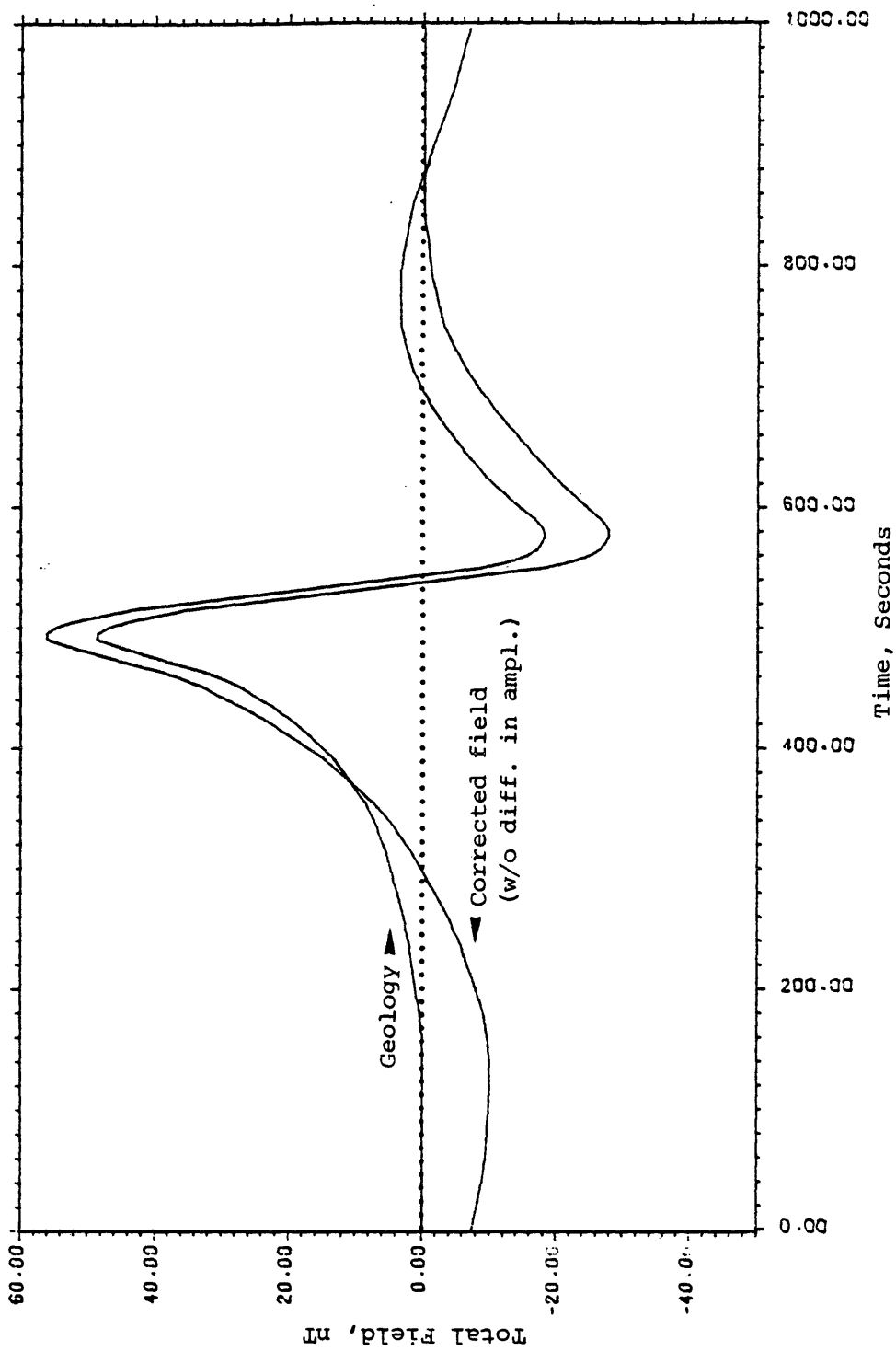

Figure 44. Model#1 field due to the geology and time-variation corrected (without difference in amplitude) Model#1 field data.

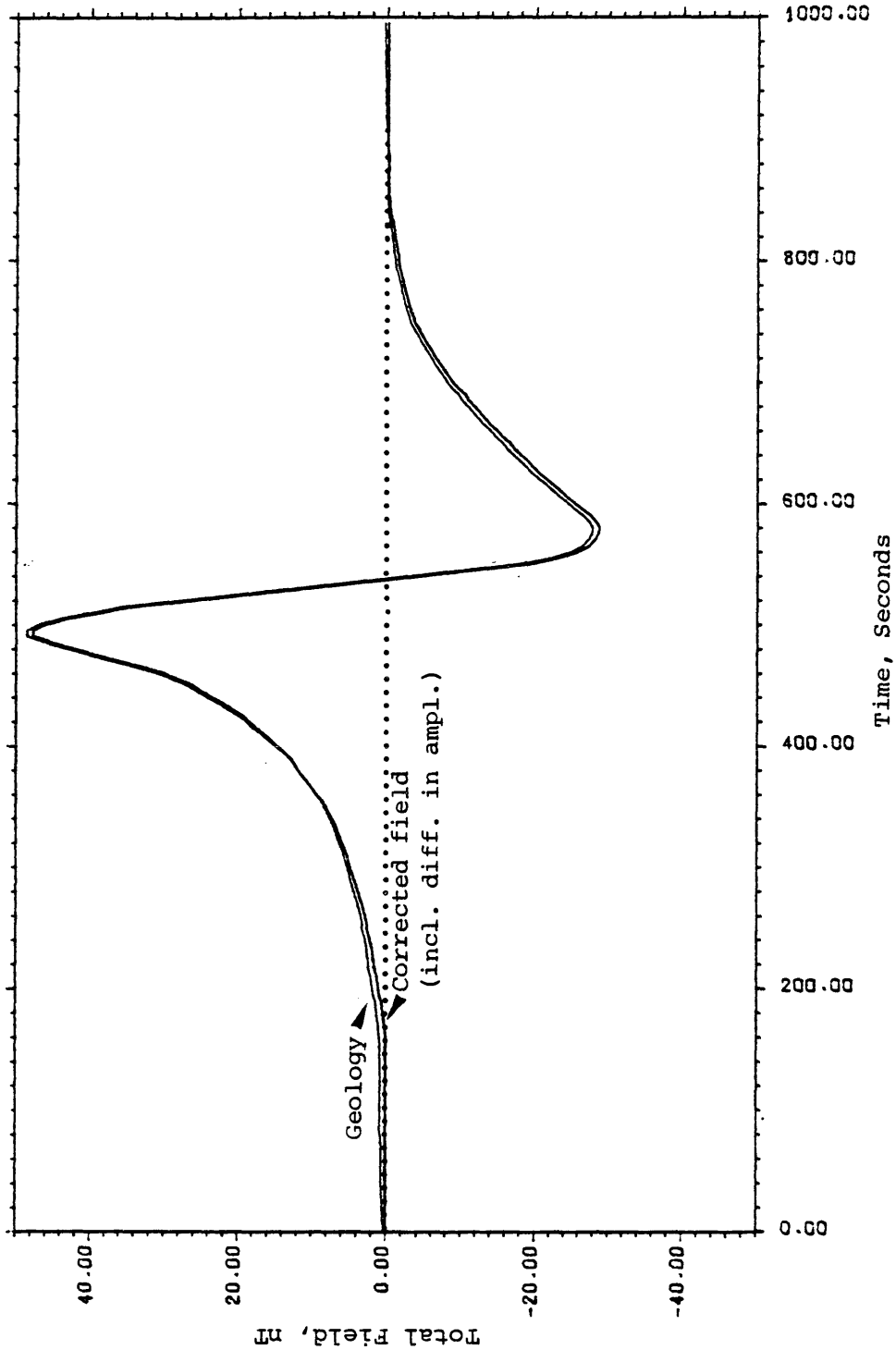

Figure 45. Model#1 field due to the geology and time-variation corrected (including difference in amplitude) Model#1 field data.

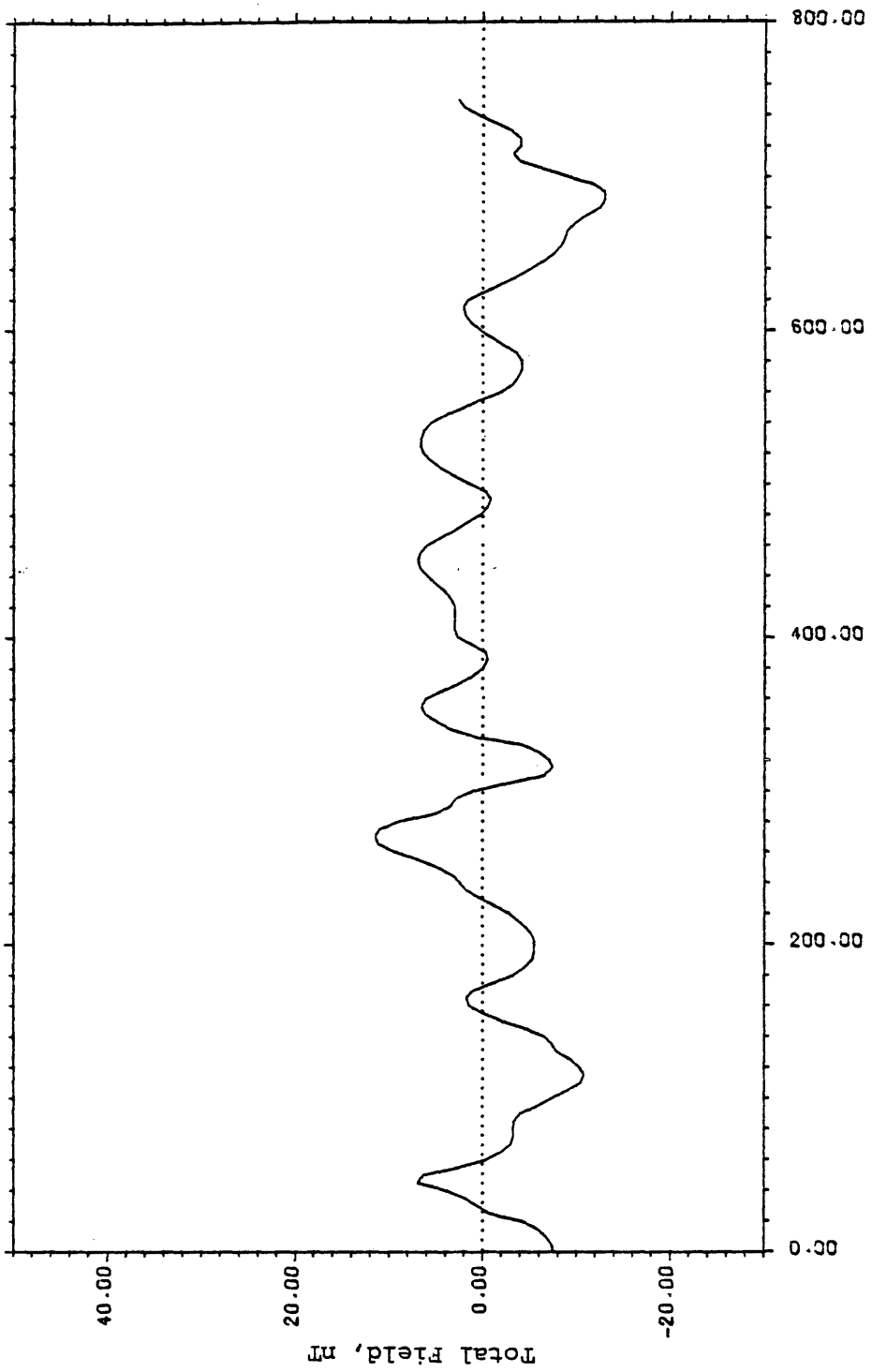

Figure 46. Model#3 base data.

different model field due to the geology, which we call the Model#3 field due to the geology as shown in Figure 47. Adding the Model#3 base data and the Model#3 field due to the geology together, we created the Model#3 field data, as shown in Figure 48. Calculating the filter from the Model#3 base and field data, we applied the filter to remove the time variations from the Model#3 field data. The corrected field and the geology are plotted together in Figure 49. From the results in Figure 49, we see that the new filtering technique also effectively removes the irregular and aperiodic time variations from the field data.

Real Data

In 1984 U.S. Geological Survey (USGS) conducted a marine magnetic gradiometer survey in the Antarctic Continental Margin area as shown in Figure 50 (Hansen and Childs, 1987). The upper part of the Figure 50 shows the locations of the survey lines in the Ross sea near the coast of the Victoria Land. A base magnetometer was operated at the Scott Observatory on Ross Island. The lower part of the Figure 50 shows the magnetic field and base data for the survey Line 404 shown in the upper part of the same figure. A portion of the field data and the corresponding portion of the base data from the Line 404

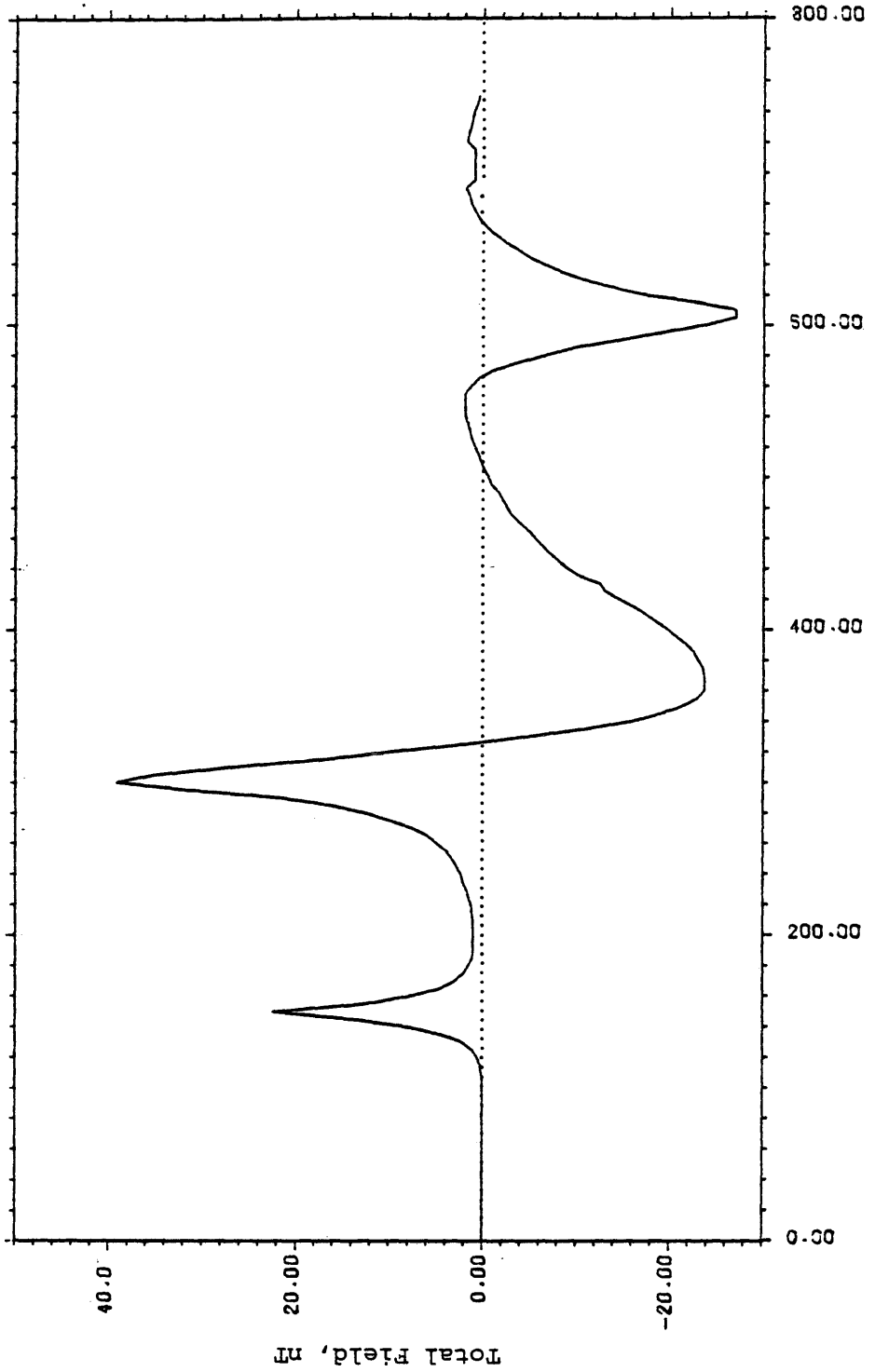

Figure 47. Model#3 field due to the geology.

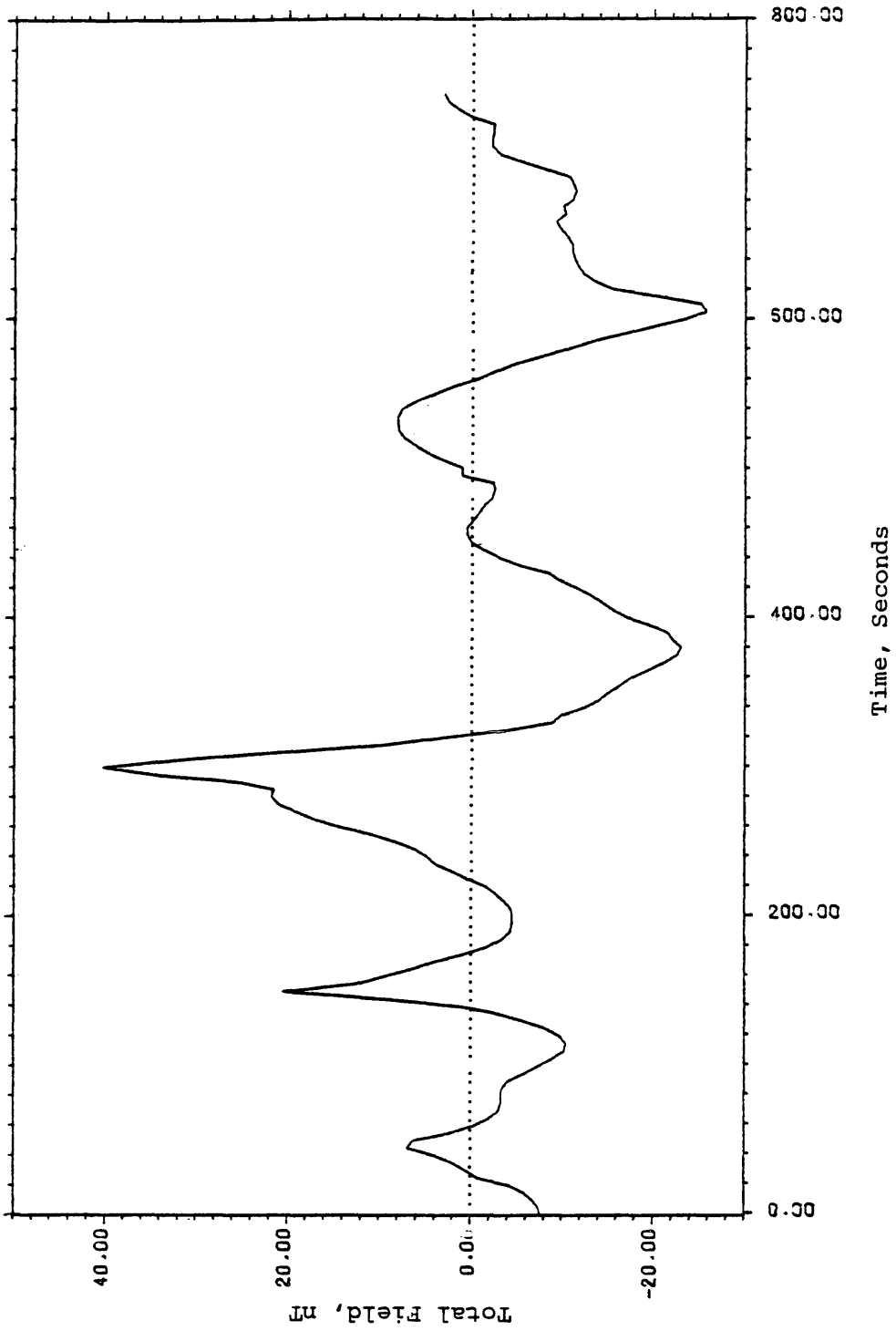

Figure 48. Model#3 field data.

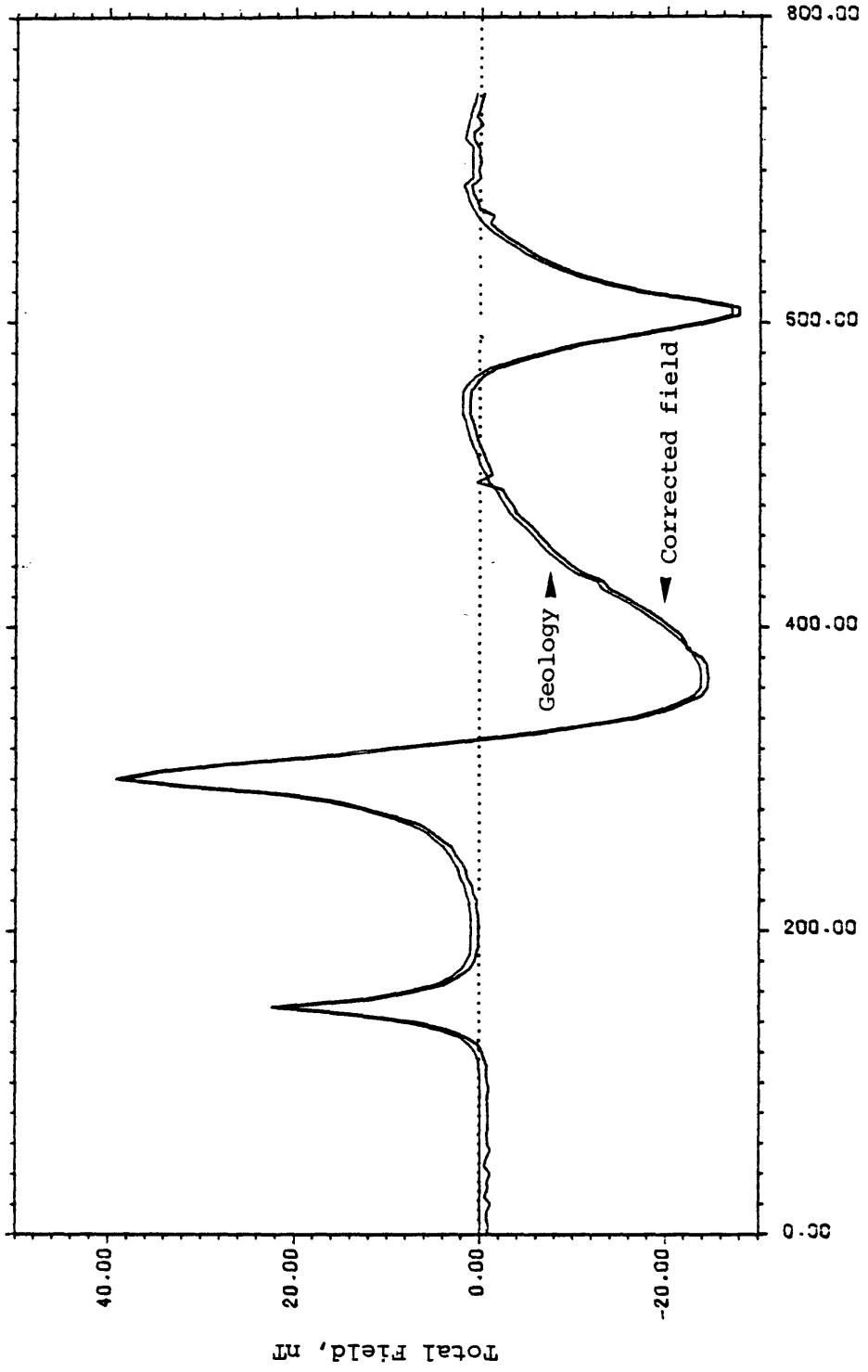

Figure 49. Model#1 field due to the geology and time-variation corrected Model#3 field data.

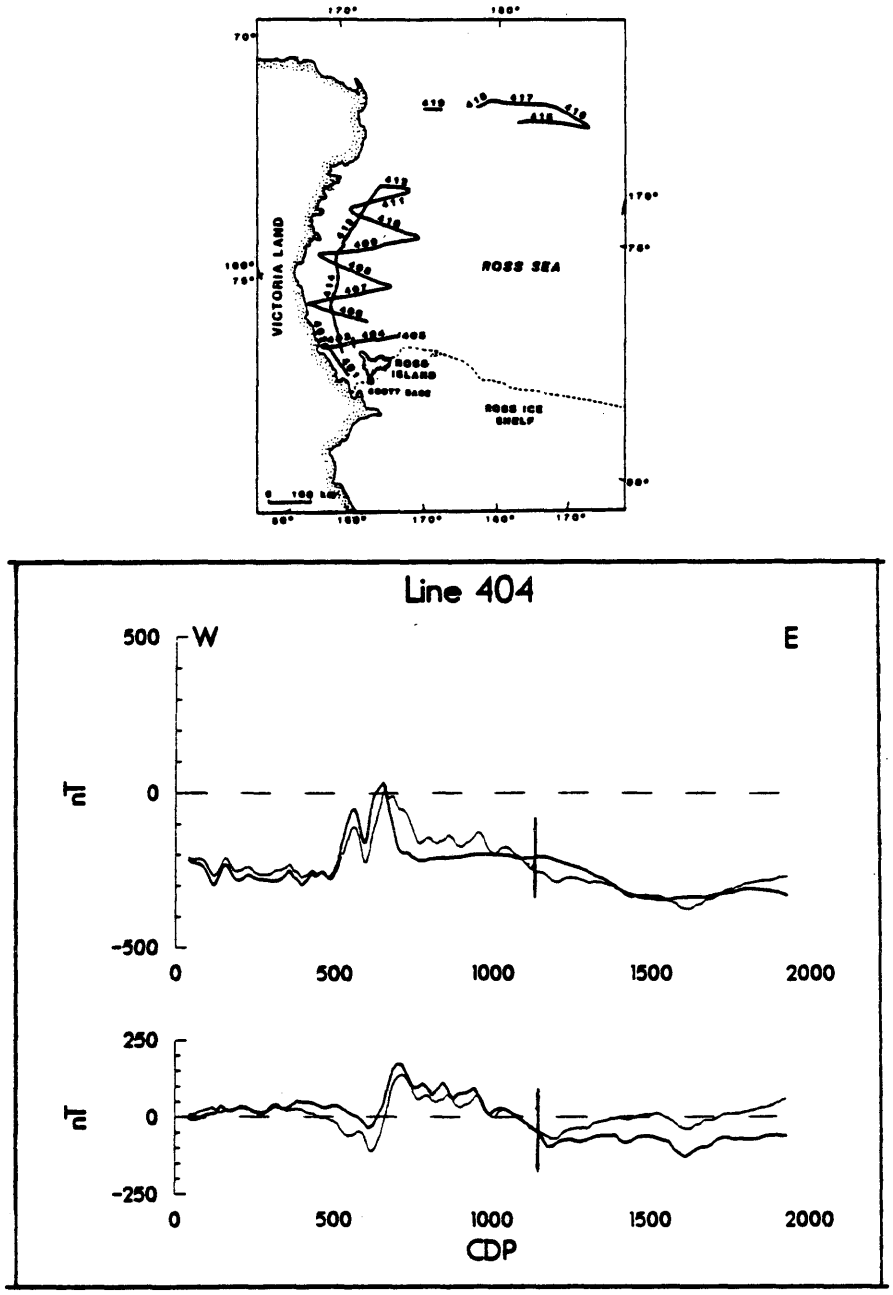

Figure 50. Upper part: Trackline map for Leg 2 of the 1984 U.S. Geological Survey Antarctic Cruise. Lower part: Magnetic data for Line 404. (Hansen and Childs, 1987)

were obtained from Dr. R. O. Hansen for removing the time variations from the field data by applying the new filtering technique. The selected portions of the field and base data are shown separately in Figures 51 and 52. The reason for choosing these gradiometer data is that we also have available the time-variation corrected field data obtained by a gradiometer reconstruction technique for comparison with the time-variation corrected field data to be obtained by applying the new filtering technique.

At the right-hand side of both the field and base data (Figures 51 and 52) we observe a similar trend of anomalies and also a phase shift between the two sets of data. This phase shift is more clearly seen in Figure 53, where these portions of the field and base data are plotted together. The phase shift shown in Figure 53 represents the phase shift between the time variations in the base and field data, because similar anomalies in the field data and the corresponding base data are assumed to be due to the time variations only. The cross phase spectrum of these portions of the field and base data, having a similar trend of anomalies, is shown in Figure 54. The dashed line suggested by the trend of the cross phase spectrum in Figure 54, and which passes through the points (0.0, 0.0) and (0.0025, -180.0) represents the phase shift between the time

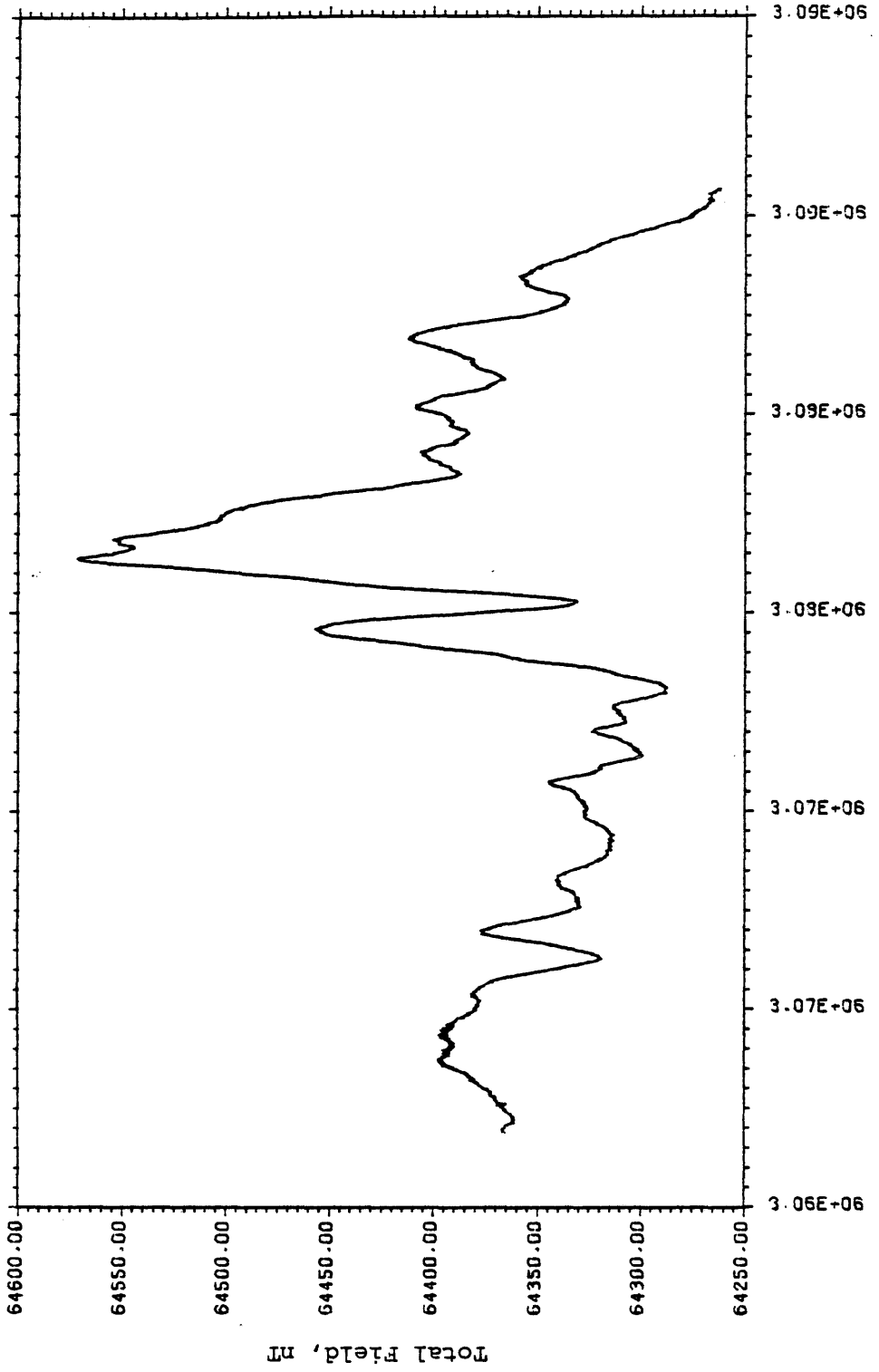

Figure 51. Field data for a portion of Line 404.

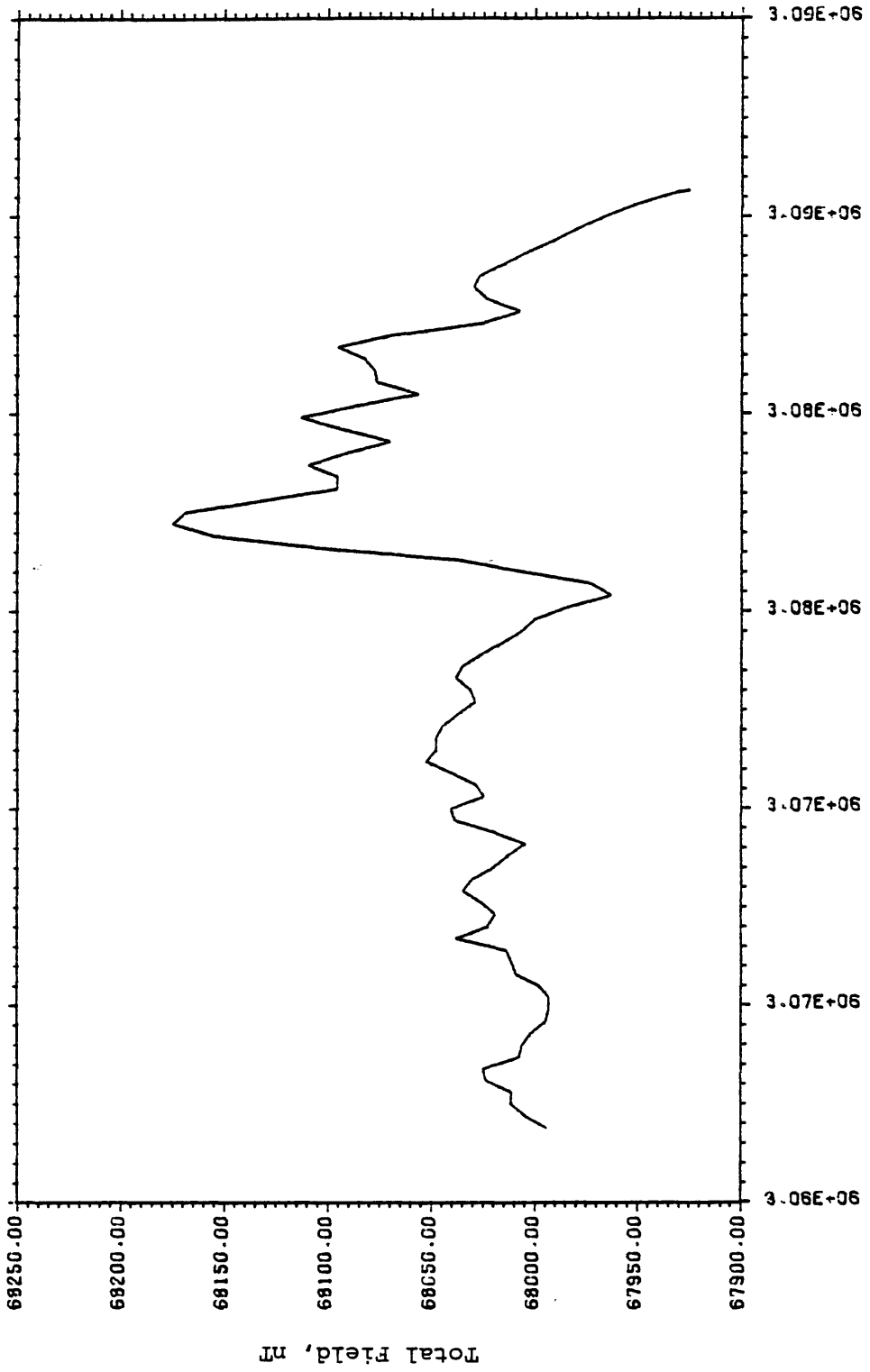

Figure 52. Base data for a portion of Line 404.

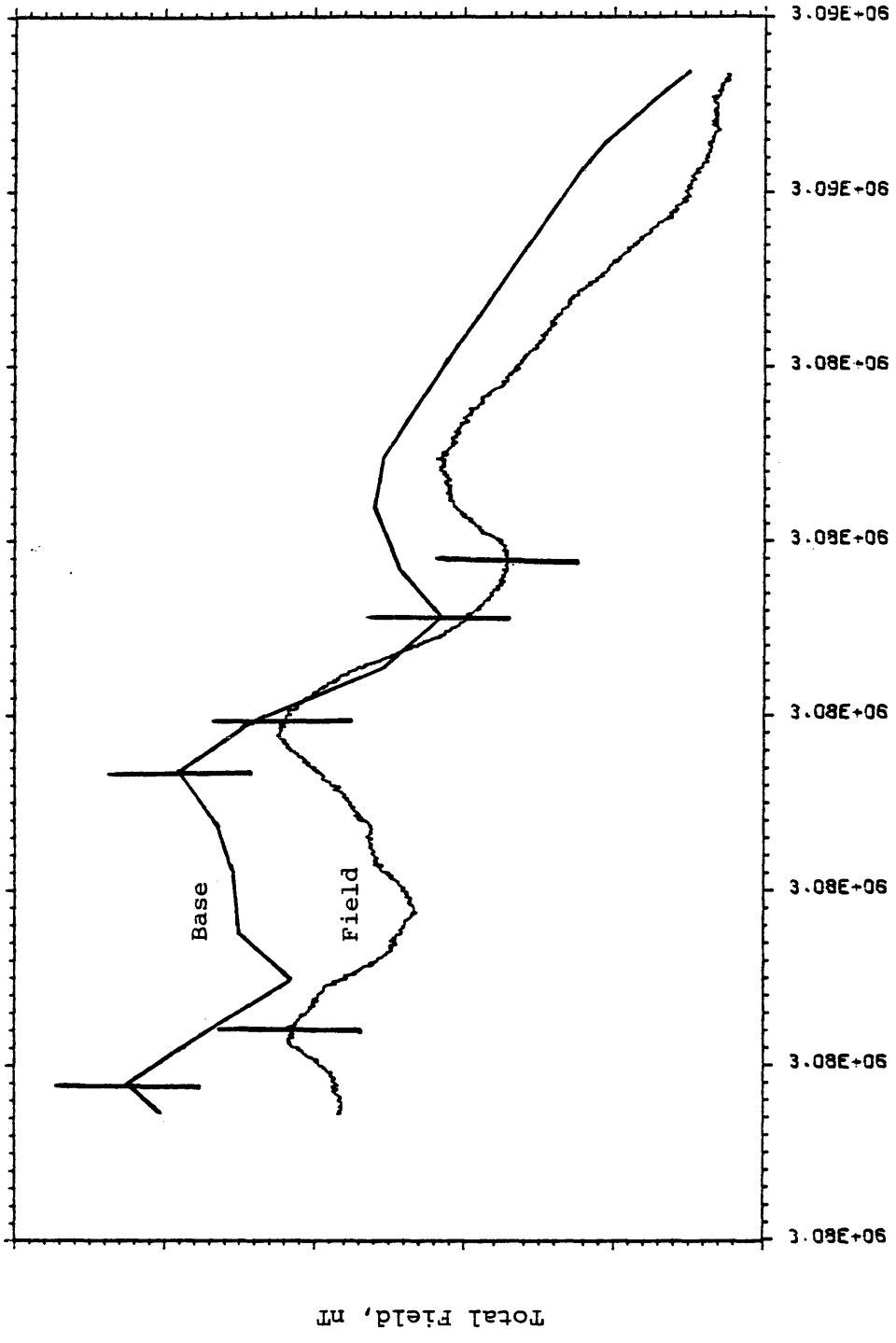

Figure 53. Field and base data for a portion of Line 404 showing similar trend of anomalies and a constant phase shift between them.

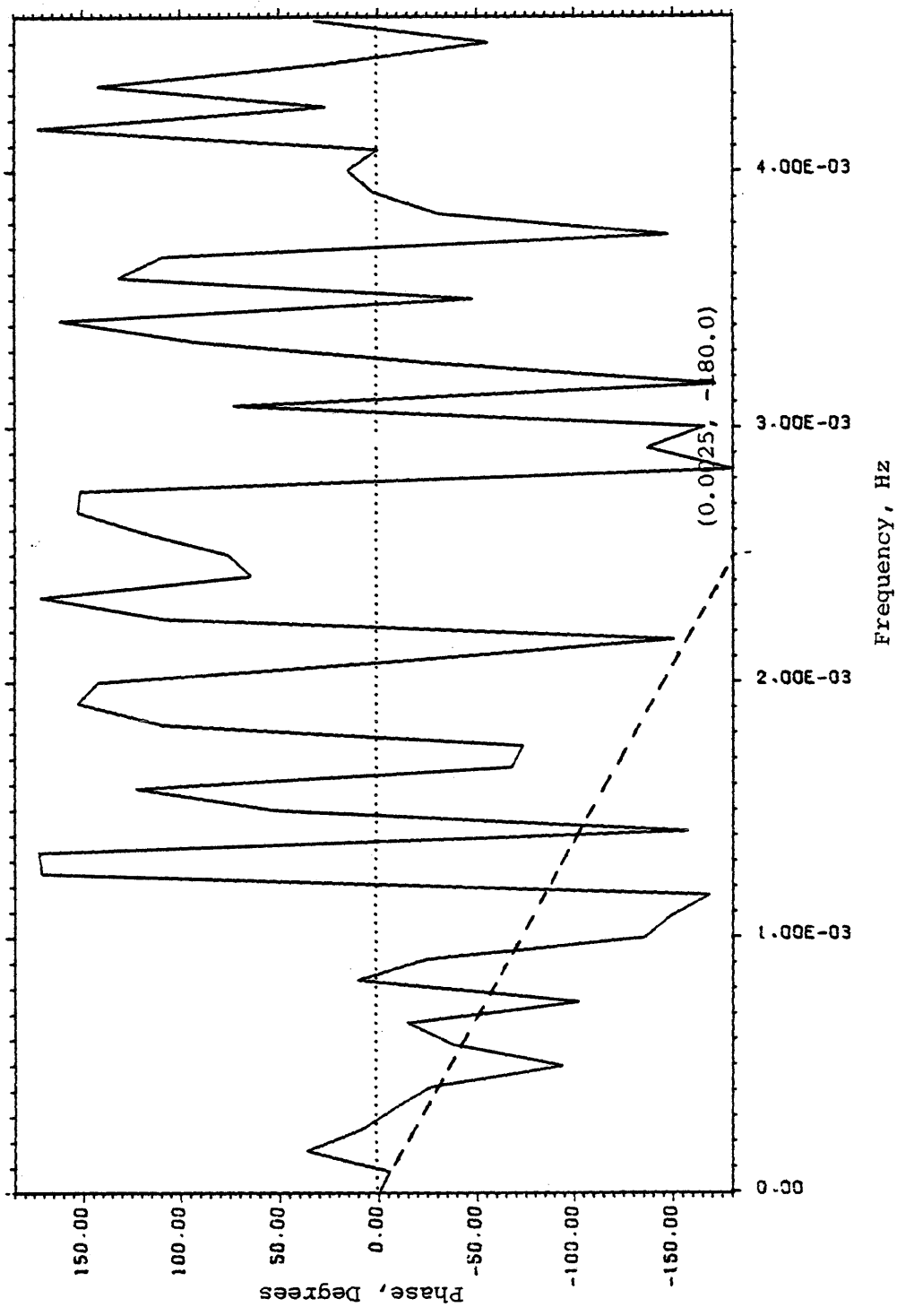

Figure 54. Cross phase spectrum of the portions of the field and base data shown in Figure 53. The dashed line represents the phase shift.

variations in the base and field data. That the dashed line correctly represents the phase shift is seen clearly from the results shown in Figure 55. In Figure 55 we have plotted together the field data and the corrected field data. Since the anomalies in this portion of the field data are due to the time variations only, after removing the time variations correctly from the field data we are supposed to get a flat time-variation corrected field. In Figure 55, we see that, by considering the phase shift represented by the dashed line in Figure 54 when we removed the time variations from the field data, we got the desired result. So, the dashed line in Figure 54 represents the correct phase shift between the time variations in the baee and field data. This result also confirms our anticipation that, in practice, we are able to estimate the phase shift between the time variations in the base and field data by locating a portion of the field data having similar trend of anomalies as in the corresponding portion of the base data.

The cross power spectrum of the field and base data is shown in Figure 56, and the auto power spectrum of the base data in Figure 57. Using the line segment approximations of the power spectra in Figures 56 and 57 and the phase shift represented by the dashed line in Figure 54, we calculated

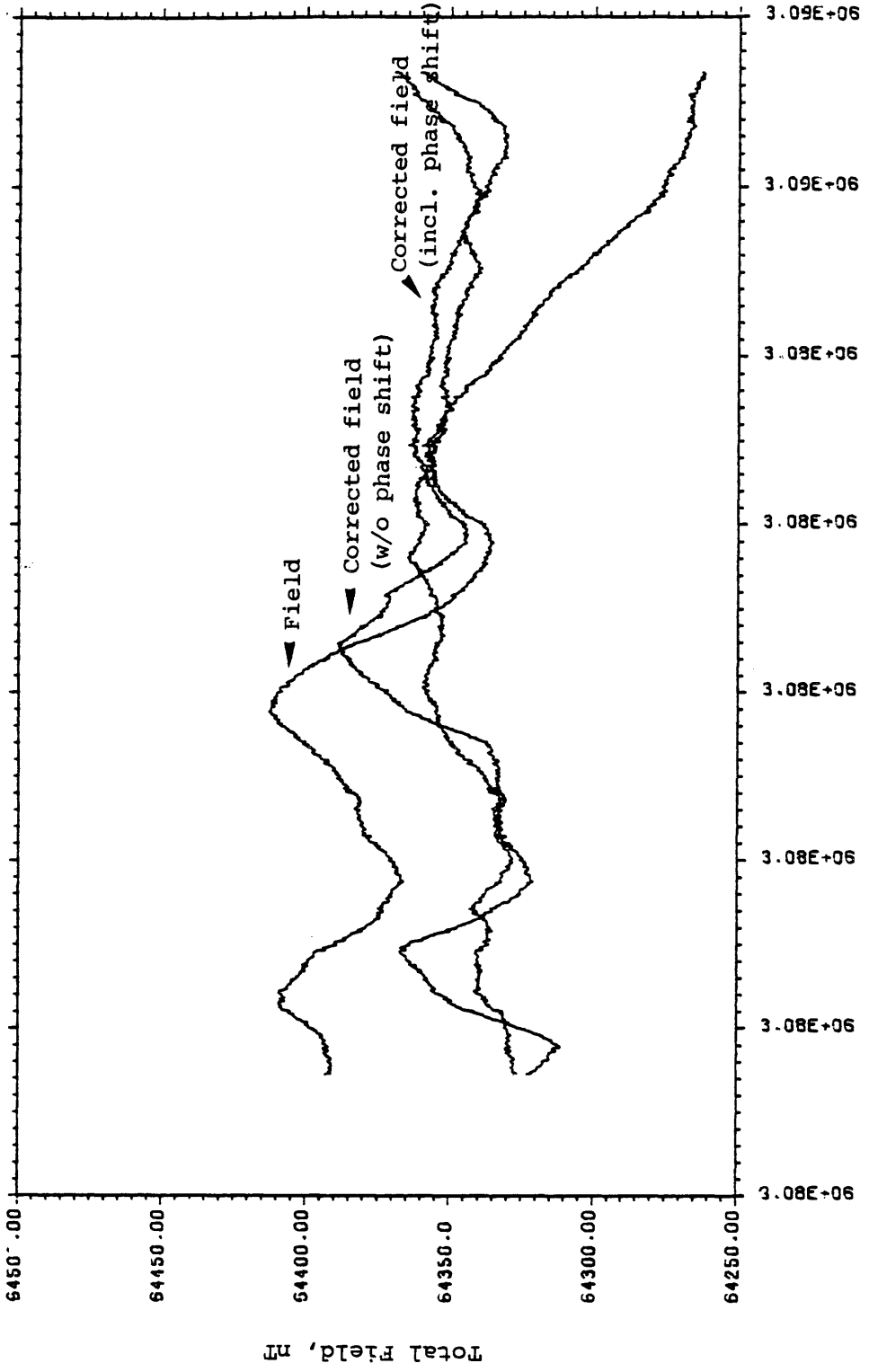

Figure 55. Field data for a portion of Line 404 (shown in Figure 53) and time-variation corrected field data.

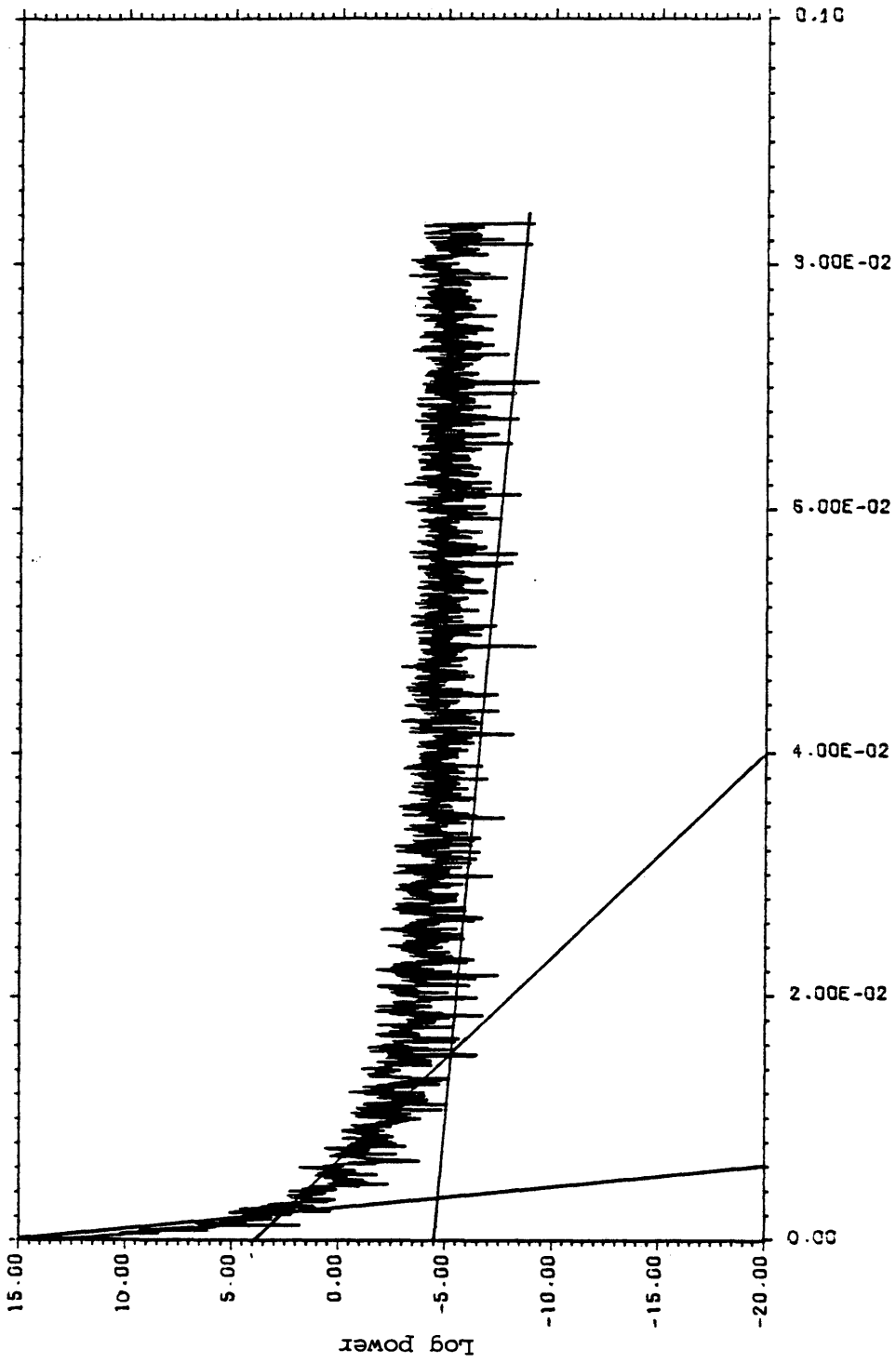

Figure 56. Cross power spectrum of the field and base data for a portion of Line 404.

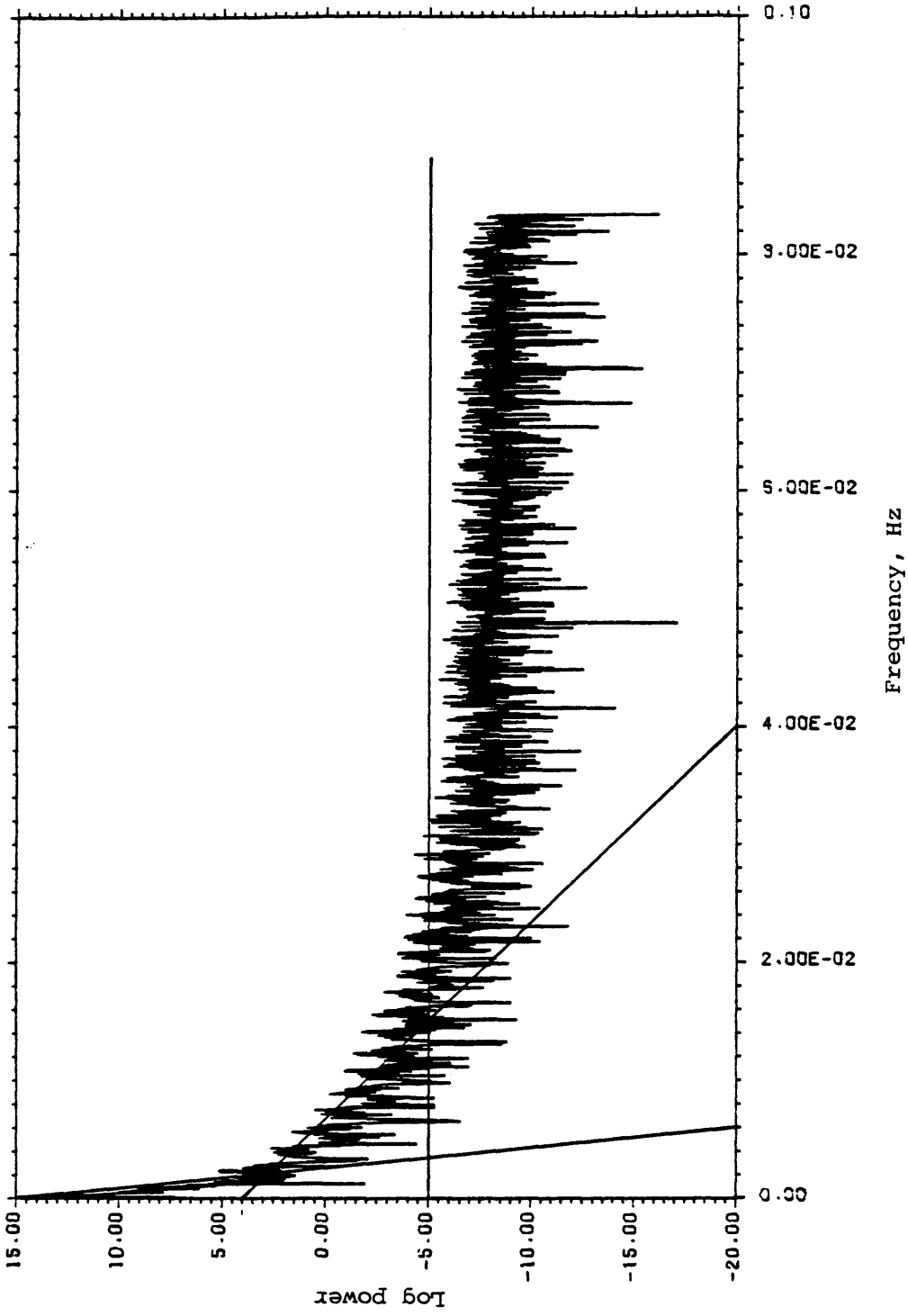

Figure 57. Auto power spectrum of the base data for a portion of Line 404.

the filter transfer function, which is shown in Figure 58. Applying the filter shown in Figure 58, we removed the time variations from the field data; the results obtained are shown in Figure 59. In Figure 59, the solid curve represents the time-variation corrected field data obtained by applying the new filtering technique and the dashed curve by the gradiometer reconstruction technique. The match between the two corrected fields is very good, although we observe a small discrepancy at the left-hand part of the profile. During our model studies, we have observed that the new filtering technique is very effective for removing low-frequency time variations from the field data. From the gradiometer reconstructed field in Figure 59, we observe that the gradiometer reconstruction technique, in contrast to the new filtering technique, is very effective for correcting high-frequency time variations. Considering these opposite characteristics of the two different techniques, the observed discrepancy in the corrected fields is not unexpected. It seems reasonable that, the slightly rising trend of the time variations towards right as can be seen in the base data (Figure 52), is more effectively removed by the new filtering technique than by the gradiometer reconstruction technique. Dr. R. O. Hansen, who was one of the participants in the removal of

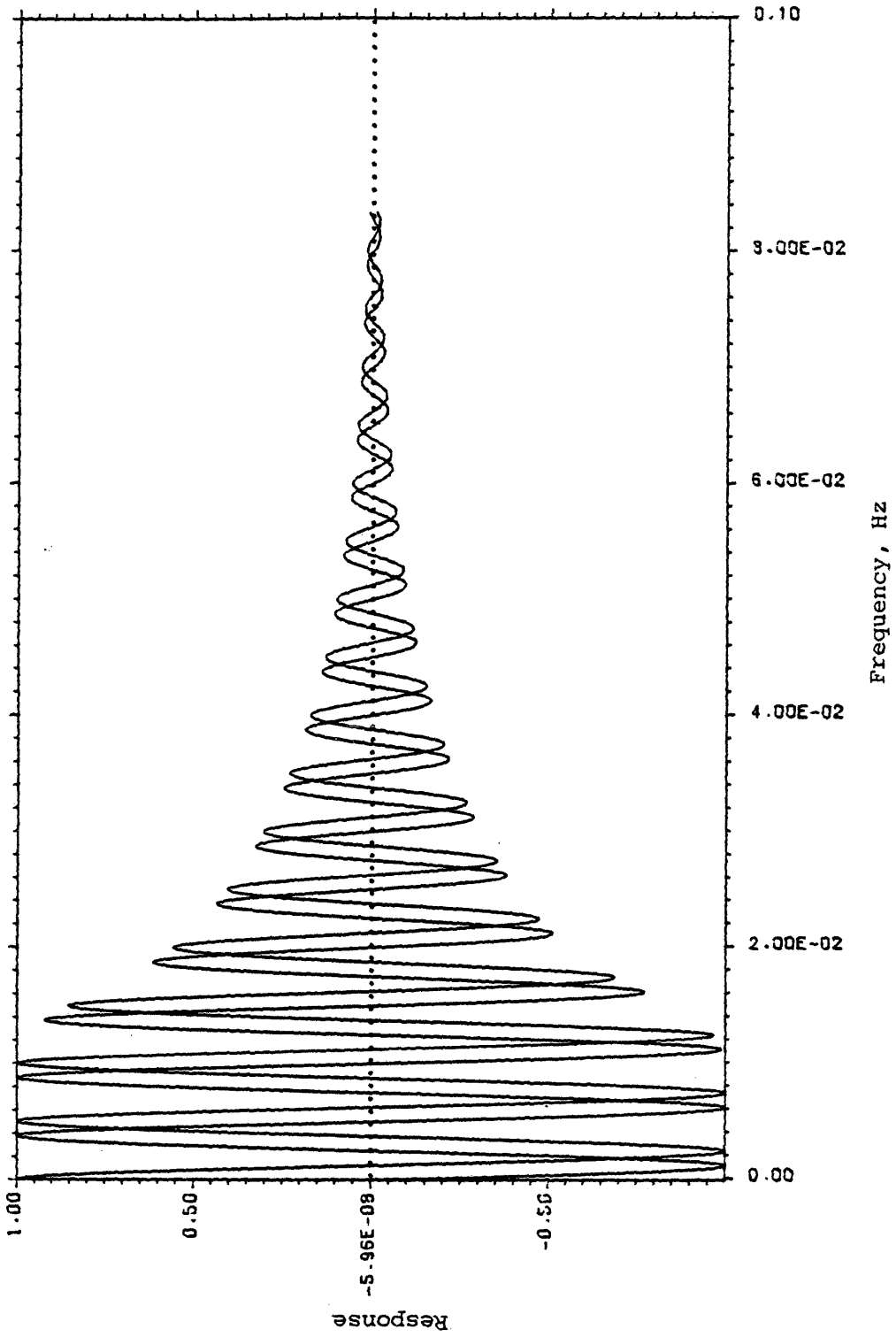

Figure 58. Filter transfer function (calculated from the power spectra in Figures 56 and 57 and using the phase shift shown in Figure 54).

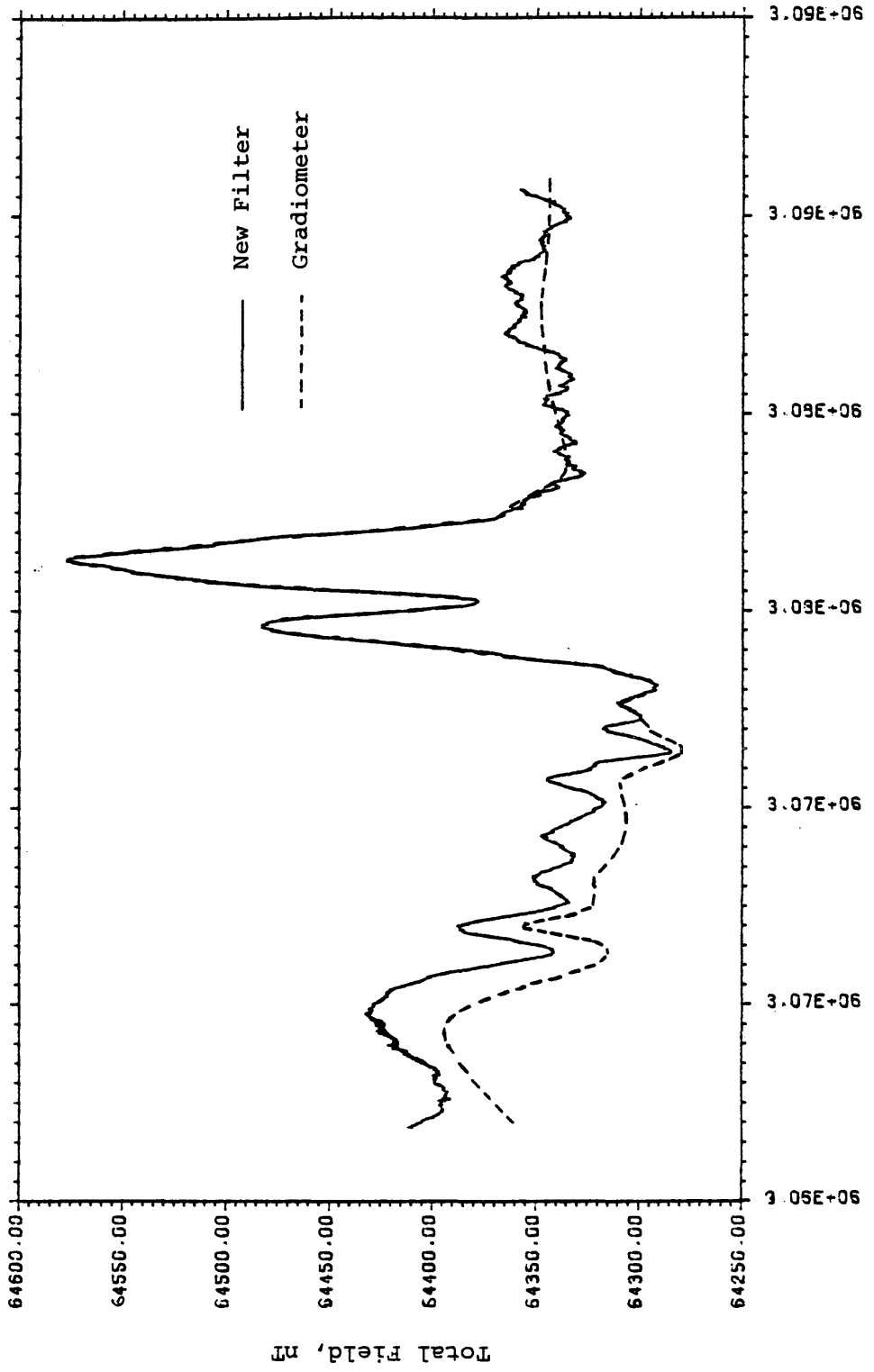

Figure 59. Time-variation corrected field data for a portion of Line 404.

the time variations from the field data by the gradiometer reconstruction technique, also thinks so.

We also applied the new filtering technique to remove the time variations from aeromagnetic data. Aeromagnetic survey data for the profile KY2700 of a survey conducted in Kentucky were obtained from TerraSense, Inc. The field and base data for the profile KY2700 are shown in Figures 60 and 61. We calculated the filter from the base and field data, and then applied the filter to remove the time variations from the field data. The corrected field and the uncorrected field are plotted together in Figure 62. We do not see any difference between the two sets of data in Figure 62. The Kentucky aeromagnetic data are very good survey data. The anomalies in the field data are of the order of two thousand nT and the anomalies in the base data, which represent the time variations, are only of the order of ten nT. Ten nT time variations in two thousand nT anomalies due to the geology are practically insignificant. In our plot of the two sets of data in Figure 62, we can not expect to see the effect of removal of the ten nT time variations from the field data containing anomalies of the order of two thousand nT.

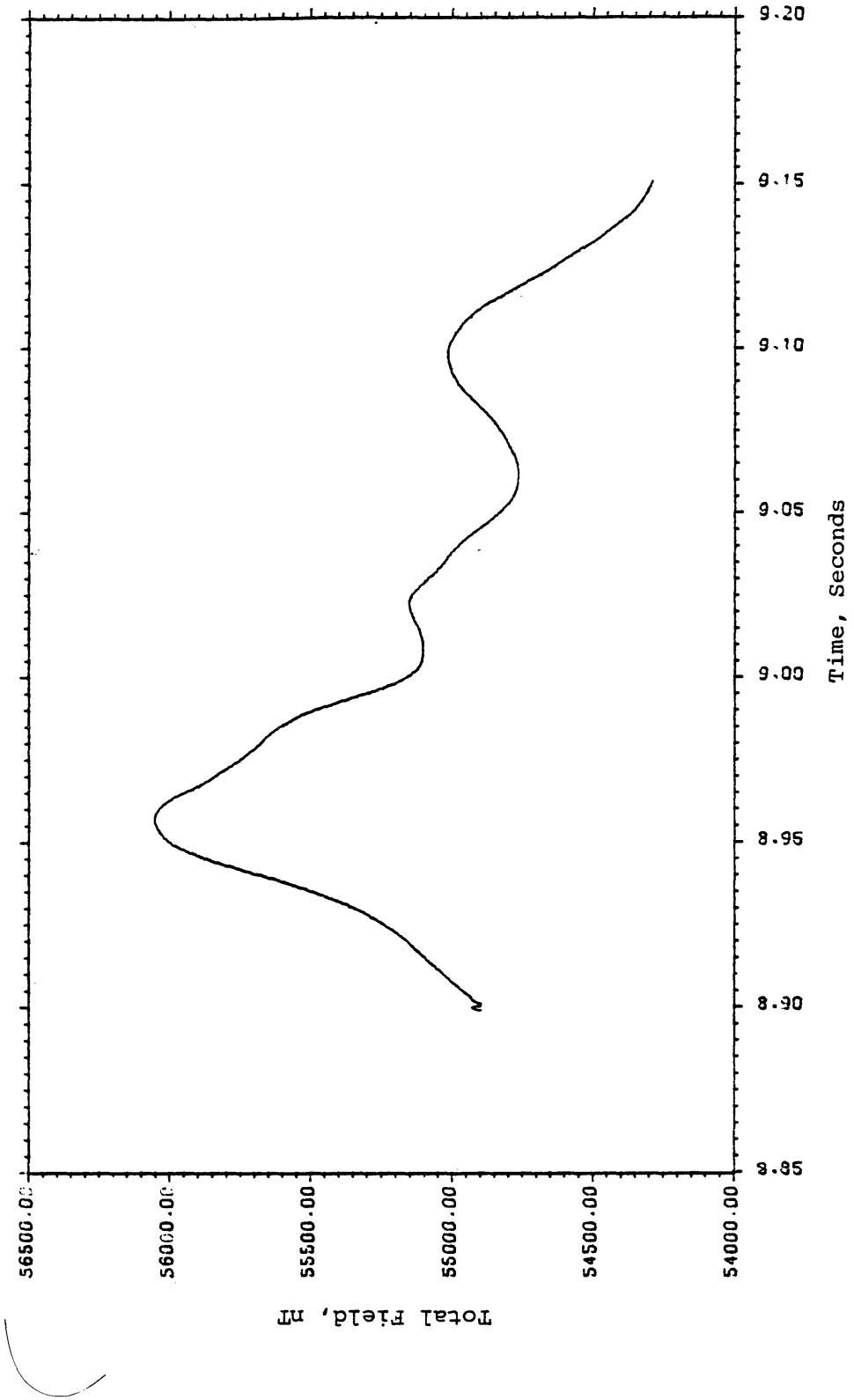

Figure 60. Field data for the profile KY2700.

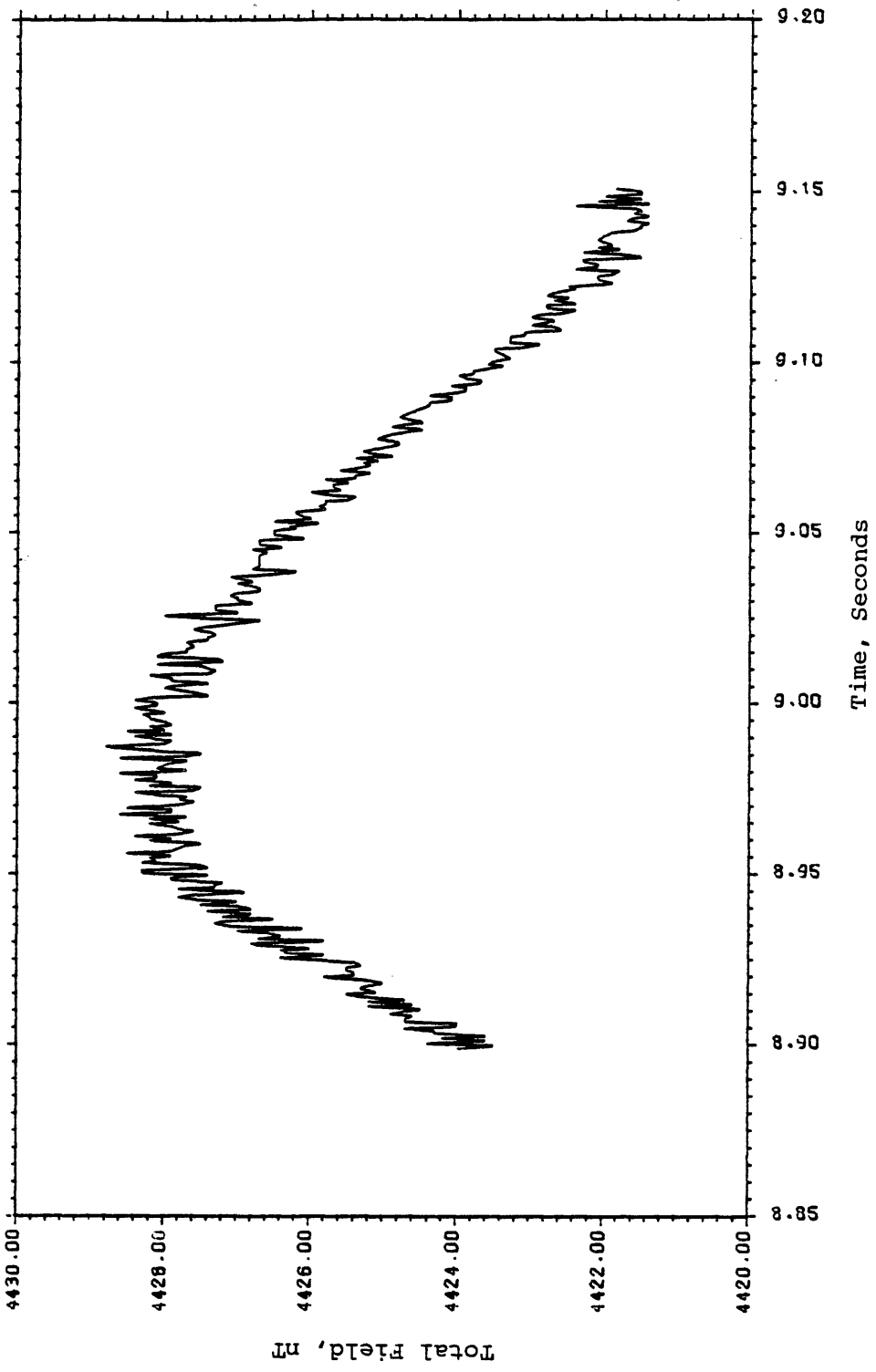

Figure 61. Base data for the profile KY2700.

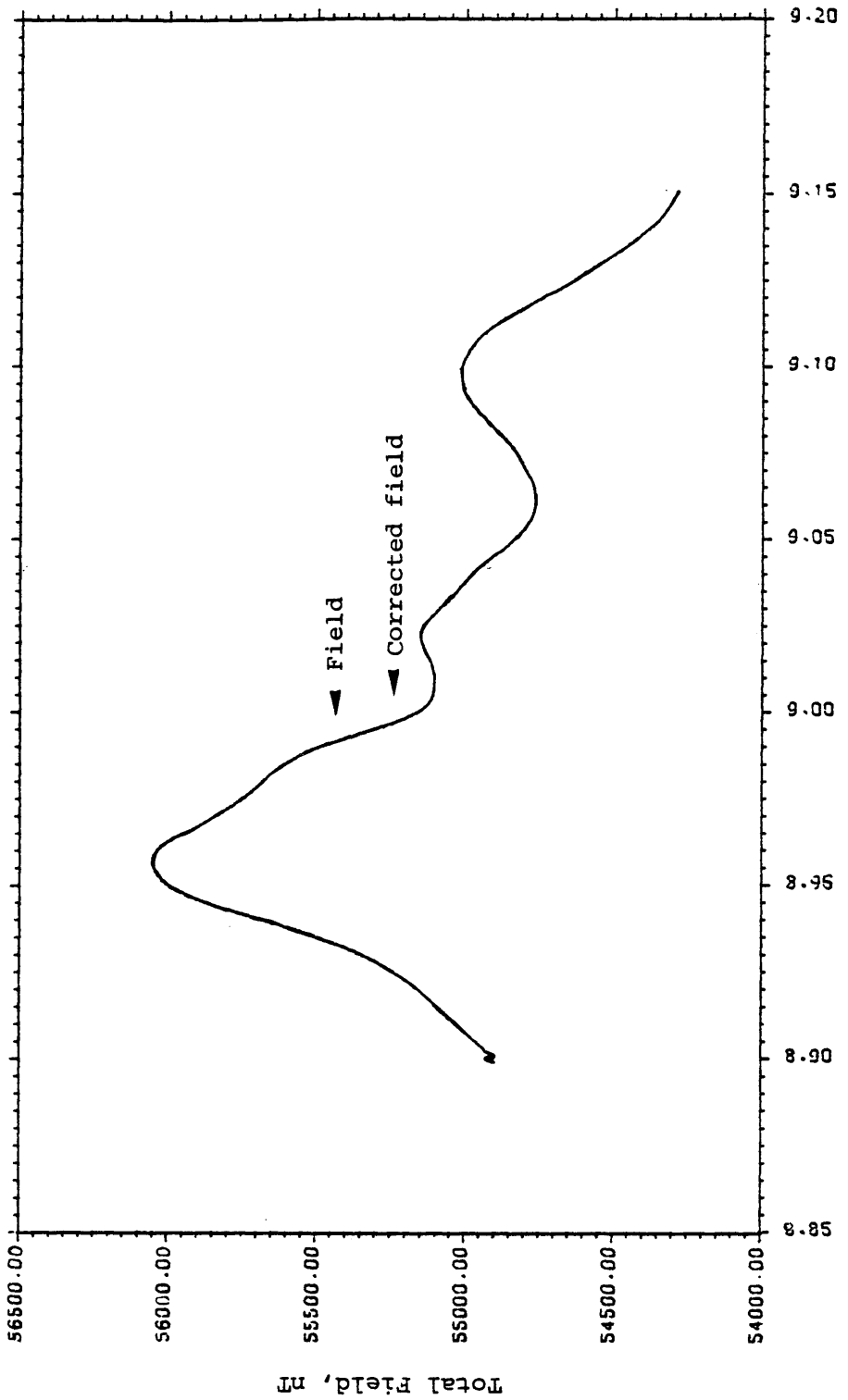

Figure 62. Field data and time-variation corrected field data for the profile KY2700.

Chapter 5

CONCLUSIONS AND RECOMMENDATIONS FOR FURTHER WORK

The new filtering technique, which is explained and tested in this thesis, effectively removes the time variations from magnetic field data. The new technique is more generally applicable than the conventional method. The results obtained by applying the technique to model and real data clearly suggest that the new filtering technique successfully removes the time variations from the field data by taking care of the differences in phase and amplitude between the time variations in the base and field data.

The differences in phase and amplitude between the time variations in the base and field data, to some extent, also depend on frequency. At present, we have difficulty in estimating more than a single phase shift and a common difference in amplitude. If we can estimate the differences in phase and amplitude at different frequencies and then incorporate them in our calculation of the filter, the new filtering technique will be more generally applicable.

The assumption that the time variations in the base and field data differ by a single phase shift and a common

difference in amplitude is fairly reasonable for most surveys. However, if the field data are collected along a long profile, then the phase and amplitude of the time variations in the field data relative to the base station may vary significantly along the profile. For example, if field data are collected along a profile crossing a coast and continuing inland for a few hundred kilometers, then the amplitude of the time variations in the field data near the coast will be remarkably different from the amplitude of the time variations in the field data far away from the coast. In such cases, to correctly remove the time variations from the field data, we are also required to take care of the variations of the phase and amplitude of the time variations in the field data. This correction might be calculated using a time-varying Wiener filter technique.

At present, our estimation of the cross power spectrum at the high-frequency tail is biased. Better estimation of the power spectrum will further improve the implementation of the new filtering technique. Maximum entropy spectral methods may provide the improved estimates.

REFERENCES

Abell, G.O., 1975, Exploration of the Universe: Holt, Rinehart and Winston, New York, p. 198-229, 535.

Hansen, R.O. and Childs, J.R., 1987, The Antarctic Continental Margin Magnetic Gradiometer Data: Suppression of Time Variations: CPCEMR Earth Science Series, v. 5B, p. 139-153.

Hill, M.N. and Mason, C.S., 1962, Diurnal Variation of the Earth's Magnetic Field at Sea: Nature, v. 195, p. 365-366.

Jacobs, J.A., 1968, The Magnetosphere and Disturbance Magnetic Fields, in Application of Natural Electromagnetic Fields in Petroleum and Mining Exploration: University of California, Berkeley, p. A.1/1-A.1/26.

Jenkins, G.M., 1961, General Considerations in the Analysis of Spectra: Technometrics, v. 3, p. 133-166.

Keller, G.V. and Frischknecht, F.C., 1966, Electrical Methods in Geophysical Prospecting: Pergamon Press, New York, p. 200.

Lilley, F.E.M., 1982, Geomagnetic Field Fluctuations over Australia in Relation to Magnetic Surveys: Bull. Aus. Soc. Explor. Geophys., v. 13, p. 68-76.

Matsushita, s. and Campbell, W.H., 1967, Physics of Geomagnetic Phenomena: Academic Press, New York, p. 301-424.

McPherron, R.L., 1968, Auroral Zone Phenomena, in Application of Natural Electromganetic Fields in Petroleum and Mining Exploration: University of California, Berkeley, p. A.3/1-A.3/72.

Morley, L.W., 1953, The Areal Distribution of Geomagnetic Activity as an Aeromagnetic Survey Problem near the Auroral Zone: Transactions, American Geophysical Union, v. 34, p. 836-840.

Porstendorfer, G., 1975, Principles of Magneto-Telluric Prospecting: Geoexploration Monographs, Series 1, No. 5, Gebruder Borntraeger, p. 7-14.

Regan, R.D. and Rodriguez, P., 1981, An Overview of the External Magnetic Field with regard to Magnetic Surveys: Geophy. Surv., v. 4, p. 255-296.

Riddihough, R.P., 1971, Diurnal Corrections to Magnetic Surveys -- An Assessment of Errors: Geophysical Prospecting, v. 19, p. 551-567.

Schmucker, U., 1970, Anomalies of Geomagnetic Variations in the southwestern United States: University of California Press, California, p. 33-54.

Vestine, E.H., Laporte, L., Lance, I. and Scott, W.E., 1947, The Geomagnetic Field, Its Description and Analysis: Carnegie Institution of Washington Publication 580, Washington, D.C., 390pp.